A REGULARIZATION APPROACH FOR RECONSTRUCTION AND VISUALIZATION OF 3-D DATA

Hebert Montegranario Riascos, M.Sc.

Thesis submitted in partial fulfillment of the requirements for the
Degree of Doctor of Philosophy

Advisor

Prof. Jairo Espinosa Ph. D.

UNIVERSIDAD NACIONAL DE COLOMBIA
Facultad de Minas
Doctorado en Ingeniería - Sistemas
Medellín, Colombia
2010

Foreword

Esta investigación se llevó a cabo gracias a una comisión de estudios que me concedió la Universidad de Antioquia como profesor de su Departamento de Matemáticas. De otra manera, habría sido mucho más difícil realizarla.

Debo agradecer a algunas personas que de una u otra forma han influido en esta aventura. A mi director Jairo Espinosa por sus oportunos comentarios y su apoyo incondicional, a Jaime Valencia y Carlos Mario Jaramillo, colegas de la Universidad de Antioquia, a los profesores Hernán Darío Álvarez, John W. Branch y su grupo de investigación por animarme a ser parte de la Facultad de Minas de la Universidad Nacional, como también al profesor Carlos Cadavid y a Clara y Lina en la Universidad EAFIT. Este trabajo está dedicado a mi esposa Zoraida y a nuestros niños Hanna y Santiago

<div align="right">

Hebert Montegranario Riascos,
Junio 2010,
Medellín.

</div>

Summary

Computer vision is an inter-disciplinary research field that has as primary objective to address visual perception through mathematical modeling of visual understanding tasks. The first part of vision –from images to surfaces- has been termed early vision and consists of a set of processes that recover physical properties of visible three-dimensional surfaces from the two dimensional images. Different arguments suggest that early vision processes correspond to conceptually independent modules that a first approximation can be studied in isolation. Surface reconstruction is one of these modules.

This thesis is about surface reconstruction from range images using some extensions of Tikhonov regularization that produces splines applicable on n-dimensional data. The central idea is that these splines can be obtained by regularization theory, using a trade-off between fidelity to data and smoothness properties; as a consequence, they are applicable both in interpolation and approximation of exact or noisy data. We propose a variational framework that includes data and *a priori* information about the solution, given in the form of functionals. We solve optimization problems which are extensions of Tikhonov theory, in order to include functionals with local and global features that can be tuned by regularization parameters. The *a priori* is thought in terms of geometric and physical properties of functionals and then added to the variational formulation. The results obtained are tested on data for surface reconstruction, showing remarkable reproducing and approximating properties. In this case we use surface reconstruction to illustrate practical applications; nevertheless, our approach has many other applications. In the core of our approach is the general theory of inverse problems and the application of some abstract ideas from functional analysis. The splines obtained are linear combinations of certain fundamental solutions of partial differential operators from elasticity theory and no prior assumption is made on a statistical model for the input data, so it can be thought in terms of nonparametric statistical inference. They are implementable in a very stable form and can be applied for both interpolation and smoothing problems.

Well-posedness of an inverse problem depends on the topological properties, then is very important the function spaces in which our optimization problems are going to be formulated and solved. Here we show how Schwartz distribution theory is a fundamental tool for modeling and understanding of reconstruction problems. Distributional spaces, such as Sobolev and Beppo-Levi spaces provides an abstract setting for including discrete and continuous function in the same framework. In this way we obtain explicit expressions for a family of interpolating and smoothing splines. This family includes the well-known Thin Plate Spline (TPS), which is used as performance criterion for testing the other members of the class. Numerical tests applied with these splines yield very promising and successful results, showing that it is possible to design new splines able to improve the properties of TPS by an appropriate selection of parameters and regularization functionals. These results also have consequences in other approaches that can be applied for solving reconstruction problems as Learning Theory, Nonparametric Statistical Inference and Neural Networks. We think that in this way we are making contributions to fill the gap between some abstract mathematical ideas and their corresponding engineering applications

List of symbols

$\mathbb{N}$	Natural numbers
$\mathbb{Z}$	Integer numbers
$\mathbb{R}^n$	The Euclidian n dimensional space
$C^k(\mathbb{R}^n)$	The space of continuously differentiable functions of order k
$\mathcal{L}^2(\mathbb{R}^n)$	Hilbert space of square integrable functions
$C_0^\infty(\mathbb{R}^n)$	Infinitely differentiable functions with compact support
$\mathcal{S}$	Space of tempered distributions
$\mathcal{D}'$	Space of distributions
$BL(\mathbb{R}^n)$	Beppo-Levi spaces
A^t	Transpose of a matrix
A^{-1}	Inverse of a matrix
$A^\dagger$	Generalized inverse
$\dfrac{\partial u}{\partial x} = u_x$	Partial derivatives
$\| \mathbf{x} \|$	Euclidian norm

Acronyms

TPS	Thin Plate Spline
GCV	Generalized Cross-Validation
CAGD	Computer Aided Geometric design
PDE	Partial Differential Equation
CV	Cross-Validation
RMS	Root Mean Square Error
MAX	Maximum Error
MAD	Minimum absolute deviations
MAE	Minimum absolute errors
MATLAB	Matrix Laboratory
SVD	Singular Value Decomposition
RKHS	Reproducing Kernel Hilbert Space
PD	Positive Definite
CPD	Conditionally Positive Definite
wp1	Well-posed condition 1
wp2	Well-posed condition 2
wp3	Well-posed condition 3
RBF	Radial basis function

Contents

Chapter 1

Introduction

Through vision, we obtain an understanding of what is in the world, where objects are located, and how they are changing with time. Because we obtain this understanding immediately, effortlessly, and without conscious introspection, we may believe that vision should therefore be a very simple task to perform. An important contribution that computational studies have made is to show how difficult vision is to perform, and how complex are the processes needed to perform visual tasks successfully.

Computer vision is an inter-disciplinary research field that has as primary objective to address visual perception through mathematical modeling of visual understanding tasks. It has evolved during the last four decades with two main goals: to develop image understanding systems and to understand biological vision. Its main focus is on theoretical studies of vision, considered as an information processing task. In the second half of the twentieth century, there were two important attempts to provide a theoretical framework for understanding vision, by David Marr [113] and James Gibson [68].

We shall focus at the level Marr called **computational theory of vision**. Marr emphasized that vision was nothing more than an information-processing task. Any such task, he argued, could be described on three levels: (i) computational theory; (ii) specific algorithms; and (iii) physical implementation.

The important point is that the levels can be considered independently. This concept of independent levels of explanation remains a paradigm of vision research. Marr attempted to set out a computational theory for vision as a whole. He suggested that visual processing passes through a series of stages, each corresponding to a different representation, from retinal image to 3D model representation of objects. Today, forty years on, most would agree that Marr's framework for investigating human vision and [113-118], in particular, his strategy of dividing the problem into different levels of analysis, has become unquestioned [74,75].

The first part of vision –from images to surfaces- has been termed **early vision** and consists of a set of processes that recover physical properties of visible three-dimensional surfaces from the two dimensional images. Different arguments [114,116] suggest that early vision processes correspond to conceptually independent modules that as first approximation can be studied in isolation. **Surface reconstruction** is one of these modules. Other early vision modules are edge detection, spatio-temporal interpolation and approximation,

computational optical flow, shape from contours, shape from texture, shape from shading and binocular stereo.

A very remarkable fact is that most early vision problems are ill-posed in the sense defined by Hadamard [81]. A problem is well posed when its solution (a) exists, (b) is unique, and (c) depends continuously on the initial data. Ill-posed problems fail to satisfy one or more of these criteria. Bertero, Poggio and Torre [18] show precisely the mathematically ill-posed structure of these problems. This fact suggests the use of **regularization methods** developed in mathematical physics for solving the ill-posed problems of early vision.

The main idea supporting **Tikhonov regularization** theory [179,132,82,83] is that the solution of an ill-posed problem can be obtained using a variational principle, which contains both the data and prior smoothness information. If we consider, for instance, 3D data, these two features are taken into account, assuming $z_i = f(a_i)$ and minimizing the functional

$$\min_{f \in \mathcal{F}} \tau[f] := \frac{1}{M} \sum_{i=1}^{M} (f(a_i) - z_i)^2 \ + \ \lambda R[f] . \qquad (1.1)$$

With this approach, we are looking for an approximation that is simultaneously close to the data and smooth. Smoothness is included with the smoothness functional or **regularizer** $R[f]$ in such a way that lower values of the functional corresponds to smoother functions, and λ is a positive number called **regularization parameter**.

1.1 Surface Reconstruction from range image data

In the area of surface reconstruction the goal is to obtain a digital representation of a real, physical object or phenomenon described by a cloud of points, which are sampled on or near the object's surface. Recently there has been a growing interest in this field motivated by the increased availability of point-cloud data obtained from medical scanners, laser scanners, vision techniques (e.g. range images), and other modalities.

Range images [36,61,20] are a special class of digital images. Each pixel of a range image expresses the distance between a known reference frame and a visible point in the scene. Therefore, a range image reproduces the 3D structure of a scene. Range images are also referred to as depth images, depth maps, xyz maps, surface profiles and 2.5D images.

Range images can be represented in two basic forms. One is a list $A = \{a_1, a_2, \ldots, a_M\} \subset \mathbb{R}^3$ of M scattered points in 3D coordinates $a_i = (x_i, y_i, z_i), i = 1, \ldots, M$ in a given reference frame (point clouds), for which no specific order is required. The other is a matrix of depth values of points along the directions of the x, y image axes, which makes spatial organization explicit. Intensity images are of limited use in terms of estimation of surfaces. Pixel values are related to surface geometry only indirectly. Range images encode the position of surface directly; therefore, the shape can be computed reasonably easy.

Apart from being ill-posed, the problem of surface reconstruction from unorganized point clouds is challenging because the topology of the real surface can be very complex, and the acquired data may be non-uniformly sampled and contaminated by noise. Moreover, the quality and accuracy of the data sets depend upon the methodologies which have been employed for acquisition (i.e. laser scanners versus stereo using uncalibrated cameras). Furthermore, reconstructing surfaces from large datasets can be prohibitively expensive in terms of computations.

Our approach to surface reconstruction will be based in the following multivariate interpolation problem:

Given a discrete set of scattered points $A = \{a_1, a_2, \ldots, a_M\} \subset \mathbb{R}^n$ and a set of possible noisy measurements $\{z_i\}_{i=1}^M$, find a continuous or sufficiently differentiable function

$$f : \mathbb{R}^n \to \mathbb{R},$$

such that f interpolates ($f(a_i) = z_i$) or approximates ($f(a_i) \approx z_i$) the data

$$D = \{(a_i, z_i) \in \mathbb{R}^n \times \mathbb{R}\}_{i=1}^M.$$

1.2 Applications of 3D reconstruction

Surface reconstruction is an important problem in computational geometry, computer aided design (CAD), computer vision, graphics, and engineering. The problem of building surfaces from unorganized sets of 3D points has recently gained a great deal of attention. In fact, in addition to being an interesting problem of topology extraction from geometric information, its applications are becoming more and more numerous. For example, the acquisition of large numbers of 3D points is becoming easier and more affordable using, for example, **3D-scanners** [20]. There are a number of other applications where objects are better described by their external surface rather than by unorganized data (clouds of points, data slices, etc.). For example, in medical applications based on CAT scans or NMRs it is often necessary to visualize some specific tissues such as the external surface of an organ starting from the acquired 3D points. This can be achieved by selecting the points that belong to a specific class (organ boundary, tissue, etc.) and then generating the surface from their interpolation. In most cases the definition of this surface is an ill-posed problem as there is no unique way to connect points of a dataset into a surface; therefore it is often necessary to introduce constraints for globally or locally controlling the surface behavior. As a matter of fact, the resulting surface often turns out to exhibit a complex topology due to noise in the acquired data or ambiguities in the case of non-convex objects [200]. In order to overcome such problems, surface reconstruction algorithms need to incorporate specific constraints on the quality of the data fitting (surface closeness to the acquired points), on the maximum surface curvature and roughness, on the number of resulting triangles, etc.

Three dimensional object surface reconstruction and modeling plays a very important role in **reverse engineering** [146]. For example, if we want to build a geometrical model to a

3D object for reproduction, the only way is to scan the object with a digital-data acquisition device and perform surface reconstruction to get its geometrical model. While conventional engineering transforms engineering concepts and models into real parts, in reverse engineering real parts are transformed into engineering models and concepts. The existence of a computer model provides enormous gains in improving the quality and efficiency of design, manufacture and analysis. Reverse engineering typically starts with measuring an existing object so that a surface or solid model can be deduced in order to exploit the advantages of CGD/CAM technologies.

There are several application areas of reverse engineering. It is often necessary to produce a copy of a part, when no original drawings or documentation are available. In other cases we may want to re-engineer an existing part, when analysis and modifications are required to construct a new improved product. In areas where aesthetic design is particularly important such as in the automobile industry, real-scale wood or clay models are needed because stylists often rely more on evaluating real 3D objects than on viewing projections of objects on high resolution 2D screens at reduced scale. Another important area of application is to generate custom fits to human surfaces, for mating parts such as helmets, space suits or prostheses. It is important to say that there exist other meanings for reverse engineering but we refer here to surface reconstruction.

Since surface-based representation of a 3D object is crucial not only in data rendering, but also in 3D object analysis, modeling and reproduction, many surface reconstruction algorithms have been proposed in recent years. In 3D object reconstruction and display, 3D surface points can be collected either by tactile methods such as Coordinate Measuring Machines (CMM), or via non-contact methods, such as magnetic field measurement machines and optical range scanners. After surface point acquisition, the next step of 3D object reconstruction will be data fusion (patch registration and integration) to translate the surface point sets captured at different view-angles into a common coordinate system, known as the World Coordinate System (WCS), and merge the overlapping points of any two neighboring data sets. The last step of the process is surface reconstruction (surface meshing/triangulation) and rendering.

From the point of view of technology, 3D reconstruction methods can be collected under two groups: active and passive. Active methods make use of calibrated light sources such as lasers or coded light most typical example of which is the shape from optical triangulation method. Passive methods on the other hand, extract surface information by the use of 2D images of the scene. Among the most common that fall into this category are the techniques known as shape from silhouette, shape from stereo, and shape from shading. Many results are available concerning reliable reconstruction of objects using these methods. However, there is still a need for improved reconstructions since each specific method, active or passive, has its own drawbacks and deficiencies.

All techniques that recover shape are commonly called "shape-from-X," where X can be shading, stereo, texture, or silhouettes, etc. (see [9,58,93,98,148,166] and the references therein). For example, in the stereo problem, one first extracts features (e.g., corners, lines, etc.) from a collection of input images, and then solves the so-called correspondence problem, i.e., matching features across images. After obtaining depth information at the

locations of the extracted features, one needs to reconstruct the surfaces of the objects present in the scene. One way of achieving this is by using techniques that reconstruct surfaces from point clouds. Reconstructing a surface from unorganized point clouds is a challenging problem because the topology of the real surface can be very complex, the acquired data may be non-uniformly sampled and the data may be contaminated by noise. In addition, the quality and accuracy of the data sets strongly depend upon the acquisition methodology. Furthermore, the computational cost of reconstructing surfaces from large datasets can be prohibitive. Most of the existing reconstruction methods were developed postulating that precise and noise-free data is available. Therefore, they cannot meet the demands posed by noisy and/or sparse data.

1.3 Requirements of surface reconstruction

A primary goal of early vision is to recover the shapes and motions of 3D objects from their images. To achieve this goal, we must synthesize visual models that satisfy a bewildering variety of constraints. Some constraints derive from the sensory information content of images. Others reflect background knowledge about image formation and about the shapes and behaviors of real-world objects. Exploiting diverse constraints in combination has proven to be a challenge. We need models which not only integrate constraints, but which escape the confines of conventional representations that impose simplifying assumptions about shape and motion. Computational vision calls for general-purpose models having the capability to accurately represent the free-form shapes and nonrigid motions of natural objects---objects with which the human visual system copes routinely. Clearly, we are looking for models that can accommodate deformation, nonconvexity, nonplanarity, inexact symmetry, and a gamut of localized irregularities.

Many results are available concerning reliable reconstruction of objects using different methods. However, there is still a need for improved reconstructions since each specific method has its own drawbacks and deficiencies. A reconstructed surface is an intermediate representation to bridge the gap between sensor data and a symbolic description of a surface. An ideal framework or algorithm for reconstruction should have several properties [97] that Marr eloquently expresses [113] in the following conditions:

R1. Reconstruction must be invariant with respect to viewpoint, that is, to rotations and translations of the surfaces being reconstructed. This is especially important when reconstruction is part of an object recognition system. In this case a change in this intermediate representation may cause a change in any symbolic description that is derived, resulting in failure to identify objects in a scene.

R2. It is desirable to find discontinuities in both depth and orientation. A reconstruction algorithm, if detection of discontinuities is not simultaneously carried out in the reconstruction process, should at least sharply preserve regions near discontinuities for a later stage of discontinuity detection.

R3. A reconstruction framework should conduct to computationally efficient algorithms

We use these requirements as a guide for our proposal of surface reconstruction, although it is extremely difficult, if not impossible, to fully satisfy them. Nevertheless, from the early work of Marr [113] it has been shown that problems of computer vision are a set of ill-posed problems, so we have considered regularization theory as the most natural tool for dealing with these problems, in particular surface reconstruction. *The purpose of this thesis is not only to derive a method for surface reconstruction but to provide a framework and mathematical formulation for thinking and incorporating knowledge about the problem.*

1.4 The thesis objectives

1.4.1 General

Our goal is to give a general approach and a theoretical framework for solving the problem of surface reconstruction from range image data, incorporating both local and global information about the surface.

1.4.2 Specific

1. Formulation of surface reconstruction as a variational problem in terms of inverse theory.

2. To establish a regularization approach and a mathematical framework for surface reconstruction able to satisfy data and smoothness constraints on the surface.

3. To obtain criteria for the selection of smoothing functionals and regularization parameters that satisfies local or global features.

4. Validation of the proposed framework for surface reconstruction with point clouds from different objects, using criteria as accuracy and computational complexity.

Surface reconstruction is one of the fundamental problems of computer vision, a class of extremely **ill-posed inverse problems** that has originated two branches of functional analysis:

(a) The theory of generalized inverses, which is an extension of the Moore-Penrose inverse of a matrix and

(b) The regularization theory of inverse problems.

Given the difficulty of the problem we are dealing with, it is not enough to use the theory of generalized inverses. As a consequence we apply regularization theory as a variational problem on infinite-dimensional function spaces.

Naturally, trying to represent a completely arbitrary surface with a function f is next to impossible. Therefore one should make some assumptions about this function. The most common assumptions are explicit assumptions about the shape, or the form of the function. We fulfill these objectives considering our functions and our data as linear functionals on **Schwartz's distributional spaces (**generalized functions**)** [40,65,66,152,163,164,202] and analyzing the problem under the point of view of some generalizations of Tikhonov regularization.

From the practical point of view, we to obtain explicit representations for a surface in the form $f : \mathbb{R}^n \to \mathbb{R}$, making interpolation or approximation of range data $\mathbf{D} = \{(a_i, z_i) \in \mathbb{R}^2 \times \mathbb{R}\}_{i=1}^{M}$. The function f may then be used as a model or representation of the real object or phenomenon from which data are taken.

W**e** approach the problem of surface reconstruction with a generalization of the standard regularization (1.1) that satisfy the above mentioned requirements (R1, R2, R3). The regularization functionals come from a **seminorm** $R[f] = |Pf|_{\mathcal{X}}^2$, where P is a differential operator and $\mathcal{X}$ is an appropriate function space, so we can make different choices for $R[f]$.

1.5 Proposed model

Our framework uses **two regularization functionals** R_1, R_2, one functional for global smoothness and other for locality; with their corresponding regularization parameters λ_1, λ_2, included in the variational problem

$$\min_{f \in \mathcal{X}} \tau[f] = \frac{1}{M} \sum_{i=1}^{M} (f(a_i) - z_i)^2 \ + \ \lambda_1 R_1[f] + \ \lambda_2 R_2[f], \qquad \textbf{(1.2)}$$

where R_1, R_2 are functionals taken from the family of seminorms

$$R[f] = J_m[f] = \int_{\mathbb{R}^n} \sum_{|\alpha| = m} \frac{m!}{\alpha!} |\partial^\alpha f(\mathbf{x})|^2 d\mathbf{x} . \qquad (1.3)$$

These seminorms include and generalize to n dimensions the Tikhonov original proposal [170] given by the **norm** $R[f] = \sum_{m=0}^{p} \int_{\mathbb{R}} w_m (\frac{d^m f}{dx^m})^2 \, dx$.

A seminorm has the same properties of a norm with the difference that its null space can be different from zero. This property makes seminorms less restrictive than norms. Furthermore, it can be proved that a seminorm is an enough condition for solving the optimization problem [78,79,48,122].

We provide an abstract framework for the solution $S(\mathbf{x})$ of our proposal (1.2) and obtain these solutions as translates of a basis function $\Phi : [0, \infty[\to \mathbb{R}$, in the form

$$S(\mathbf{x}) = \sum_{j=1}^{M} \alpha_j \Phi(\| \mathbf{x} - a_j \|) + p(\mathbf{x}). \qquad (1.4)$$

These splines are linear combinations in terms of the fundamental solutions (Green's functions) of operators formed by different combinations of Δ^m, where Δ is the Laplacian operator and $\Delta^m f = \Delta(\Delta^{m-1} f)$. They include **Thin Plate Spline** (TPS) and splines in tension [63, 178]. For example, when $m = n = 2$, $J_m[f]$ represents the potential energy of deformation of a thin plate, so if an elastic material is deformed to satisfy the constraints $f(a_i) = z_i$, the plate fits these points, minimizing its potential energy

$$J_2[f] = \int_{\mathbb{R}^2} (\frac{\partial^2 f}{\partial x^2})^2 + 2(\frac{\partial^2 f}{\partial x \partial y})^2 + (\frac{\partial^2 f}{\partial y^2})^2 \, dx \, dy. \qquad (1.5)$$

In this approach, we satisfy requirements (R1, R2, R3) of surface reconstruction in the following way:

R1. Our solutions to regularization framework have radial form given by (1.4). As a consequence they are invariant to rotations and translations.

R2. We use local and global functional with two regularization parameters one for locality and other for global smoothness.

R3. And they have robust implementation because they have explicit mathematical expressions as linear combinations of translates of a basis function whose weights are found solving a system of linear equations.

This work is mainly inspired in *Marr and Poggio* [113-118] with their formulation of computational vision as a set of inverse problems; *D. Terzopoulos* [174-178], in the addition of proper functional for improving standard regularization, and *J. Duchon* [47-50] in his distributional approach for the solution of variational problems.

We preserve the main virtues of these three viewpoints and we also provide some contributions that make a difference with them. For example, Terzopoulos [167] do not give demonstrations of our explicit expressions $S(\mathbf{x})$ for the solution of the variational problem, instead, he used finite element methods for managing discontinuities; we do it by tuning the regularization parameters. On the other side, Duchon [48] handle variational problems in a distributional approach but he does not consider noisy data.

1.6 Contents and contributions

This work is based in and at the same time is a generalization of these previous publications of the author [129-131]

- Montegranario, H., Espinosa, J. (2007). Regularization approach for surface reconstruction from point Clouds. *Applied Mathematics and Computation* .188, 583–595.

- Montegranario, H. (2008). A unified framework for 3D reconstruction. *PAMM - Proc. Appl. Math. Mech.* 7, 2140017–2140018.

- Montegranario, H., Espinosa, J. (2009). A general framework for regularization of n-dimensional inverse problems. VII Congreso Colombiano de Modelamiento Numérico. Bogota.2009

In the first paper [129] we made a proposal of regularization for surface reconstruction from point clouds in the framework of radial basis functions. In the second paper [130] we make a generalization to several kinds of data and the third one we contribute some practical applications. Now, in this thesis our work goes further in order to formulate the general problem of surface reconstruction in terms of inverse problems theory. We are showing splines and radial basis functions as a particular case of our framework. The key idea is the extension of Tikhonov regularization to include global and local characteristics of data to be reconstructed. We propose a regularization approach under a unified variational framework that includes fidelity to data and generalization of the surface and makes a proper choice of the *a priori* knowledge in the form of regularization functionals.

Traditionally, surface reconstruction problems and their solutions are considered for particular problems, and different methods have been developed for each case. Unlike this, we face the problem with an integrated framework. The advantage of this approach is that provide the engineering community with a tool that helps to bridge the distance between theory and applications. Our approach lies heavily on inverse problems theory and approximation theory, so we can obtain robust methods and algorithms.

Up to now, many researchers do not have paid enough attention to criteria for choice of regularization functionals. We tackle this problem selecting these functionals by physical and geometric criteria, providing a heuristic reasoning that enriches the mathematical formulation.

In **chapter 1**, we state the problem of surface reconstruction from range data and its importance for engineering and technology. We then identify the question as an inverse problem with many applications in the so called inverse engineering pipeline, making emphasis in reconstruction from point clouds. We then explain the purpose and contributions of the thesis, mainly inspired in : Marr and Poggio with their formulation of computational vision as a set of inverse problems; D. Terzopoulos, in the addition of proper functional for improving standard regularization, and J. Duchon in his distributional approach for the solution of regularization.

Next, in **chapter 2** we place our work into the past and present of surface reconstruction. We review the state of the art and make a classification of methods for surface reconstruction. Currently there is a wide variety of methods; a situation which may produce confusion among developers of applications; so this problem deserves a conceptually based

taxonomy. We propose to classify the different procedures as: g*eometric, statistical and regularization* methods.

In **chapter 3** we state one of our contributions to the philosophical basis of inverse problems, showing a set of problems as noise, complexity and others, which should be identified and tackled in surface reconstruction problems. We have called them *the seven intrinsic problems of surface reconstruction*, and its statement is done in terms of how regularization theory contributes to their solution.

In **chapter 4** we do the mathematical statement of this thesis problem: The problem of surface reconstruction from point clouds. Using ideas from functional analysis, we make an integrated treatment of the problem, showing how inner product spaces and seminorms provide an abstract setting for surface reconstruction. Our framework uses two regularization functionals, one for global smoothness and other for locality; with their corresponding regularization parameters, we distinguish two basic problems: interpolation and smoothing. The first alternative can be applied on exact data, the second one, for noisy data. One important fact is that our proposal of regularization includes and solves both problems in a unified variational framework.

In **chapter 5**, we show how the study of seminorms, provide us a set of criteria for choosing the functionals which later will be used as regularizers. Although theoretically many functionals could be used for this task, some extra criteria or constraint should be imposed to its choice. We show that physical and geometrical criteria provide a firm guide in this decision. Seminorms associated with classical problems of continuum mechanics, as for instance the concept of deformation potential energy, are shown to be very useful and enrich the solutions of variational problems with very suggestive heuristic interpretations. This interpretation enables us for handling global and local features in terms of regularization functionals.

Chapters 6, it is the most theoretical one and provides strong and very refined mathematical tools. Here we use Schwartz distribution theory (generalized functions) for n-dimensional surface reconstruction. Distributional function spaces combine continuous and discrete functions in a unified framework, making possible the reconstruction of scattered data which are the basis of modern meshless methods. With distribution theory, we can develop a successful generalization of minimum norm problems from one to n dimensions. Although this treatment of inverse theory is more abstract than usual and requires a big amount of functional analysis, our reward is a theory that provides constructive proofs and implementable algorithms. Following this framework, we find that some ideas of classical analysis, as reproducing kernel Hilbert spaces and Green's functions yield very practical results for constructing interpolating and smoothing splines.

Chapter 7 contains applications and algorithmic implementations; here we apply the ideas developed in the former chapters to obtain concrete and explicit solutions to surface reconstruction. Here is shown the way in which variational methods are applied to interpolation of point clouds data and its solutions are obtained as linear combination of translates of radial basis functions, implementable as the solution of a linear system. The

ideas from distribution theory are combined with Hilbert space properties in a general abstract framework that includes (m,s)-splines and τ-splines.

In **chapter 8** we present general results for our proposed model, considering data with or without noise. The most interesting aspect is that these results provide general solutions in the form of radial functions that include two regularization parameters. In the same way, we obtain practical algorithms for interpolation and approximation of range data.

Finally in **chapter 9**, the properties and applicability of our models are analyzed using exact and noisy data. We use different criteria in order to find the best performer among a family of splines that resulted as a consequence our proposed model of regularization. We find that these splines fit the properties we are looking for, about the detection of local and global features in the data. From these splines only thin plate spline is well known. The analysis shows that our results are a good alternative for problems of reconstruction, performing equally well to TPS and better than it in complex situations (for example, noisy data), where models better than TPS are necessary. In **chapter 10** we make conclusions and future research.

1.7 Brief contents by chapter

Chap 1.　　　Statement of thesis problem and its relevance in engineering and science

Chap 2.　　　The state of the art and methods of surface reconstruction

Chap 3.　　　The key problem in terms of regularization theory

Chap 4.　　　Regularization theory in surface reconstruction

Chap 5.　　　The physical meaning

Chap 6.　　　The math tools

Chap 7.　　　Interpolation

Chap 8.　　　Smoothing

Chap 9.　　　Applications
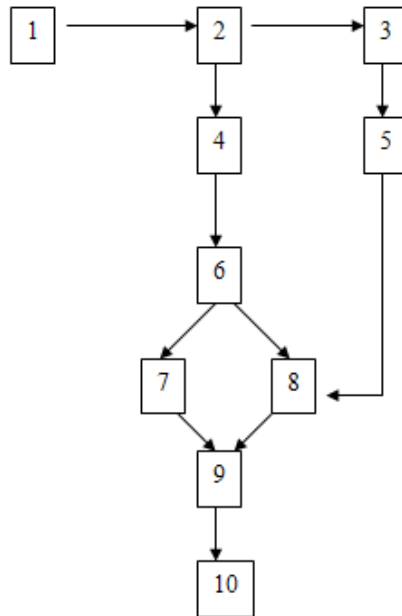
Chap 10.　　　Conclusions

Fig. 1.1 Structure of the chapters

The logical dependence of chapters (Fig. 1.1) can be used by different readers, in the following manner:

- Inverse problems applications: Chapters 1, 2,3,5,8

- Distribution theory and its applications: Chapters 6, 7, 8

- Applications of splines: Chapters 4,6,7,9

Chapter 2

Review and classification of methods for surface reconstruction

2. 1 Introduction

The computer graphics, computer-aided design and computer vision literatures are filled with an amazingly diverse array of approaches to surface description. The reason for this variety is that there is no single representation of surfaces that satisfies the needs of every problem in every application area.

Apart from being ill-posed, the problem of surface reconstruction from unorganized point clouds is challenging because the topology of the real surface can be very complex, and the acquired data may be non-uniformly sampled and contaminated by noise. Moreover, the quality and accuracy of the data sets depend upon the methodologies which have been employed for acquisition. Furthermore, reconstructing surfaces from large datasets can be prohibitively expensive in terms of computations.

Methods to digitize and reconstruct the shapes of complex three dimensional objects have evolved rapidly in recent years. The speed and accuracy of digitizing technologies owe much to advances in the areas of physics and electrical engineering, including the development of lasers, CCD's, and high speed sampling and timing circuitry. Such technologies allow us to take detailed shape measurements with precision better than 1 part per 1000 at rates exceeding 10,000 samples per second. To capture the complete shape of an object, many thousands, sometimes millions of samples must be acquired. The resulting mass of data requires algorithms that can efficiently and reliably generate computer models from these samples.

Surface reconstruction from unorganized data set is very challenging in three and higher dimensions. Furthermore the ordering or connectivity of data set and the topology of the real surface can be very complicated in three and higher dimensions. A desirable reconstruction procedure should be able to deal with complicated topology and geometry as well as noise and non-uniformity of the data to construct a surface that is a good approximation of the data set and has some smoothness (regularity). Moreover, the reconstructed surface should have a representation and data structure that is not only good for static rendering but also good for deformation, animation and other dynamic operation on surfaces. None of the present approaches possess all of these properties.

In general, surfaces can be expressed in an **implicit** or **explicit form**. An explicit form of a surface is the graph of a function of two variables.

Definition 2.1. Let $f : \Omega \subset \mathbb{R}^n \to \mathbb{R}$. The **graph** of f it is the subset of $\mathbb{R}^{n+1}$ consisting of the points $(x_1, \cdots, x_n, f(x_1, \cdots, x_n))$, for $(x_1, \cdots, x_n) \in \Omega$ an open subset of $\mathbb{R}^n$. In symbols

$$graph\, f = \{(x_1, \cdots, x_n, f(x_1, \cdots, x_n)) \in \mathbb{R}^{n+1} : (x_1, \cdots, x_n) \in \Omega\},$$

for the case $n = 1$ the graph is, intuitively speaking, a curve, while for $n = 2$, it is a surface. In the context of vision, the depth maps produced from stereo algorithm or a range finder can be interpreted as the sample data set from a surface in the explicit form $z = f(x, y)$, where z is the distance from the viewer to the object points in a scene and (x, y) are the image plane coordinates. The implicit form of a surface in $\mathbb{R}^3$ is expressed as the function

$$f : \mathbb{R}^3 \to \mathbb{R}; \ \ f(x, y, z) = \text{constant},$$

where (x, y, z) are the Cartesian coordinates of the surface points. Of course, the explicit form is a special case of the implicit equation. In fact, all surfaces in the explicit form can be transformed to an implicit form but not vice versa. Another useful representation of a surface is the parameterized form. A parametric surface in $\mathbb{R}^3$ is a smooth map $\mathbf{x} : \Omega \subset \mathbb{R}^2 \to \mathbb{R}^3$, where Ω is a connected open set in $\mathbb{R}^2$ such that $d\mathbf{x}_p$ has rank 2 for each $p \in \Omega$. In this way the surface Σ will be a set of points $\mathbf{x}$ of the form

$$\mathbf{x}(u_1, u_2) = (x_1(u_1, u_2), \ x_2(u_1, u_2), \ x_3(u_1, u_2)), \qquad (u_1, u_2) \in \Omega.$$

Explicit (boundary) representations describe the surface in terms of point connections, and traditional approaches are based on Delaunay triangulation and Voronoi diagrams [6,52]. Another well known explicit approach is a parametric surface description based on NURBS [140,149]. One example of surface-oriented solution, proposed in [140,90] is based on the computation of the signed Euclidean distance between each sample point and a linearly regressed plane that approximates the local tangent plane. Curless and Levoy [38] developed an explicit algorithm tuned for laser range data, which is able to guarantee a good rejection of outliers (points whose coordinates were not correctly acquired). Another well-known approach is the α-shape [53,54], which associates a polyhedral shape to an unorganized set of points through a parameterized construction.

Now we propose a classification for surface reconstruction methods. Our approach can be compared to previous works in the areas of shape representation, reconstruction, smoothing, and surface regularization. The large number of published methods requires a comprehensive classification, but it is nearly impossible to perform a perfect survey. We describe some of the most well-known approaches, with a bias towards those more closely related to our regularization framework.

2.2 Geometric methods

One of the key concepts in these methods is a triangular mesh, because it is obtained directly from the data; this is a simple representation of the topology of the object, but if other properties are required, a better representation is needed. In this context the problem of surface reconstruction can be stated as follows: Let Σ be a surface of object O, and assume that Σ is a smooth twice-differentiable two dimensional manifold, embedded in an Euclidian three-dimensional space $\mathbb{R}^3$. Given a discrete set of points

$$A = \{a_1, a_2, \ldots, a_M\} \subset \mathbb{R}^3,$$

that samples the surface Σ; find a surface Σ' that approximates Σ, using the data set A. The reconstructed mesh Σ' must be topologically equivalent to the surface Σ of the original object. In order to get this, a good idea is to take advantage of the different geometric viewpoints under which one can see an object and its surface. This is done studying properties that may be *local, intrinsic or global;* examples of these are respectively, *tangent planes, Gaussian curvature or Gauss-Bonnet theorem*. All the properties considered should be, sooner or later, discretizable in order to be applicable on point clouds

Geometric methods range from the simple but very useful triangular mesh to more sophisticated tools that come from fields such as algebraic topology or Differential geometry. These developments have conducted to a new branch of geometry – **discrete differential geometry** [22], whose aim is to develop discrete equivalents of the geometric notions and methods of classical differential geometry, where a surface Σ can be seen as a collection of points in $\mathbb{R}^3$.

A popular approach in computer vision is to reconstruct a triangulated surface using **Delaunay triangulations** and **Voronoi diagrams**. The reconstructed surface is usually a subset of the faces of the Delaunay triangulations. A lot of research has been done with this approach [52,90] and efficient algorithms have been designed to compute Delaunay triangulations and Voronoi diagrams. Although this approach is very versatile and can deal with general data sets, the constructed surface is only piecewise linear and it is difficult to handle non-uniform and noisy data. Recently, implicit surfaces or **volumetric representations** have been used most frequently in recent years for surface reconstruction from **point** clouds. These are based on well established algorithms of computer tomography like **marching cubes** and therefore are easily implemented. They produce approximated surfaces, so that error smoothing is carried out automatically. The method of Hoppe [90] is able to detect and model sharp object features. Curless and Levoy [38] can handle millions of data points. Levoy et al. [106] used this reconstruction method for their huge **Digital Michelangelo Project.**

The traditional approach [21,133,183] uses a combination of smooth basis functions such as blobs, to find a scalar function such that all data points are close to an isocontour of that scalar function. This isocontour represents the constructed implicit surface. However computation costs are very high for large data sets, since the construction is global which

results in solving a large linear system. The second approach uses the data set to define a signed distance function on rectangular grids and denotes the zero isocontour of the signed distance function as the reconstructed implicit surface [15,29]. The construction of the signed distance function uses a discrete approach and needs an estimation of local tangent planes or normals for the orientation, i.e. a distinction needs to be made between inside and outside.

Using the signed distance representation, many surface operations such as Boolean operations, ray tracing and offset become quite simple [139, 195]. Efficient algorithms [129,184], are available to turn an implicit surface into a triangulated surface. In [41] implicit surfaces are used for animation and the **level set method** is used for surface reconstruction from **range data** in [36]. In fact the level set method [201] provides a general framework for the deformation of implicit surfaces according to arbitrary physical and/or geometric rules.

Triangle meshes are so-called unstructured grids [193] and therefore it is not possible to use conventional modeling or signal processing methods like tensor product surfaces or linear filters. Unfortunately, no basic theory exists for handling unstructured data in order to estimate surface normals and curvature, interpolate curved surfaces, and subdivide or smooth triangle meshes. An approach for general meshes was proposed by Taubin [173]. He has generalized the discrete **Fourier transformation** by interpreting frequencies as eigenvectors of a discrete Laplacian. Defining such a Laplacian for irregular meshes allows to use linear signal processing tools like high and low pass filters, data compression and multiresolution hierarchies. However, the translation of concepts of linear signal theory is not the optimal choice for modeling geometry data. Surfaces of three-dimensional objects usually consist of segments with low bandwidth and transients with high frequency between them. They have no "reasonable" shape, as it is presupposed for linear filters. "Optimal" filters like Wiener or matched filters usually minimize the root mean square (RMS) error. Oscillations of the signal are allowed, if they are small. For visualization or milling of surfaces, curvature variations are much more disturbing than small deviations from the ideal shape. A smoothing filter for geometric data should therefore minimize curvature variations.

2.3 Statistical methods

Statistical methods explain data $D = \{(a_i, z_i) \in \mathbb{R}^n \times \mathbb{R}\}_{i=1}^{M}$ from a surface, with a stochastic model by considering that the observations z_i, constitute a realization of an stochastic process. Under this point of view the surface reconstruction problem is solved by finding the response $f(\mathrm{x})$ of an unknown function f at a new point $\mathbf{x}$ of a set Ω, from a sample of input-response pairs $(a_j, f(a_j))$ given by observation or experiment. Now the response z_j at a_j is not a fixed function of a_j but rather a realization of a random variable $Z(a_j)$. It is assumed that for each $\mathrm{x} \in \Omega$ there is a real-valued random variable $Z(\mathrm{x})$ which replaces f in the deterministic approach. The purpose is to get information about the expectation

$E(Z(\mathbf{x}))$ of $Z(\mathrm{x})$ with bounded positive variance $E\left\{[Z(\mathbf{x})-E(Z(\mathbf{x})]^2\right\}$. If $\mathbf{x}$ is close to $\mathbf{y}$ the random variables $Z(\mathbf{x})$ and $Z(\mathbf{y})$ will be correlated. This is described by a covariance kernel $\mathrm{cov}(\mathbf{x},\mathbf{y}) := E(Z(\mathbf{x})\cdot Z(\mathbf{y}))$.

The stochastic solution to ill-posed problems is a straightforward application of Bayesian interpretation of regularization [99]. In a Bayesian approach [188,18,119], the stabilizer corresponds to a smoothness prior, and the error term to a model of the noise in the data (usually gaussian and additive). Following Girosi *et al.* [70]; for surface reconstruction, it is supposed that $\mathrm{D}=\{(a_i,z_i)\in\mathbb{R}^n\times\mathbb{R}\}_{i=1}^M$ are noisy data obtained from sampling the function f, thus

$$f(a_i)=z_i+\varepsilon_i, \ i=1,\ldots,M, \tag{2.1}$$

where ε_i are random independent variables with a given distribution. The problem is to recover f or an estimate of it from the set of data D. f is the realization of a random field with a known prior probability distribution. The Bayesian interpretation find the function f which maximizes the conditional probability of the function f given D $P[f\,|\,D]$ by using Bayes rule

$$P[f\,|\,D]\propto P[D\,|\,f]\,P[f], \tag{2.2}$$

where $P[D\,|\,f]$ it is the conditional probability of D given f. $P[f]$ is the *a priori* probability of the random field f, and embodies the *a priori* knowledge of the function. Assuming the noise variables in equation (2.1) are normally distributed with variance σ then

$$P[D\,|\,f]\propto e^{-\frac{1}{2\sigma^2}\sum_{i=1}^M(f(a_i)-z_i)^2}.$$

Taking a model known in statistical physics it is defined $P[f]\propto e^{-\lambda R[f]}$, hence replacing in (2.2)

$$P[f\,|\,D]\propto e^{-\frac{1}{2\sigma^2}\sum_{i=1}^M(f(a_i)-z_i)^2+2\lambda H[f]}. \tag{2.3}$$

One estimate of the function f from the probability distribution (2.3) is the maximum a posteriori (MAP) estimate that maximizes the a posteriori probability $P[f\,|\,D]$ and therefore maximizes the exponent in (2.3). The MAP estimate therefore minimize the functional

$$\tau[f]=\sum_{i=1}^M(f(a_i)-z_i)^2+\lambda\,R[f], \tag{2.4}$$

which it is the well-known regularization model.

In statistical methods 3D objects can be represented by *regression models*. Fitting data to a model is a basic statistical tool that has been frequently used in computer vision. Objects in range images are simply represented by the *polynomial surface model*. With the estimated surface parameters, the range image analysis such as reconstruction and segmentation can be achieved easily. The model parameters are commonly estimated by the *least squares* (LS) method that yields optimum results for the Gaussian noise case. However, it becomes unreliable if non-Gaussian noise (e.g., impulse noise) is added. *Statistical approaches to surface parameter estimation* include robust estimators such as the *M-estimator*, least median of squares *(LMedS) method*, least trimmed squares *(LTS) method*, and so on [151,121,105].

Robust estimation techniques have been used to recover the parameters of a surface patch because they are robust to outliers. Outliers have values far from the local trend, resulting in a large measurement error. The local window size employed in a robust estimator is a user-specified parameter. The surface parameters are accurately estimated in a large homogeneous region whereas the estimation error becomes large near abrupt discontinuities. Thus, it is difficult to select a single optimal window size (resolution) that yields reliable parameter estimation results over an entire image. Optimal parameters, therefore, can be estimated in different applications by integrating the surface parameters obtained at various resolutions [138]. Range image reconstruction based on the estimated surface parameters can be regarded as a means of noise suppression. Noise that corrupts the range images is modeled by Gaussian and impulse noise mixture [101].

Waqar *et al*. [190] develop a technique based on nonparametric kernel density estimation to robustly filter a noisy point set which is scattered over a surface and contains outliers. Given a set 3D scattered points, a density function of the data is estimated, the main idea of this filtering approach consists on defining an appropriate density estimation to determine those cluster centers which deliver an accurate and smooth approximation of the sampled surface. Recently, robust statistics and statistical learning techniques have gained popularity in Computer Graphics and have been successfully applied to surface reconstruction [60,95, 160,169].

2.4 Regularization methods

Regularization methods are based in variational principles. Variational methods have been employed with considerable success in computer vision, particularly for surface reconstruction problems. Formulations of this type require the solution of computationally complex Euler–Lagrange partial differential equations (PDEs) to obtain the desired reconstructions. These methods have played an important role in the analytic formulation of most **early vision** problems [92,134,176,178]. Early vision has traditionally been considered as an array of special reconstruction methods operating on images. They include the reconstruction of 2-D image intensity gradient.and flow fields, as well as the reconstruction of 3-D surface depth, orientation, and motion fields. A broad range of visual reconstruction problems may be unified mathematically as well-posed variational principles. These can be characterized as optimal approximation problems involving a class of generalized multidimensional spline functionals [26-28,32,175].

Jean Duchon, a mathematician at the University Joseph Fourier in Grenoble, France, suggested a variational approach minimizing the integral of Δf, which also leads to the thin plate splines. This work was done in the mid 1970s and is considered to be the foundation of the variational approach to radial basis functions [47-50]. The method introduced by Duchon followed the ideas of Attéia [10] and Laurent [104], for the general theory of Hilbertian splines and involved a reproducing kernel. The reproducing kernel of Aronszajn [8] or the Hilbertian kernel of Schwartz [163] gives the explicit characterization of the (m,s) splines. It is widely known that the (m,s)-splines belong to a variety of radial basis functions which are conditionally positive definite functions [57,26,112,158].

Barrow and Tenenbaum [12] were among the first to introduce the surface reconstruction problem in vision. They implemented the solution for the interpolation of approximately uniformly curved surfaces from initial orientation values and constraints. The solution applies a relaxation algorithm that involves using an array of simple parallel processes performing iterative local averaging. This technique, although very simple, has many drawbacks. It does not deal with local and global properties, yields an interpolated surface that is not invariant to 3-D rigid motion, and is computationally inefficient.

The early work of Grimson [78,79] presents a theory of visual surface interpolation where range data is obtained from a pair of stereo images. The theory deals with determining a best-fit surface to a sparse set of depth values obtained from the Marr and Poggio [117] stereo algorithm. Grimson minimized what he called the quadratic variation E (1.5) of the surface $f(x,y)$

$$E = \iint_{\Omega} f_{xx}^2 + 2f_{xy}^2 + f_{yy}^2 \, dy \, dx \,, \tag{2.5}$$

where Ω is a region in the image plane at which the depth constraints are specified. This functional also happens to be a particular case of the seminorm we are using in this work and represents the energy of a thin plate [47-50]. The minimization yields the thin plate splines; this function was applied earlier by Schumaker [162] for interpolation of scattered 3-D data.

Grimson [78] developed an iterative algorithm based upon the biharmonic equation that results from applying Euler's equations to minimize E. His work does not apply to the general surface reconstruction problem since it did not deal with surface or orientation discontinuities. The reconstructed surface is invariant to image plane rotations and translations.

Boult and Kender [29] discuss an approach for visual surface reconstruction that is based on semireproducing spline kernels of Duchon [48]. Semireproducing kernel splines are defined in terms of the reproducing kernels for the semi-Hilbert space [8,10]. The major computational component of the method is the solution to a dense linear system of equations. The algorithm results in a true functional form of the surface allowing for symbolic manipulations (e.g., differentiation or integration). If the norm used in the problem is isotropic, then the kernel is rotation, translation, and scale invariant. Hence, the

reconstruction is invariant to such transformations applied to the data with respect to the image plane. Since the resulting linear system is dense and often indefinite, this limits the approaches that can be used in its solution.

Terzopoulos [174-178] pioneered finite-differencing techniques to compute approximate derivatives used in minimizing the thin-plate energy functional of a height-field. He developed computational molecules from the discrete formulations of the partial derivatives and uses a multi-resolution method to solve the surface. He presents a technique for visible surface computation from multiresolution images. His primary contribution was improved computational efficiency and also the integration of surface depth and orientation discontinuity information into the surface reconstruction problem. He used multigrid methods [178] to speed up his algorithm by orders of magnitude over the single grid approach. His surface reconstruction process treats surfaces of objects as thin plate patches bounded by depth discontinuities and joined by membrane strips along loci of orientation discontinuities. The description of the surfaces thus obtained is invariant to image plane transformations (rotations and translations in image plane) but not to three-dimensional rigid motion. The "controlled continuity stabilizer" in the functional that is minimized by Terzopoulos is similar to spline in tension.

Both Grimson [78] and Terzopoulos [176,177] used the standard discrete biharmonic operator or their surface reconstruction algorithms. Grimson used finite-difference methods while Terzopoulos used more general finite-element techniques.

In [142], Poggio and Torre suggest that the mathematical theory developed for regularizing ill posed problems leads in a natural way to the solution of early vision problems in terms of variational problems. They argued that this is a theoretical framework for some of the variational solutions already obtained in the analysis of early vision processes. Thus the computational ill posed nature of these problems dictates a specific class of algorithms for solving them, based on variational principles. They show that these variational principles follow in a natural and rigorous way from the ill posed nature of early vision problems.

In a series of papers [71-73], Girosi and coworkers established relations between the problem of function approximation and regularization theory. The approach regularizes the ill posed problem of function approximation from sparse data by assuming an appropriate prior on the class of approximating functions which follows the technique introduced by Tikhonov, identifying the approximating function as the minimizer of a cost functional that includes an error term and smoothness functional. They show that regularization principles lead to approximation schemes that are equivalent to networks with one hidden layer, called regularization networks. In particular, they described how a certain class of radial stabilizers-and the associated priors in the equivalent Bayesian formulation lead to a subclass of regularization networks, the already known radial basis functions network.

Recently, Turk [183] used variational surface and thin plate spline by specifying locations in 3D through which the surface should pass, and also identifying locations that are interior or exterior to the surface. A 3D implicit function is created from these constraints using a variational scattered data interpolation approach. They call the iso-surface of this function a variational implicit surface.

In [150] it is proposed a variational technique for reconstructing surfaces from a large set of unorganized 3D data points and their associated normal vectors. The surface is represented as the zero level set of an implicit volume model which fits the data points and normal constraints. The resulting model use explicit solutions in terms of radial basis functions. Gokmen and Li [76] presents an edge detection and surface reconstruction algorithm using regularization, in which the smoothness is controlled spatially over the image space but they only use one regularization parameter. Beatson *et al.* [14] apply a method for surface reconstruction from scattered range data by fitting a Radial Basis Function (RBF) to the data and convolving with a smoothing kernel (low pass filtering). These splines are a particular case of our approach.

There exist well known relations between regularization theory and other variational approaches. In [70] Girosi *et al.* show that regularization principles conduct to approximation schemes called regularization networks. In particular, standard smoothness functionals lead to radial basis functions. Additive splines as well as some tensor product splines can be obtained from appropriate classes of smoothness functionals. In the probabilistic interpretation of regularization, the different classes of basis functions correspond to different classes of prior probabilities on the approximating function spaces, and therefore to different types of smoothness assumptions.

Parallel to the problems of computer vision there has been a great development of variational approach and splines in surface reconstruction from the point of view of approximation theory. These developments have conducted to Radial basis function theory and meshfree methods [57,191]. Originally, the motivation came from applications in geodesy, geophysics, mapping, or meteorology. Later, applications were found in many other areas such as in the numerical solution of PDEs, computer graphics, artificial intelligence, statistical learning theory, neural networks, signal and image processing, sampling theory, statistics (kriging) and optimization.

Donald Shepard, suggested the use of what are now called Shepard functions in the late 1960s [165]. Rolland Hardy, who was a geodesist, introduced the so-called multiquadrics (MQs) in the early 1970s. Hardy's work was primarily concerned with applications in geodesy and mapping [85]. Robert L. Harder and Robert N. Desmarais [84] who were aerospace engineers at MacNeal-Schwendler Corporation (MSC Software), and NASA's Langley Research Center, introduced the thin plate splines in 1972. Their work was concerned mostly with aircraft design. Meinguet introduced what he called surface splines in the late 1970s. Surface splines and thin plate splines fall under what are called as polyharmonic splines [122-125].

Richard Franke [63,64], a mathematician at the Naval Postgraduate School in Monterey, California, compared various scattered data interpolation methods, and concluded MQs and TPSs were the best. Franke also conjectured that the interpolation matrix for MQs is invertible. Madych and Nelson proved Franke's conjecture based on a variational approach [105]. Charles Micchelli, also proved Franke's conjecture [126-128]. His proofs are rooted in the work of Bochner, from 1932 [23,24] and Schoenberg (from 1937) [158,159]; on positive definite and completely monotone functions. Grace Wahba, a statistician at the

University of Wisconsin, studied the use of thin plate splines for statistical purposes in the context of smoothing noisy data and data on spheres, and introduced the ANOVA and cross validation approaches to the radial basis function setting [186-189].

Robert Schaback, introduced compactly supported radial basis functions (CSRBFs) in [154], and a very popular family of CSRBFs was presented by Holger Wendland in his Ph.D. thesis [192] and in [191]. Both of these authors have contributed extensively to the field of radial basis functions for surface reconstruction [155,156].

Chapter 3

The seven intrinsic problems of surface reconstruction

3.1 Introduction

The recovery and representation of 3-D geometric information of the real world is one of the most challenging problems in computer vision research and its literature is filled with an amazingly diverse array of approaches to surface description. The reason for this variety is that there is no single representation of surfaces that satisfies the needs of every problem in every application area.

Apart from being ill-posed, the problem of surface reconstruction from unorganized point clouds is challenging because the topology of the real surface can be very complex, and the acquired data may be non-uniformly sampled or contaminated by noise. Moreover, the quality and accuracy of the data sets depend upon the methodologies which have been employed for acquisition. Furthermore, reconstructing surfaces from large datasets can be prohibitively expensive in terms of computations.

Commonly, reconstruction problems correspond to solving a compact operator equation. But compact operators cannot have a bounded inverse. This means that the problems we are dealing with are intrinsically ill-posed. In this chapter we study this and other difficulties that arise when considering surface reconstruction from scattered data.

3.2 The problems of surface reconstruction

Surface reconstruction shares a common structure with the rest of inverse problems in which the input-output relation in the operator equation $Af = z$, takes the form of a Fredholm integral operator of the first kind with $(A f)(s) = \int_a^b K(s,t) f(t)dt$, where $K(s,t)$ is called the kernel of the operator and represents a simplified model of the process. The assumption of linearity is very important, because in spite of the increasing power of computers, only in the case of linear problems it is possible to get a solution in almost real time for large scale problems. The source of great mathematical problem is that, on all three counts of Hadamard conditions, Fredholm integral equations of the first kind are ill-posed. These are compact operators, and then cannot have a bounded inverse [100,172,132].

We claim that these limit situations have an intrinsic nature; therefore we should look for, not a definite solution for them but for the best way to deal with them. Next, we study those which we consider the most critical **intrinsic problems** of surface reconstruction from scattered data giving a way to treat the problem using the properties of our regularization framework.

3.2.1 Reproduction-generalization dilemma

In surfaces reconstruction from scattered data $A = \{a_1, a_2, \ldots, a_M\}$, the resulting function f that models the surface should be such that it generalizes well, i.e. it should give practically useful values of $f(\mathbf{x})$ to new points $\mathbf{x} \notin A$. Furthermore, it should be *stable* in the sense that small changes in the training data do not change f too much. However, these goals are in conflict with good reproduction of data. Sometimes we could obtain a highly stable but useless model, while *over fitting* occurs if there is too much emphasis on data reproduction, leading to unstable models with bad generalization properties.

Problem: *Surface reconstruction is subject to the **reproduction-generalization dilemma** and need a careful balance between generalization and stability properties on one hand and data reproducing quality on the other.*

This is called the *bias-variance dilemma* under certain probabilistic hypotheses, but it also occurs in deterministic settings. This problem can be illustrated by the uncertainty principle in its multiple forms. For example, it is impossible for a signal f to be to be both band-limited and time-limited; that is, it is impossible for f and its Fourier transform f both to vanish outside a finite interval unless f is identically zero.

Solution: In our regularization approach (3.1), we treat the reproduction-generalization dilemma on surfaces, using one term for reproduction or fidelity to data and other for generalization, with two functionals (local and global) that handle different degrees of smoothness by tuning parameters λ_1 and λ_2 in the following scheme

$$\min_{f \in \mathfrak{F}} \boldsymbol{\tau}_{\lambda_1, \lambda_2, z_\delta} [f] = \underbrace{\frac{1}{M} \sum_{i=1}^{M} (f(a_i) - z_i)^2}_{\text{data reproduction}} + \underbrace{\lambda_1 R_1[f] + \lambda_2 R_2[f]}_{\text{Generalization}}. \qquad (3.1)$$

3.2.2 Restrictions on the choice of spaces

Problem: *Given a surface reconstruction problem from scattered data, there is not enough information to come up with a useful solution of the reconstruction problem. In particular, the simple numbers do not say how to define f or which space of functions to pick it from. We are facing an ill-posed problem with plenty of indistinguishable approximate solutions.*

Surface reconstruction problem requires minimum conditions in order to be well posed. This is done by working in a linear or vector space. There are also practical reasons for this, because:

- If the values $z_j = f(a_j)$, from the surface are multiplied by a fixed scalar factor α, then the new data should be recovered by the function αf instead of f.

- If data $z_j = f(a_j)$ and $z_j = g(a_j)$ at the same locations $A = \{a_1, a_2, \ldots, a_M\} \subset \mathbb{R}^n$ are recovered by functions f and g, respectively, then the data $f(a_j) + g(a_j)$ should be recovered by the function $f + g$.

But, from a practical point of view, all mathematical a-priori assumptions on f are useless if we are not taking the application into account. For example, if we take a linear subspace $\mathfrak{F}$ of dimension $M \geq 2$ of a space of multivariate functions in such a manner that $\mathfrak{F}$ does not depend on the set $A = \{a_1, a_2, \ldots, a_M\}$. There will always be a degenerated set Ω. It is to say, there exist a function $g \in \mathfrak{F}$, different from zero that vanishes on Ω. This is undesirable because we can add to the solution f, all the functions of the form αg, without altering the reproduction of data. Furthermore, the recovery process will have a non-unique solution and will be numerically unstable (see Mairhuber-Curtis theorem [191]).

Solution: To define the problem of surface reconstruction into functional spaces with data dependent inner products. We do this in chapter 7 (see formula 7.1). This is the reason for obtaining solutions in the subspace $\mathfrak{F}_{A,K} = \{\sum_{j=1}^{M} \alpha_j K(\mathbf{x}, a_j) : \alpha_j \in \mathbb{R}\}$.

3.2.3...The Curse of dimensionality

The curse of the dimensionality (term coined by Bellman in 1961 [16,17]) refers to the following

Problem: *in the absence of simplifying assumptions, the sample size needed to estimate a function of several variables to a given degree of accuracy grows exponentially with the number of variables.*

Let us say that we wanted to do a second-order polynomial fit. In 1D this is simply $y = a_0 + a_1 x + a_2 x^2$. In 2D, we have $y = a_0 + a_1 x + a_2 y^2 + a_3 x y + a_4 x^2 + a_5 y^2$, we have gone from three to six terms. In 3D we need ten terms:

$$y = a_0 + a_1 x + a_2 y + a_3 z + a_4 x y + a_5 x z + a_6 y z + a_7 x^2 + a_8 y^2 + a_9 z^3.$$

It is known that $\begin{pmatrix} k+n \\ n \end{pmatrix}$ is the dimension of $\Pi_k(\mathbb{R}^n)$, then as we increase the order of the polynomial, the exponent of the number of terms required increases accordingly.

Solution: If our problem is to approximate the surface f, by the solution $S(\mathbf{x})$ of the regularization problems (3.1). The solutions (as we proof in chapter 6) can be written as linear combinations of translates containing the original data, in the form

$$S(\mathbf{x}) = \sum_{j=1}^{M} \alpha_j K(\mathbf{x} - a_i), \qquad (3.2)$$

then, given the approximation error ε, with data $A = \{a_1, a_2, \ldots, a_M\} \subset \mathbb{R}^d$, in a d-dimensional space, we are looking for approximations with a degree of smoothness s such that

$$\| f - \sum_{j=1}^{M} \alpha_j K(\mathbf{x} - a_i) \| \leq \varepsilon_M. \qquad (3.3)$$

Usually [69], ε_M is such that $\varepsilon_M \propto \left(\dfrac{1}{M} \right)^{\frac{s}{d}}$. It is common to say that the curse of dimensionality is the d factor and the "blessing" of smoothness is the s factor. This means that fixing the dimension d of the surface, if we want to "beat the curse of dimensionality" we have to increase the smoothness degree s.

We do it into our approach, by defining regularization in functions spaces for which the rate of convergence to zero of the error ε_M is *independent of any number of dimensions* (see [69]). This avoidance of the curse of dimensionality is due to the fact that these functions are more and more constrained as the dimension increases. Examples include spaces of the *Sobolev* type, in which the number of weak derivatives (in the sense of Schwartz distributions) is required to be larger than the number of dimensions.

3.2.4 Noise

Problem: *Noise is ubiquitous in measured data.*

Noise it is a disturbance that affects a signal and that may distort the information carried by the signal. In the case of observational data, noise may have many sources including quantization and noise from image video systems. Important object features, such as corner points or edges are not directly recorded; instead, they have to be modelled from data in a separate process. In range sensor for point clouds, noise may have very high frequency due to measurement errors. Some reconstruction methods tends to smooth any high frequency feature such as corners and wrinkles that belongs to the geometry of the object creating inaccuracy in the reconstructed object. Many of the errors that are caused by the measuring process (noise, aliasing, outliers, etc.) can be filtered at the level of raw sensor data. A

special class of errors (calibration and registration errors) first appears after merging the different views.

Surface mesh models built using measurement data obtained using 3D range scanners necessarily contains some type of noise. To remove the noise in surface mesh models, many mesh denoising algorithms have been developed, for example [34,37,41,44,157] and other references therein. In evaluating the effectiveness of denoising algorithms both visual and numerical comparisons are used [170]. For meshes corresponding to real scanned data, however, we can in most cases only perform visual comparisons, because ground truth data required for evaluation are almost always unavailable. However, to provide a more objective evaluation and more through testing, numerical comparisons are required. Having synthetic models of real scanner noise would be useful for evaluating denoising algorithms. Any synthetic model used for evaluating denoising algorithms should take an exact model surface and add noise, which has to be removed by the algorithms. The noise should have the same characteristics as noise in real measurement data. Experimentally, measurement noise is often assumed to be Gaussian in a wide range of disciplines. Thus, various mesh denoising algorithms have been developed based on the Gaussian noise assumption [39], while others used synthetic models with Gaussian white noise (that is, independent Gaussian noise per mesh vertex) in evaluation of their algorithms [34,96,170,196,198].

Point datasets routinely generated by optical and photometric range finders usually are corrupted by noise. In order to remove these deficiencies from scanned point clouds, a large variety of denoising approaches based on low-pass filtering [110], MLS fitting [5,43,120] and partial differential equations (PDEs) [103] has been proposed.

A very important consequence of being ill-posed is that mathematical modelling of the surface reconstruction cannot uniquely consist in establishing the equations relating the data to the solution; it must also include a model of the noise perturbing the data and, as far as possible, a model of known properties of the solution. Then the data are a linear transform of an original signal f corrupted by noise, so that we have

$$z_i = Kf(a_i) + \varepsilon_i, \qquad\qquad (3.4)$$

where K is some known compact linear operator defined on a Hilbert space $\mathcal{H}$ and ε_i is a white noise with unknown variance σ^2. Since K is compact, the equation (3.3) cannot be directly inverted since K^{-1} is not a bounded operator.

Solution: The solution $S(\mathbf{x})$ to our regularization schemes (3.1) may be considered as the result of applying a low-pass filter to the data. In frequency space it can be shown that λ controls the half-power point of the filter and m (m refers to seminorm $J_m[f]$ in (1.3)) the steepness of the roll-off [189]. Further, under certain conditions the regularization functional $R[f] = J_m[f]$ can be written as $R[f] = \int |f(\xi)|^2 \|\xi\|^{2s} d\xi$. If this seminorm is defined in the Hilbert space associated with a kernel K and its Fourier transform $K(\xi) = \|\xi\|^{-2m}$, the seminorm reduces to the form

$$R[f] = \int_{\mathbb{R}^n} \frac{|f(\xi)|^2}{K(\xi)} d\xi, \qquad (3.5)$$

in this case $K(\xi)$ can be viewed as a low-pass filter [189,70], which plays a roll of smoothing in the sense that the solution surface f can be viewed as the convolution of the observation with a smoothing filter $f(\mathbf{x}) = z(\mathbf{x}) * B(\mathbf{x})$, where $*$ denotes the operation of convolution product and $B(\mathbf{x})$ is the inverse Fourier transform of $B(\xi)$ given by

$$B(\xi) = \frac{K(\xi)}{\lambda + K(\xi)}. \qquad (3.6)$$

When $\lambda = 0$ $f = z$, then $B(\xi) = 1, B(\mathbf{x}) = \delta(\mathbf{x})$, which corresponds to an interpolation problem in the noiseless situation [70].

3.2.5 Error bounds

Error estimates and error bounds are fundamental in any approximation process. Remember that the surface reconstruction problem pretends to recover the surface f from data $D = \{(a_i, z_i) \in \mathbb{R}^2 \times \mathbb{R}\}_{i=1}^M$. From this information is desired to compute another value $f(\mathbf{x})$. As it is usual in approximation theory, we are looking for an element S in a subset or subspace and then use $S(\mathbf{x})$ to approximate $f(\mathbf{x})$ with an error ε, such that

$$|f(\mathbf{x}) - S(\mathbf{x})|_{\mathfrak{F}} \leq \varepsilon. \qquad (3.7)$$

It is desirable to obtain an a priori measure of the error ε. But in general, the information we have about f is that f is an element of a known linear space of functions $\mathfrak{F}$; then the value $S(\mathbf{x})$ at a fixed point $\mathbf{x}$ is a linear combination $\sum_{i=1}^M \alpha_i f_i(\mathbf{x})$ of certain elements f_i of $\mathfrak{F}$.

Problem: *The intrinsic problem here is that it is **impossible** to give finite bounds for error, in terms of $f(a_1), \ldots, f(a_M)$, if the only additional information is that f is the element of a linear space $\mathfrak{F}$.*

Moreover, it can be demonstrated that it is impossible to obtain finite bounds for ε if the only **additional information** is that f is an element of $\mathfrak{F}$ (see [77]). This is true no matter how restricted the infinite-dimensional space $\mathfrak{F}$ is by conditions of continuity, differentiability, analyticity, and so on. Therefore is meaningless to speak of the goodness of a linear approximation without reference to some nonlinear constraint in $\mathfrak{F}$.

Solution: The variational properties of regularization method provide the additional information necessary for calculating bounds of the approximation error. The basic idea is to build a semi-inner product $(\, , \,)_{\mathfrak{F}}$, using data and the variational properties of regularization functionals (semi-norms), then using orthogonality properties and Cauchy-Schwarz inequality is possible to obtain error bounds in the form

$$
\begin{aligned}
|f - S|^2 &= (f - S, f - S)_{\mathfrak{F}} \\
&= (f, f - S)_{\mathfrak{F}} \le |f|_{\mathfrak{F}} \, \|f - S\|_2.
\end{aligned}
\tag{3.8}
$$

This is the most frequent method for obtaining error bounds in surface reconstruction methods (see [77,109,27,28]).

3.2.6   The Computational complexity

An important question about surface reconstruction is what the theoretical limitations are on the speed of interpolation and approximation algorithms. The computational complexity of any procedure or algorithm can be considered or expressed by means of a function $T(n)$ that gives its execution time in terms of the size n of the input.

Problem: *The tasks associated with reconstruction problems may have a very high computational complexity, including issues as amount of data, implemented algorithms, or the available hardware.*

In this thesis, we obtain interpolators with the form

$$
S_{\lambda}(\mathbf{x}) = \sum_{j=1}^{M} \alpha_j \Phi(\| \mathbf{x} - a_j \|) + p(\mathbf{x}),
\tag{3.9}
$$

where the basis functions $\Phi(\| \mathbf{x} - a_j \|)$ are the Green's functions of the Gram's operator associated with the stabilizer. If the stabilizer exhibits radial symmetry, the basis functions are radially symmetric as well and a radial basis function is obtained. M is the number of centers or points in the cloud. In order to find α_i, $i = 1, \ldots, M$, we have to solve the linear system

$$
\begin{bmatrix} A + \lambda I & P \\ P^t & 0 \end{bmatrix} \begin{bmatrix} \alpha \\ \beta \end{bmatrix} = \begin{bmatrix} z \\ 0 \end{bmatrix},
\tag{3.10}
$$

with
$A_{i,j} = \Phi(\| a_i - a_j \|), \quad i, j = 1, \cdots, M, P_{ij} = p_j(a_i), i = 1, \ldots, M, j = 1, \ldots, N, z = (z_1, \ldots, z_M),$
such that $\boldsymbol{\alpha} = (\alpha_1, \ldots, \alpha_M) \in \mathbb{R}^M, \boldsymbol{\beta} = (\beta_1, \ldots, \beta_M) \in \mathbb{R}^N$, and the polynomials $\{p_j\}_{j=1}^{N}$ form a basis for $\Pi_{m-1}(\mathbb{R}^n)$ (see chapters 6, 7 for more details).

The dimension of the linear system is equal to the number of centres M, giving a complexity $T(M) = O(M^3)$. If we consider that usually a point cloud may have one million centres or more, it is easy to imagine the huge number of floating point operations we are dealing with.

The interpolation matrix A is not sparse and, except for symmetry, has no obvious structure that can be exploited in solving the system. Solution via a symmetric solver will require $\dfrac{M^3}{6} + O(M^2)$ flops. Moreover, a single direct evaluation of expression (3.4) requires $O(M)$ operations.

Solution: There exists a diversity of solutions

- Simplify the data set reducing the number of centers a_i in order to make them computationally manageable (see [15,191]).

- The computation of some basis functions $\Phi(\| \mathbf{x} - a_j \|)$ require more floating point operations, so we could choose the most convenient.

- Fast methods for solving the interpolation matrix A and the evaluation of $S(\mathbf{x})$. For example, Beatson and Powell [14] proposed to use the smoothness of the interpolant and required the cardinality properties be satisfied at a small number of points in the domain. This method was further developed by the groups of Powell and Beatson for obtaining a fast method. The culmination of this work was an iterative Krylov subspace algorithm [59,80].

3.2.7 Local and global properties

Visual surfaces have both microscopic and macroscopic properties. A point cloud of an scanned surface may come from objects of different form and topology. So the shape of the surface varies from simple to a highly complex one, with rapid variations in the local surface orientation. This complexity can be measured with the derivatives of the surface. A surface that curves continuously, without breaks or creases and cusps will be referred to as a **regular surface**. More exactly, if $f : \Omega \subset \mathbb{R}^2 \to \mathbb{R}$ is a differentiable function in an open set Ω of $\mathbb{R}^2$, then the graph of f, that is the subset of $\mathbb{R}^3$ given by $(x, y, f(x, y))$ for $(x, y) \in \Omega$, is a regular surface. Regularity is measured by the smoothness degree of the surface. This is a hierarchical concept related to the order of continuity in the surface´s partial derivatives. Loosely speaking, the more continuous the derivatives, the smoother the surface.

Problem: *A surface reconstruction approach should be able to reproduce local and global behaviour of the surface.*

Given a set of scattered data $A = \{a_1, a_2, \ldots, a_M\}$ on a surface, there will be many possible surfaces consistent with these initial points. How do we distinguish the correct one? Mathematically, we need to be able to compare two possible surfaces, to determine which is "better". This can be done by defining a functional $R[f]$ from the space of all possible surfaces to the real numbers, so that comparing surfaces can be accomplished by comparing corresponding real numbers, provided $R[f] < R[g]$ whenever surface f is better than surface g. The best surface to fit through the known points is the one that minimizes $R[\cdot]$.

Solution: These functionals are chosen in such a way that permits different smoothness degree. One attractive formal characterization of smoothness is readily related to physical models, in particular we apply functionals coming from elasticity theory to deduce explicit expressions that performs local approximation and fits a global surface to initial data (see chapter 5).

Chapter **4**

Regularization and inverse theory in surface reconstruction

4.1 Introduction

In surface reconstruction one is faced with the task of discovering the nature of objects that produced the point cloud for the surface received by the camera. A proper computational formulation of these problems recognizes that they involve inverse processes that are mathematically ill-posed. This allows one to derive systematically, computational schemes based upon regularization theory that ensure existence of solution and stability of inversion process. Such approaches often suggest particular types of algorithms for efficient solution to the problems. The concepts of regularization theory give a comprehensive framework to formulation of the problems in vision: at all three levels of problem, algorithm, and implementation. Furthermore, the mathematical theory of regularization provides a useful theory for incorporating prior knowledge, constraints, and quality of solution.

4.2 Regularization and inverse problems.

In this section we show how regularization theory provides a framework for formulation of inverse problems of computer vision, in particular, surface reconstruction. A general formulation of inverse problems is that one is given the sensed data z, which is produced through the action of an operator A, acting upon the data, we wish to recover f from the operator equation

$$A f = z. \tag{4.1}$$

In surface reconstruction, f is a corrupted version of z and A is an integral operator that models the laser scanning process. A problem involving inversion of this operator is well-posed [82,179,132] if we can ensure existence, uniqueness, and stability of solutions.

For a variety of reasons, failure of one or more of these conditions is common and thus the problem is ill-posed. For example A may not be full rank (so that the solution is not unique - extra information may be required to restrict the solution space), or A may be invertible but ill-conditioned (thus small changes in data lead to large deviations in solution - which

can be disastrous in the presence of noise), or A may be of rank greater than the number of degrees of freedom (the system is over-determined and thus a solution may not exist if any of the measurements contains noise).

Additional constraints and assumptions restrict the solution space, but in the presence of noise, the problem can become ill-posed in either of the last two senses. Standard regularization theory provides mathematical tools that enable one to turn an ill-posed problem into a well posed problem.

4.3   Ill-posed problems and regularization

From the point of view of modern mathematics, all problems can be classified as being either correctly posed or incorrectly posed. In the language of functional analysis, this fact can be stated in the following manner.

Let $\mathcal{X}$ and $\mathcal{Y}$ be Banach spaces and the continuous operator $A:\mathcal{X} \to \mathcal{Y}$ (not necessarily linear). The equation $A f = z$, represents a correct, correctly posed or **well-posed** problem in the sense of Hadamard if the operator A has a continuous inverse $A^{-1}:\mathcal{Y} \to \mathcal{X}$. In other words

(**wp1**) Exists a solution: $\forall z \in \mathcal{Y}$ there exists a solution $f \in \mathcal{X}$.

(**wp2**) The solution is unique: $\forall z \in \mathcal{Y}$ there is no more than one $f \in \mathcal{X}$ such that $A f = z$.

(**wp3**) The solution f^* depends continuously on the data: $\| f - f^* \|_{\mathcal{X}} \to 0$ when $\| z - z^* \|_{\mathcal{Y}} \to 0$.

If one of these three conditions is not satisfied, the problem $A f = z$ is called ill-posed. Given that we want to find f given z it is also called **ill-posed inverse problem**.

These conditions do not have the same degree of importance [94]. If the uniqueness condition (**wp2**) is not satisfied then the problem does not make sense. However, if (**wp1**) is not satisfied, it only means that there are not conditions to guarantee existence of a solution. On the other side, one may think (as Hadamard did) that without (**wp3**) the problem $A f = z$ does not have physical sense and is incomputable. Nevertheless, choosing a proper notion of convergence and the space $\mathcal{X}$, it is possible to fix the situation. For instance $\mathcal{X}$ and $\mathcal{Y}$ may be taken from the classical spaces $C^k(\mathbb{R}^n)$ or $W^{m,p}(\mathbb{R}^n)$. These spaces are a natural setting for mathematical physics and partial differential equations. They reflect physical reality and generate stable computational algorithms.

Now we will deal with Tikhonov regularization. The main idea supporting this approach [100] is that the solution of an ill-posed problem can be obtained using a variational

principle, which contains both the data and prior smoothness information. For the stable approximation of a solution of the operator equation $Af = z$; where it is assumed that only noisy data z_δ of the exact data z are available. Tikhonov or variational regularization propose to minimize a functional in the general form

$$\tau_{\lambda, z_\delta} = \rho[Af, z_\delta] + \lambda R[f], \qquad (4.2)$$

only assuming that ρ is a functional measuring the error between Af and z_δ, $\lambda > 0$ and $R[\cdot]$ is a nonnegative functional. The real number λ is called regularization parameter. The idea is to find a solution for $Af = z$ as an element minimizing the functional (4.5). One may think that this element is $\|Af - z\|$, but it does not work because is equivalent to (4.4) and therefore will also be ill-posed. Another idea could be to use Moore-Penrose generalized inverse $f^\dagger = A^\dagger z$, defined as the minimum norm solution of the problem $\min_{f \in \mathcal{X}} \|Az - z_\delta\|_{\mathcal{X}}^2$. However the operator $A^\dagger$ is usually not bounded. The viewpoint of regularization is to use the "improved" functional τ_{λ, z_δ}.

4.4 Surface reconstruction as an inverse problem

The original idea of regularization is to replace an ill-posed Fredholm integral equation of the first kind

$$\int_0^1 K(s,t) f(t) dt = z(s),$$

by a nearby well-posed Fredholm integral equation of the second kind. Here $f(t)$ is the unknown function and $K(s,t)$ is the **kernel** of the operator.

In abstract features this equation may be written in operator form as $Af = z$, where A is a linear integral operator such that $Af(s) = \int_a^b K(s,t) f(t) dt$.

Let A_x be the integral operator with $A_x f = f(x)$. In a point cloud $D = \{(a_i, z_i) \in \mathbb{R}^n \times \mathbb{R}\}_{i=1}^M$ we have noisy data that can be modeled as

$$z_i = A_{a_i}(f) + \varepsilon_i = \int_a^b K(a_i, t) f(t_i) dt + \varepsilon_i, \quad i = 1, \ldots, M. \qquad (4.3)$$

This is a discrete (noisy) Fredholm integral equation of the first kind. In vector form we will denote $z = (z_1, z_2, \ldots, z_M)$, such that

$$z = A_M f + \varepsilon, \quad \text{where} \quad (A_M f)_i = \int_a^b K(a_i, t) f(t_i) dt. \quad (4.4)$$

Commonly, the errors $\{\varepsilon_i\}$ are i.i.d. (independent and identically distributed) random variables from a normal distribution $N(0,\sigma^2)$ (see [188]).

4.5 Regularization of surface reconstruction

Let $\mathcal{X}$ and $\mathcal{Y}$ be two Hilbert spaces and $A:\mathcal{X}\to\mathcal{Y}$ a linear bounded operator. The Tikhonov regularization scheme [132,142,184] is given by

$$\min_{f\in\mathcal{X}}\boldsymbol{\tau}_{\lambda,z_\delta} = \| Af - z_\delta \|^2_\mathcal{Y} +\lambda \| f \|^2_\mathcal{X} . \tag{4.5}$$

Observe that in general, the spaces $\mathcal{X},\mathcal{Y}$ have different metrics. Now, we adapt this framework to the particular case of surface reconstruction. Let $\mathcal{X}$ be a reproducing kernel Hilbert space [8,188] with continuous kernel $K:\Omega\times\Omega\to\mathbb{R}$. If $\mathbf{x}\in\Omega$, we let $K_\mathbf{x}(\mathbf{s})=K(\mathbf{s},\mathbf{x})$ and by the Riesz representation theorem[100,104,152], define the bounded linear operator

$$(Af)(\mathbf{x}) = (f,K_\mathbf{x})_\mathcal{X} = f(\mathbf{x}). \tag{4.6}$$

Given the data $\mathrm{D} = \{(a_i,z_i)\in\mathbb{R}^n\times\mathbb{R}\}^M_{i=1}$, from a point cloud, we obtain a discretized version $A_\mathbf{x}:\mathcal{X}\to\mathbb{R}^M$ of A in the following way

$$(A_\mathbf{x}f)_i = (f,K_{a_i})_\mathcal{X} = f(a_i), \tag{4.7}$$

where $\mathcal{Y}=\mathbb{R}^M$, has the inner product $(\mathbf{z},\mathbf{z}')_{\mathbb{R}^M} = \dfrac{1}{M}\sum_{i=1}^M z_i z_i'$. Then it is straightforward to see that

$$\| A_\mathbf{x}f - \mathbf{z} \|^2_{\mathbb{R}^M} = \frac{1}{M}\sum_{i=1}^M (f(a_i) - z_i)^2, \tag{4.8}$$

Using this setting, we see surface reconstruction as the minimization of the functional $\boldsymbol{\tau}_{\lambda,z_\delta}$, given by

$$\min_{f\in\mathcal{X}}\boldsymbol{\tau}_{\lambda,z_\delta}[f] = \| A_\mathbf{x}f - \mathbf{z} \|^2_{\mathbb{R}^M} + \lambda R[f]$$

$$= \frac{1}{M}\sum_{i=1}^M (f(a_i) - z_i)^2 + \lambda R[f], \tag{4.9}$$

where

$$R[f] = \int_{\mathbb{R}^n}\sum_{|\alpha|=m}\frac{m!}{\alpha!}|\partial^\alpha f(\mathbf{x})|^2 d\mathbf{x}.$$

35

4.5.1 Interpolation and approximation by regularization

It is a well-known fact that the classical methods of interpolation (Lagrange polynomials, for example) have serious problems for fitting data from real problems. Given a set of knots there exist many ways to interpolate them, so in order to choose one is necessary to add more information other than the knots. Cubic splines were one of the first successful answers to this problem, adding the requirement of a smoothing functional.

Depending on the origin of data and kind of application, it is possible to do interpolation ($S(\mathbf{x}) = f(\mathbf{x})$) or approximation ($S(\mathbf{x}) \approx f(\mathbf{x})$). For example, some range scanners data are accurate enough for obtaining good results using interpolation, but if we are going to interpolate noisy data, the advisable way is to make approximation on the data. We may state both problems in terms of regularization over a function space $\mathcal{X}$.

P1. *Interpolation problem*

$$\min_{f \in \mathcal{X}} R[f], \qquad \text{with } \{f(a_i) = z_i\}_{i=1}^{M}. \qquad (4.10a)$$

P2. *Smoothing problem*

$$\min_{f \in \mathcal{X}} \tau_{\lambda, z_\delta} = \frac{1}{M} \sum_{i=1}^{M} (f(a_i) - z_i)^2 \; + \; \lambda R[f], \text{ with } \quad \{f(a_i) \approx z_i\}_{i=1}^{M}. \qquad (4.10b)$$

4.5.2 Proposed model

Finally, we extend the approach (4.6) considering two regularization functionals R_1 and R_2 in the form

$$\min_{f \in \mathcal{X}} \tau_{\lambda_1, \lambda_2, z_\delta} [f] = \frac{1}{M} \sum_{i=1}^{M} (f(a_i) - z_i)^2 \; + \; \lambda_1 R_1[f] + \lambda_2 R_2[f]. \qquad (4.11)$$

The idea is to integrate local and global features of the surface or phenomenon in order to obtain models that fit the three requirements for surface reconstruction. The first term is controlling fidelity to data and functionals R_1, R_2 are properly combined for handling the degree of smoothness or generalization by tuning parameters λ_1 and λ_2. This is one of the most important properties of regularization approach, that is, the possibility to add *a priori* knowledge about the model in the form of functionals, into an integrated variational approach.

Chapter **5**

Regularization functionals and their physical interpretations

5.1 Introduction

At first glance, it seems to be impossible to compute the solution of a problem numerically if the solution does not depend continuously on the data, i.e., for the case of ill-posed problems. Under additional a priori information about the solution, such as smoothness and bounds on the derivatives, however, it is possible to restore stability and construct efficient numerical algorithms.

The main purpose of this chapter is to develop some criteria for choosing smoothing or regularization functionals $R[f]$. In order to do a heuristic discussion we consider the behaviour of curves and surfaces under geometrical criteria, as for instance, Gaussian and mean curvature as well as physical criteria, based on continuum mechanics.

Fig. 5.1: Dirac deltas do exist, don't they? (La Ferté pedestrian bridge in Stuttgart, Germany) [86].

Using the ideas of variational calculus we show the strong relationship between regularization and the physical realities represented by classical partial differential operators of mathematical physics. It is also important to take into account more subtle

mathematical properties in the functionals in order to produce solvable minimization problems and according to the reality of data.

5.2 Plate and membrane models

Variational calculus is the most reliable guide for dealing with the partial differential equations of mathematical physics. The models we will use as criteria for choosing regularization or smoothing functionals comes originally from continuum mechanics, in particular elasticity theory. An elastic body is defined to be a solid which, once deformed will revert to its original shape if the forces causing the deformation are removed. These problems of stable equilibrium, are governed by the variational principle of minimal potential energy:

A mechanical system with the potential energy $U(q_1, q_2, \ldots, q_n)$ is in equilibrium at a particular set of values of the coordinates $q_1, q_2, \ldots, q_n$ if and only if the potential energy is stationary for this set of values.

An example in one dimension is the vibrating string and in further dimensions the **plate and membrane** models. They have shown to be very useful for modeling and reconstruction of surfaces. A **membrane** [86,87,181,176] is a portion of a surface, plane at rest, with potential energy proportional to change in area; the proportionality factor is known as tension. Now, suppose that the membrane at rest covers a region Ω of the plane and that the deformation $f(x, y)$ is normal to the equilibrium plane. Suppose this deformation is small in the sense that higher powers of the partial derivatives f_x, f_y of f are negligible compared with lower ones. Then the expression $\iint_\Omega \sqrt{1 + f_x^2 + f_y^2}\, dy\, dx$ for the area may be replaced by $\iint_\Omega [1 + \frac{1}{2}(f_x^2 + f_y^2)]\, dy\, dx$ and the potential energy by $\frac{1}{2}\iint_\Omega (f_x^2 + f_y^2)\, dy\, dx$.

For the equilibrium problem of the membrane we suppose that the displacement $f(x, y)$ of the membrane have prescribed values on its boundary and that no external forces act on the membrane, then the equilibrium position is characterized by the following variational problem.

The displacement $f(x, y)$ in the equilibrium position is the function for which the potential energy functional

$$R[f] = \iint_\Omega (f_x^2 + f_y^2)\, dy\, dx, \qquad (5.1)$$

attains the least possible value among the functions which are continuous in the closed set Ω , take on the prescribed boundary value, and possesses continuous first and piecewise continuous second derivatives in the interior. Observe that the functional (5.1) is the

Duchon seminorm $R[f] = J_m[f] = \int_{\mathbb{R}^n} \sum_{|\alpha|=m} \frac{1}{\alpha!} |\partial^\alpha f|^2$ in $\mathbb{R}^2$ with $m=1$. When $m=2$, we obtain the elastic potential energy of a plate.

A **plate** is the body $\Omega \times]-\frac{h}{2}, \frac{h}{2}[$ of thickness h, that occupies the region Ω in $\mathbb{R}^2$, one of its dimensions, in the z direction, say, is very smaller than the other two, so that geometrically the plate is flat.

If for the equilibrium problem of the plate we suppose similar conditions to membrane problem, then the displacement $f(x, y)$ in the equilibrium position is the function which minimize the potential energy functional

$$J_2[f] = \int_{\mathbb{R}^2} (\frac{\partial^2 f}{\partial x^2})^2 + 2(\frac{\partial^2 f}{\partial x \partial y})^2 + (\frac{\partial^2 f}{\partial y^2})^2 \, dx\, dy \, .$$

The governing equation for the deflection of an elastic thin plate is

$$D\Delta^2 f = g \, ,$$

where $\Delta^2 = \frac{\partial^4}{\partial x^4} + 2\frac{\partial^4}{\partial x^2 \partial y^2} + \frac{\partial^4}{\partial y^4}$, is the biharmonic operator, D is called the bending stiffness; depends on the material and the geometry, and is defined by $D = Eh^3/12(1-\gamma^2)$, where E and γ are constants known respectively as Young's modulus and Poisson's ratio [147].

(a)   (b)
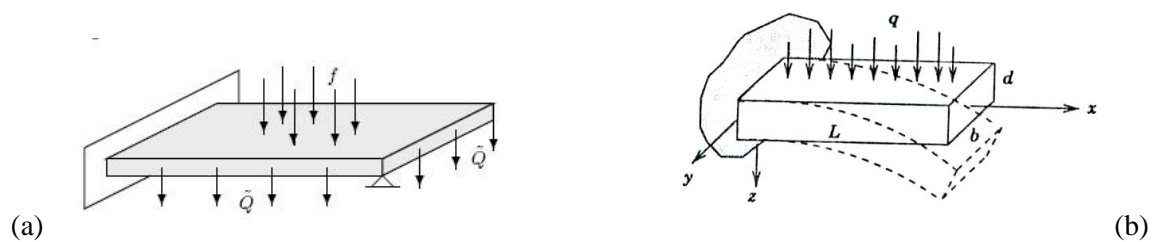
Figure 5.2: (a) Plate and (b) beam are classical models that have inspired variational theory of splines.

The one-dimensional version of plate model is the deflection of a beam. A beam is a body rectilinear in shape and whose length is considerable greater than its two other dimensions. We want to find the in-plane deflection f of the beam (fig.5. 2) while subject to a force of intensity g per unit length. The beam has length L, width b and depth d; b and d are assumed to be much smaller than its length. The governing equation for deflection of the beam is

$$EI \frac{d^4 f}{dx^4} = g(x),$$

where E: modulus of elasticity, I: moment of inertia of a cross section about the neutral axis [153,87,153].

The beam model explains the original idea of splines. The term spline is derived from the analogy to a draughtsman's approach to pass a thin metal or wooden strip through a given set of constrained points called ducks (fig 5.3).

(a)   (b)
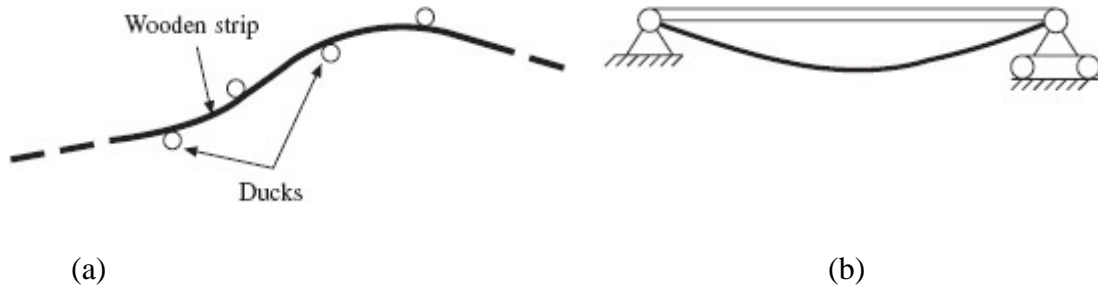
Figure 5.3: Physical interpretation of one dimensional cubic spline [153].

We can imagine any segment between consecutive ducks (fig. 5.3 (b)) to be a thin simply supported beam across which the bending moment varies linearly. Applying the linearized Euler-Bernoulli beam equation for small deformations

$$EI\kappa = EI \frac{d^2 f}{dx^2} = Ax + B \ .$$

Where EI is the flexural rigidity of the beam, κ the curvature, A and B known constants. Solving for the deflection yields a cubic polynomial

$$f = \frac{A}{6EI} x^3 + \frac{B}{2EI} x^2 + C_1 x + C_2 .$$

In general [35,188], this cubic spline has the form

$$S(x) = \sum_{i=0}^{M} \alpha_i (x - a_i)_+^3 + \beta_0 + \beta_1 x,$$

and minimize the functional $R[f] = \int_a^b (f")^2$. This is an approximation to the total curvature of the curve, because if in the formula

$$k = \frac{f"}{\sqrt{(1 + f'^2)^3}},$$

for the curvature of the curve $(x, f(x))$, we consider f' small, then $k \approx f"$ and $R[f]$ approximates the total curvature $\int_a^b k^2(x) dx$, of the curve.

40

5.3 Weak formulation

There exist a very close relationship between differential equations and variational problems. Many of the PDE of mathematical physics and applied mathematics are in fact the Euler-Lagrange equations for the minimum of some functional. Laplace's equation

$$\Delta f = f_{xx} + f_{yy} = 0,$$

 is the Euler-Lagrange equation for the potential energy functional of the membrane,

$$R[f] = \iint_{\Omega} |\nabla f|^2 \, dydx = \iint_{\Omega} (f_x^2 + f_y^2) \, dy \, dx,$$

called the Dirichlet integral. If we consider the Dirichlet boundary value problem for the Poisson equation

$$\begin{cases} -\Delta f = g & in \ \ \Omega \subset \mathbb{R}^2 \\ f = 0 & on \ \ \partial\Omega \end{cases}, \tag{5.2}$$

with $g \in C(\Omega)$, the desired classical solution of this equation belongs to $C^2(\Omega)$ and vanishes on $\partial\Omega$. Multiplying eq. (5.2) by an arbitrary function φ with compact support (i.e. $\varphi = 0$ on $\partial\Omega$) we have $-\int_{\Omega} \varphi \Delta f = \int_{\Omega} \varphi g$. Then, using integration by parts

$$-\int_{\Omega} \varphi \Delta f = \int_{\Omega} \nabla \varphi \cdot \nabla f - \int_{\partial\Omega} \varphi \frac{\partial f}{\partial \hat{n}} \, dS = \int_{\Omega} \varphi g,$$

we obtain

$$\int_{\Omega} \nabla \varphi \cdot \nabla f = \int_{\Omega} \varphi g \ \ \forall \varphi \in C_0^{\infty}(\Omega).$$

This is equivalent to finding $u \in H_0^1(\Omega)$ such that using L_2 - inner product

$$(\nabla \varphi, \nabla f) = \langle g, \varphi \rangle \ \ \forall \varphi \in H_0^1(\Omega). \tag{5.3}$$

This is called the **variational or week form** of equation 5.2, which in contrast is called strong form. In the next chapter we treat its relation with Schwartz distribution theory.

5.4 Fundamental solutions

Given that our central problem is the reconstruction from scattered data, we will need physical interpretations of operator equations in the form $Pf = g$, where P is a partial differential operator, and g may be Dirac's delta δ . If in the plate problem g represents the force acting on the plate then $g = \delta$ represents a point load acting at $\mathbf{x} = 0$ and the corresponding equation is

$$\Delta f = \delta.$$

Historically, depending of the kind of application, the solutions to $P(D) = \delta$ have taken different names: impulse response, Green's functions or fundamental solution.

The point- force Green function $K(\mathbf{x})$ for a spline in tension must satisfy

$$D\Delta^2 K(\mathbf{x}) - T\Delta K(\mathbf{x}) = \delta,$$

where Δ^2 and Δ are the biharmonic and Laplace operators, respectively. The general situation of M data constraints $f(a_i) = z_i$ at the locations $A = \{a_1, a_2, \cdots, a_M\} \subset \mathbb{R}^n$, results (using distribution theory) in the equation

$$D\Delta^2 f(\mathbf{x}) - T\Delta f(\mathbf{x}) = \sum_{i=1}^{M} \alpha_i \, \delta(\mathbf{x} - a_i),$$

with solution (see chapter 7)

$$f(\mathbf{x}) = \sum_{i=1}^{M} \alpha_i K(\mathbf{x} - a_i). \qquad (5.4)$$

5.5 Criteria for selection of regularization functionals

In general any functional able to measure the amount of rapid variations of the surface (that is, the amount of variation in the local surface orientation) could be used as stabilizer $R[f]$. This suggests that this functional should measure some factor of the second −order derivative of the surface. Although every requirement restricts the number of possible regularization functionals, we would also like

- Functionals that measure local and global features.
- Rotation invariant functionals.
- Functionals with geometrical or physical interpretation.
- Functionals that fit certain mathematical requirements.

All the requirements are hard to fulfill. There are very complicated functionals that yield surfaces of high quality. But the minimization procedure is very costly or simple functionals that do not lead to good surfaces.

Then, thinking **geometrically,** one possibility is to measure the curvature of the surface, which implicitly reflects variation in surface orientation. It may be used mean curvature H or Gaussian curvature K. They both depend on the principal curvatures k_1 and k_2 (see [22,45,136]). At any point of the surface there exists an infinite number of normal sections that is, planes that intersect the surface containing the normal vector of the surface and defining curves over the surface. There are two sections of particular interest, one with maximum curvature and other with minimum curvature. It can be shown that the directions

corresponding to these two curves are orthogonal. These directions are called the principal directions and the curvatures of the corresponding sections are the principal curvatures

$$K = k_1 k_2, \qquad\qquad H = k_1 + k_2.$$

For a surface in the form $(x, y, f(x, y))$, these curvatures are given by

$$H = \frac{\partial}{\partial x}\left(\frac{f_x}{\sqrt{1 + f_x^2 + f_y^2}}\right) + \frac{\partial}{\partial y}\left(\frac{f_y}{\sqrt{1 + f_x^2 + f_y^2}}\right),$$

and

$$K = \frac{f_{xx} f_{yy} - f_{xy}^2}{(1 + f_x^2 + f_y^2)^2}.$$

We may define regularization functionals that takes measures over the whole surface in the form

$$R_1[f] = \iint H^2\, dy\, dx$$

$$= \iint \frac{[f_{xx}(1 + f_y^2) + f_{yy}(1 + f_x^2) - 2 f_x f_y f_{xy}]^2}{(1 + f_x^2 + f_y^2)^3}\, dy\, dx.$$

If f_x and f_y are assumed to be small, then

$$R_1[f] \approx \iint (f_{xx} + f_{yy})^2\, dy\, dx = \iint (\Delta f)^2\, dy\, dx. \qquad (5.5)$$

Assuming similar conditions we can define other functional

$$R_2[f] = \iint K^2\, dy\, dx \approx \iint (f_{xx} f_{yy} - f_{xy}^2)\, dy\, dx. \qquad (5.6)$$

Note that R_1 and R_2 are both functionals containing second order derivatives. The relation with the regularization functionals used in this thesis is the following:

Physically we may think in energy functionals. Thin plate energy functional has an exact and simple version

$$E_{exact} = \int_\Omega (k_1^2 + k_2^2)\, dS,$$

$$E_{simple} = \int_\Omega f_{xx}^2 + 2 f_{xy}^2 + f_{yy}^2\, dy\, dx,$$

From the physical point of view represents the bending energy of a thin plate having the shape of the surface represented by f. When this surface is not very complex, E_{simple} is a good approximation to E_{exact}. Since E_{simple} is quadratic, is much easier to minimize than the highly non linear functional E_{exact} which may also be written as

43

$$E_{exact} = \int_\Omega a(k_1^2 + k_2^2) + 2(1-b)k_1 k_2 \ dS \,,$$

where a,b are constants describing properties of the material (resistance to bending and sheering).

5.6   The Resolution of the functional

In general, it is extremely difficult to find a functional that measures surface consistency and satisfies the conditions of an inner product. Hence if the regularization functional $R[f]$ comes from a semi-inner product on a semi Hilbert space of possible surfaces, then the most consistent surface is unique up to possibly an element of the null space $\mathcal{N}$ of the functional. The null space is simply the set of surfaces that cannot be distinguished by the functional from the surface that is zero everywhere. It is to say, we can consider a vector space $\mathcal{X}$ of functions with seminorm $|f|_{\mathcal{X}}$ and null space

$$\mathcal{N} = \{\, u \in \mathcal{X} : |u|_{\mathcal{X}} = 0 \},\qquad\qquad (5.7)$$

that induces a normed space $\mathcal{X}/\mathcal{N}$, called the quotient space. The induced norm on $\mathcal{X}/\mathcal{N}$ is clearly well-defined and is given by:

$$|f + N|_{\mathcal{X}} = |f|_{\mathcal{X}}.\qquad\qquad (5.8)$$

This means that we can study our problems on the space $\mathcal{X}/\mathcal{N}$ in order to use the properties of norms.

Based on the form of the null space, we can determine whether or not the differences in minimal surfaces are intuitively indistinguishable. Then this criteria that may be used to determine the "best" functional, using the size of the null space, since this determine the resolution of the functional, that is, the level at which the functional cannot distinguish between two different surfaces. For example, it is better to use the quadratic variation

$$R[f] = \int_{\mathbb{R}^n} \sum_{|\alpha|=m} \frac{m!}{\alpha!} |\partial^\alpha f(\mathbf{x})|^2 d\mathbf{x} \,,$$

because is unable to distinguish between two different surfaces only when they differ by a plane, while the square Laplacian in the functional $\int_{\mathbb{R}^n} (\nabla^2 f)^2$ cannot distinguish between two surfaces differing by any harmonic function. It is to say, the null space on the first functional is smaller than the second one.

5.7 Adding more functionals

To illustrate the way these physical interpretations may help our understanding and analysis of surface reconstruction, let us consider the interpolation problem. The idea in this case is to choose a proper condition added to the interpolation constraints $f(a_i) = z_i$ in order to obtain a well-posed problem. Let us suppose we have a thin plate of a flexible material, plane when no external force is applied on it and we impose the condition of crossing the points represented by data $D = \{(a_i, z_i) \in \mathbb{R}^2 \times \mathbb{R}\}_{i=1}^M$.

In equilibrium, the plate tends to form a smooth surface. It is a well-known fact that the plate minimizes its potential energy, which is expressed up to certain degree of approximation minimizing the TPS functional

$$R_1[f] = \int_{R^2} [(\frac{\partial^2 f}{\partial x^2})^2 + 2\,(\frac{\partial^2 f}{\partial x \partial y})^2 + (\frac{\partial^2 f}{\partial y^2})^2]\, dy\, dx\,.$$

The interpolant satisfying these conditions is the well known Thin Plate Spline. This model is very suitable for certain cases, but arise some problems when we have regions with rapid change of gradients in the modelled phenomenon. Physically this may be interpreted as the resistance of the plate to be stressed beyond its flexibility. This resistance of the plate may be avoided taking a more general model minimizing the functional

$$R[f] = R_1[f] + \lambda_1 \int_{R^2} [(\frac{\partial f}{\partial x})^2 + (\frac{\partial f}{\partial y})^2]\, dy\, dx, \tag{5.9}$$

where $\lambda_1 \geq 0$ is a regularization coefficient. When $\lambda_1 \rightarrow 0$, we again obtain the TPS model. On the other side, if $\lambda_1 \rightarrow \infty$ the resulting spline represents the surface, being not a plate but an elastic membrane (rubber sheet) crossing the interpolation points. This membrane overcomes the difficulties of TPS. The solution to (5.9) may be interpreted as a thin plate with tension applied on its boundaries and it is called **spline with tension** [27,63]. In this case the shape will depend on the amount of tension being exerted as well as the stiffness of the material.

This process of extending the energy functionals to include more complex conditions in the form of adequate functionals is the core of this thesis work. We take TPS as initial model to obtain explicit expressions of splines that may deal with some of its limitations, especially the reconstruction of local and global properties of shapes from point clouds. In general, we are interested in partial differential operators $P(D)$, with constant coefficients c_α

$$P(D) = \sum_{|\alpha| \leq m} c_\alpha D^\alpha\,, \tag{5.10}$$

whose properties mainly depend on its **principal part** $\sum_{|\alpha| = m} c_\alpha D^\alpha$, formed by its higher order terms [87].

Chapter 6

Distribution spaces and regularization for surface reconstruction

6.1 Distributions and inverse problems

The theory of distributions has its origins in problems of partial differential equations of mathematical physics. However, as usual, after being rigorously formulated in mathematical terms, the theory has developed very far from the immediate applications and has become very useful in other disciplines, particularly surface reconstruction from scattered range data. Distribution theory was created mainly by Sobolev and Schwartz [163,164,167] to give answers to problems of mathematical physics. After obtaining a solid mathematical foundation, during the last decades, it became an independent discipline. Distribution Theory (or generalized functions) "re-establishes differentiation as a simple operation of analysis" [163].

Using the variational properties of splines with an abstract approach on distribution spaces, Duchon [48] obtained expressions for the now well-known thin plate spline. Using the Sobolev embedding theorem, he found spaces that are included into the space of continuous functions $\mathbf{C}(\mathbb{R}^n)$, making possible the work of interpolation. During the last decades, it has been necessary to develop very subtle mathematical models and algorithms for tackling the reconstruction problem and there still remain many others to be solved. Nevertheless, they all have common features that can be treated into the framework of **inverse problems** theory [94,129,55,132].

In this chapter we review distribution theory and some distribution spaces, highlighting the facts concerning surface reconstruction. The reader should consult the references [51,65,91,163,164] for a better comprehension. We show how distribution spaces are specially suited for dealing with inverse problems of 3D reconstruction, providing a variational framework that conducts to the generalization from classical cubic spline to multivariate interpolation and approximation. The results of this approach include the well-known thin plate spline and other radial basis functions.

Although surface reconstruction is an ill-posed inverse problem, distribution theory gives a setting to construct spaces where they become well-posed. In this theory, discontinuous functions can be handled as easily as continuous or differentiable functions into a unified framework, making it appropriate for dealing with discrete data. We will show how this

framework may serve as a tool for the double task of modelling these data and at the same time to provide solutions for its reconstruction.

In this thesis, we use Schwartz's approach to generalized functions considering them as continuous linear functionals on the space of infinitely differentiable functions with compact support. This setting is adequate for introducing the concept of generalized differentiation, which makes possible the calculus of distributions with all its practical consequences. The **delta functional** $\delta(x)$, contradictorily defined by Dirac, as $\int \delta(x)\varphi(x)dx = \varphi(0)$; is a generalized function in the theory of distributions, established rigorously by L. Schwartz. The spaces of distributions and its consequences for multivariate approximation and spline theory have appeared in several publications [47-49,108,109]. In this work we want to remark

- How distribution spaces and calculus on distributions provide an appropriate framework for solutions of ill-posed problems.

- The role played by fundamental solutions of differential operators for finding explicit forms of interpolants.

6.2   The derivative problem

Let us consider the classical problem of differentiation. Given a function f, It is possible to find its derivative by the classical rules for differentiation. If the function is given by a formula, a composition of elementary functions or an integral depending on a parameter, then its derivative is also given by a formula. However if the problem is to find the numerical derivative of a function on the basis of experimental data, the problem becomes ill-posed [55,100].

Our main task is to find or construct spaces where approximation problems can be well-posed, this is, to fulfill properties (wp1, 2, 3). Nevertheless, classical spaces like $C^k[a,b]$ may not be adequate for this purpose. For example, there may exist a sequence f_n of functions in $C^1(\mathbb{R})$ such that converge uniformly to f but $f \notin C^1(\mathbb{R})$. As we can see, many of these problems (like the non invertibility of the order of differentiation) are on derivatives and it may happen that $\dfrac{\partial^2 f}{\partial x \partial y} \neq \dfrac{\partial^2 f}{\partial y \partial x}$.

Therefore, it is necessary a more versatile viewpoint for differentiation of a function: derivation in the sense of distributions. Even more; the spaces of distributions solve the existence problems (wp1) but this is not enough for uniqueness (wp2) and regularity (wp3). These problems are solved taking subspaces of distributions with some additional properties. For numerical analysis the most useful spaces are those as close as possible to Euclidian and Hilbert spaces; these are Sobolev spaces, which may be introduced using the

concept of functional on a linear (vector) space and some results from approximation theory.

6.3 Distributions

If X is a function space, i.e. a space whose elements are functions (e.g. $C[a,b]$) then a real (complex) function $T : X \to \mathbb{R}$ on X is called a functional. The set X' of all continuous linear functionals on X is called the dual space of X. Especially interesting for us is the so-called space of *test functions,* the set of infinitely differentiable functions on $\mathbb{R}^n$ with compact support, symbolized $C_0^\infty(\mathbb{R}^n)$, $\mathcal{D}(\mathbb{R}^n)$ or simply by $\mathcal{D}$. The elements of the linear space $\mathcal{D}'(\mathbb{R}^n)$ are called **distributions** (or generalized functions) and are characterized by their "actions" $T(\varphi)$ or $\langle T, \varphi \rangle$ ("Duality bracket") over the elements $\varphi \in \mathcal{D}(\mathbb{R}^n)$. For instance $\langle \delta, \varphi \rangle = \varphi(0)$ is the action of the delta functional over φ. In general each $a \in \mathbb{R}^n$ determines a linear functional $\delta_{(a)} = \delta(\mathbf{x} - a)$ on $\mathcal{D}(\mathbb{R}^n)$ by the expression $\langle \delta_{(a)}, \varphi \rangle = \varphi(a)$. This is a way to solve the formal inconsistency settled by Dirac's sampling property. An important thing to note is that any locally integrable function f, will define a distribution by

$$\langle f, \varphi \rangle = \int_{\mathbb{R}^n} f(\mathbf{x}) \varphi(\mathbf{x}) d\mathbf{x} \quad \forall \varphi \in C_0^\infty(\mathbb{R}^n). \tag{6.1}$$

These are called **regular** distributions. If this is not the case, they are called **singular** distributions (for example, δ). By abuse of notation singular distributions are also denoted by the symbol $f(x)$ used for ordinary functions and are written as in (6.1). The main goal now is to extend as many operations as possible from functions to distributions (derivatives, convolution, Fourier transform). One key idea is that the definition of operations on distributions should coincide with the definition for regular distributions. From

$$\int (f\alpha)\varphi = \int f(\alpha \varphi),$$

it follows that the product of a distribution T en $\mathcal{D}'(\mathbb{R}^n)$ and a function $\alpha \in C^\infty$ is defined as

$$\langle \alpha T, \varphi \rangle = \langle T, \alpha \varphi \rangle.$$

Nevertheless, this should be done carefully, because it may arise several limitations; for example, it will not be possible to multiply distributions nor define the Fourier transform without making extra assumptions. It is a well-known fact that classical spaces may not be suitable in order to formulate well-posedness. The derivative concept is in the core of this difficulty, so it is necessary to get a more versatile definition of derivative. It is known that classical differentiation is an ill-posed problem, because taking derivatives of a function

48

amplifies its oscillations resulting in less smooth functions. On the contrary, integration is an smoothing operation.

Distributional **derivatives** are motivated using integration by parts and the compact support of $\varphi \in \mathcal{D}(\mathbb{R}^n)$, with the following definition

$$\langle \frac{\partial f}{\partial x_k}, \varphi \rangle = \int_{\mathbb{R}^n} \frac{\partial f}{\partial x_k} \varphi = -\int_{\mathbb{R}^n} f \frac{\partial \varphi}{\partial x_k} = -\langle f, \frac{\partial \varphi}{\partial x_k} \rangle,$$

then, $\langle \frac{\partial T}{\partial x_k}, \varphi \rangle = -\langle T, \frac{\partial \varphi}{\partial x_k} \rangle$ for $T \in \mathcal{D}'(\mathbb{R}^n)$. As a consequence, the derivative δ' of the delta distribution it is expressed as $\langle \delta', \varphi \rangle = -\langle \delta, \varphi' \rangle = \varphi'(0)$. A distribution T has derivatives of all orders. This is expressed as

$$\langle \partial^\alpha T, \varphi \rangle = (-1)^{|\alpha|} \langle T, \partial^\alpha \varphi \rangle \quad \forall \ \varphi \in \mathcal{D}(\mathbb{R}^n). \tag{6.2}$$

This means that the derivative of a non-differentiable function can be defined in terms of relations with smooth functions of compact support. A direct consequence is that a distribution T is indefinitely differentiable and $\frac{\partial^2 T}{\partial x_j x_k} = \frac{\partial^2 T}{\partial x_k x_j}$. It is also important to remember that distribution spaces may be defined on a bounded region $\Omega \subset \mathbb{R}^n$; but for reconstruction from scattered data it is convenient to take $\Omega = \mathbb{R}^n$, such as in the above definitions. In this manner, the boundary conditions are shifted to ∞ and is not necessary to solve boundary value problems which may conduct to unbounded Green functions [188,189]. Another problem is that some interpolants are not easy to compute, because their characterization involves a kernel given by a series, then things are much simpler replacing Ω by the whole plane $\mathbb{R}^2$.

6.3.1 Convolution

An operation with very useful properties in theory and applications is the **convolution product** of two functions u and v $u*v(\mathbf{x}) = \int_{\mathbb{R}^n} u(\mathbf{x}-\mathbf{t})v(\mathbf{t})\,d\mathbf{t}$ .Several conditions on u and v are necessary to ensure that the integral exists [163]. If S and T are distributions on $\mathbb{R}^n$ then their convolution product $S*T$ is a new distribution on $\mathbb{R}^n$, defined by

$$S*T = \langle S_{\mathbf{x}}, \langle T_{\mathbf{y}}, \varphi(\mathbf{x}+\mathbf{y}) \rangle \rangle \quad \forall \varphi \in \mathcal{D}(\mathbb{R}^n).$$

Convolution product is particularly useful because of its regularizing properties, i.e. make a function regular or smooth. Convolution becomes a very powerful and general operation when considered from a distributional point of view. Some kinds of differential, difference,

and integral equations are all special cases of convolution equations. A great variety of equations of mathematical physics can be compactly represented by the simple form

$$u * v = f.$$

Linear translation invariant systems are modelled by this kind of convolution equation. The convolution of a distribution $T \in \mathscr{D}'(\mathbb{R}^n)$ with $\varphi \in \mathcal{D}(\mathbb{R}^n)$ is a C^∞ function $T * \varphi$ on $\mathbb{R}^n$. $T * \varphi$ is called the **regularization** of T. Besides of being commutative and associative, convolution of distributions has other useful properties as

(a) $\delta * T = T$;
(b) $\delta_{(a)} * T = \tau_a T$;
(c) $\delta' * T = T'$;
(d) $\delta_{(a)} * h(\mathbf{x}) = h(\mathbf{x} - a)$.   (6.3)

In general, if D is a differential operator with constant coefficients in $\mathbb{R}^n$, $D\delta * T = DT$.

Thus, if D is the Laplacian operator $\Delta = \sum_{i=1}^{n} \frac{\partial^2}{\partial x_i^2}$ in $\mathbb{R}^n$, then $\Delta\delta * T = \Delta T$.

6.3.2 The Schwartz Space $\mathcal{S}$

A very important problem when extending the Fourier transform of a function f

$$\mathscr{F}[f] = f\,(\xi) = \int_{\mathbb{R}^n} f(\mathbf{x}) e^{-i\mathbf{x}\cdot\xi} d\mathbf{x}, \quad \xi = (\xi_1, \xi_2, \cdots, \xi_n).$$

to distributions is that if $\varphi \in \mathcal{D}$ it is possible that $\varphi \notin \mathcal{D}$. In order to obtain a useful definition of Fourier transform, Schwartz defined the space $\mathcal{S}$ of functions $\varphi \in C^\infty$ such that φ and all its derivatives $\partial^\alpha \varphi$ vanish at infinity more rapidly that any power of $\|\mathbf{x}\|$. For example $p(\mathbf{x})e^{-\|\mathbf{x}\|^2}$ belongs to $\mathcal{S}$ with p any polynomial. With this in mind, is defined the space of tempered distributions as the dual space $\mathcal{S}'(\mathbb{R}^n)$. As a consequence $\varphi \in \mathcal{S}$ implies $\varphi \in \mathcal{S}$ and it is possible to define $\langle T, \varphi \rangle = \langle T, \varphi \rangle \ \forall T \in \mathcal{S}'$; preserving in this way, the well-known nice properties of Fourier transform ($\delta = 1$, for example). One important property for applications on reconstruction is that the Fourier transform of a radial function (say $f(\mathbf{x}) = f_0(r)$) is also radial (say $f(\xi) = f_0(\rho)$), $r = \|\mathbf{x}\| = (\sum_{i=1}^{n} x_i^2)^{1/2}$; $\rho = \|\xi\|$

$$= (\sum_{i=1}^{n} \xi_i^2)^{1/2}.$$

Very useful for us will be the following results taken from Gel'fand and Shilov book [66]

$$\mathcal{F}[r^\lambda] = C\rho^{-\lambda-n} \qquad , C = 2^{\lambda+n}\,\pi^{\frac{1}{2}n}\,\frac{\Gamma(\frac{\lambda+n}{2})}{\Gamma(\frac{-\lambda}{2})},$$

$$\mathcal{F}[r^\lambda \ln r] = C_1\rho^{-\lambda-n} + C_2\rho^{-\lambda-n}\ln\rho. \tag{6.4}$$

C_1, C_2 are also given in terms of the Gamma function.

6.3.3 Fundamental solutions

A fundamental solution of linear differential operator $P = \sum_{|\alpha|\le m} c_\alpha \partial^\alpha$ with constant coefficients is a distribution $K(\mathbf{x},\mathbf{y})$, such that $P_{\mathbf{x}}(K(\mathbf{x},\mathbf{y})) = \delta(\mathbf{x\text{-}y})$. If $\Delta K = \delta$ then K is called a potential. Here P is applied to K as a function of $\mathbf{x}$ and $\mathbf{y}$ is a parameter.

Fundamental solutions have the remarkable property of being part of the solution of inhomogeneous differential equations. Reasoning formally and using properties (6.3), if $PK = \delta$, then $P(K * g) = (PK) * g = \delta * g = g$, therefore

$$K * g \text{ is a solution of } Pf = g. \tag{6.5}$$

This is a well-known fact in the theory of differential equations. In this and the next chapters, it is shown its great utility for multivariate approximation. The most remarkable fact that concern us about fundamental solutions is that the interpolants we are going to construct are expressed as a linear combination of translates of the fundamental solution for a differential operator. Fundamental solutions are called Green's functions when they are subjected to boundary conditions. According to Malgrange-Ehrenpreis theorem [91], every operator $P = \sum_{|\alpha|\le m} c_\alpha \partial^\alpha$ has a fundamental solution. Fundamental solutions take different names, depending of the specific fields where they arise: impulse response, Green's functions, influence functions. These multiple names are strongly related with the history of physico-mathematical sciences [199].

One of the most important fundamental solutions comes from the iterated Laplacian operator $\Delta^m u$. If K is a fundamental solution of the operator Δ^m, then $\Delta^m K = \delta$. Taking Fourier transform on both sides, $(-1)^m \rho^{2m} E = 1$ and using formulas (6.4) are obtained the fundamental solutions

$$K(\mathbf{x},\mathbf{y}) = \Phi_{m.n}(\|\mathbf{x\text{ - }y}\|), \tag{6.6}$$

$$\Phi_{m,n}(r) = \begin{cases} c\,r^{2m-n}\ln r, & n \text{ even} \\ d\,r^{2m-n}, & n \text{ odd} \end{cases}, \tag{6.7}$$

$$c = \frac{(-1)^{m+(n-2)/2}}{2^{2m-1} \pi^{n/2} (m-1)!(m-n/2)!}, \quad d = \frac{\Gamma(n/2-m)}{2^{2m} \pi^{n/2} (m-1)!} .$$

6.3.4 Sobolev and Beppo Levi spaces

The well-known classical spaces (e.g. the space of continuous functions) may fail when dealing with ill-posed problems. Distribution theory gives a setting to construct spaces where surface reconstruction becomes well posed. The space of distributions $\mathcal{D}'(\mathbb{R}^n)$ as described above provides answers for conditions of existence and uniqueness. However, this space is "very large", therefore, the issues on regularity are treated into some of its subspaces. It is possible to reconstruct the space $\mathbf{L}^2(\mathbb{R}^n)$ as a Hilbert space of distributions, unifying this theory with the theory of $\mathbf{L}^2(\mathbb{R}^n)$ spaces; this leads naturally to Sobolev spaces, very convenient for the pure and numerical treatment.

The key idea of Sobolev techniques it is to assume that the distributions which solve a particular problem really come from a function f, but without making any smoothness assumption about f. The next step in the method, is to take advantage of the most general and operational properties of distributions and apply them to solve the problem. Once this is done it is possible to use the so called Sobolev embedding properties in order to determine the smoothness degree of the solution. If m is a nonnegative integer and $p \in [1,\infty[$, The Sobolev space $W^{m,p}(\mathbb{R}^n)$, is the vector space

$$W^{m,p}(\mathbb{R}^n) = \{u \in \mathcal{D}'(\mathbb{R}^n): \partial^\alpha u \in L^p(\mathbb{R}^n), |\alpha| \leq m\},$$

provided with the norm $\|u\|_{W^{m,p}}^2 = \sum_{|\alpha| \leq m} \|\partial^\alpha u\|_{L^p(\mathbb{R}^n)}^p$.

The spaces $W^{m,2}(\mathbb{R}^n)$ ($p=2$) are symbolized as $H^m(\mathbb{R}^n)$ and consists of those functions in $\mathbf{L}^2(\mathbb{R}^n)$ that, together with all their distributional derivatives of order $|\alpha| \leq m$, belong to $\mathbf{L}^2(\mathbb{R}^n)$

$$H^m(\mathbb{R}^n) = \{u : \partial^\alpha u \in \mathbf{L}^2(\mathbb{R}^n), \forall |\alpha| \leq m\}.$$

We consider real value functions only, and make $H^m(\mathbb{R}^n)$ an inner product space with the Sobolev Inner product

$$(u,v)_{H^m} = \int_{\mathbb{R}^n} \sum_{|\alpha| \leq m} (\partial^\alpha u)(\partial^\alpha v) \, dx \quad u,v \in H^m.$$

This inner product generates the Sobolev norm $\|u\|_{H^m}^2 = \int_{\mathbb{R}^n} \sum_{|\alpha| \leq m} (\partial^\alpha u)^2 dx$.

One important fact about these spaces is that $H^m(\mathbb{R}^n)$ is a Hilbert space with respect to the norm $\|\cdot\|_{H^m}$. In general, for $s \in \mathbb{R}$, is defined as

$$H^s(\mathbb{R}^n) = \left\{ u \in S'(\mathbb{R}^n) : (1+\|\xi\|)^{s/2}\hat{u} \in L^2(\mathbb{R}^n) \right\},$$

with the scalar product $(u,v) = \int_{\mathbb{R}^n} (1+\|\xi\|)^s \hat{u}(\xi)\hat{v}(\xi)d\xi$. It can be shown [202] that when $s = m \in \mathbb{N}$, $H^s(\mathbb{R}^n)$ is topologically equivalent to $H^m(\mathbb{R}^n)$.

Now, our interest is to find a proper abstract setting for a natural n-dimensional generalization of the minimal norm interpolation problem. This is provided by **homogenous Sobolev spaces** or **Beppo Levi spaces** $BL^m(\mathbb{R}^n)$ of order m over $\mathbb{R}^n$

$$BL^m(\mathbb{R}^n) = \left\{ u \in \mathcal{D}' : \partial^\alpha u \in L^2(\mathbb{R}^n); |\alpha| = m \right\}.$$

In words, this is the vector space of all the (Schwartz) distributions for which all the partial derivatives (in the distributional sense) of (total) order m are square integrable in $\mathbb{R}^n$. Due to its "weaker" definition, in $BL^m(\mathbb{R}^n)$ there is not a norm but the rotation invariant semi-norm defined by (1.3)

$$R[u] = \sum_{|\alpha|=m} \frac{m!}{\alpha!}\int_{\mathbb{R}^n} |\partial^\alpha u(\mathbf{x})|^2 \, d\mathbf{x}, \qquad (6.8)$$

corresponding to the semi-inner product

$$(u,v) = \sum_{|\alpha|=m}^{n} \frac{m!}{\alpha!}\int_{\mathbb{R}^n} (\partial^\alpha u)(\partial^\alpha v)d\mathbf{x}. \qquad (6.8a)$$

A semi-inner product has nearly all the properties of an inner product, but its null space is different from cero. It can be shown that the null space of (6.8) is the space $\Pi_{m-1}(\mathbb{R}^n)$, of polynomials of total degree no greater than $m-1$; the dimension of $\Pi_k(\mathbb{R}^n)$ is $\begin{pmatrix} k+n \\ n \end{pmatrix}$; for instance, $\{1, x, y, x^2, y^2, xy\}$ is a base for $\Pi_2(\mathbb{R}^2)$. An important relation between Sobolev and Beppo-Levi spaces is that the intersection of all Beppo-Levi spaces $BL^k(\mathbb{R}^n)$ of order $k \le m$ yields the Sobolev space $W_m^2(\mathbb{R}^n) = \bigcap_{k \le m} BL^k(\mathbb{R}^n)$.

With the above setting, distribution theory provides a very efficient tool for treating with very complex problems; nevertheless, it is very important to remember that in order to have a realistic application this should be done with spaces of continuous functions. This is the method used in partial differential equations, where the problems are first solved in the realm of distributions and then if these distribution solutions are classical solutions. Sobolev embedding theorems answers this question.

By the **Sobolev embedding theorem** [2], it is well known that for $m > \dfrac{n}{2}$, the inclusion

$H^m(\mathbb{R}^n) \subseteq C(\mathbb{R}^n)$ holds, or, to be more precise, that every equivalence class in $H^m(\mathbb{R}^n)$ contains a continuous representer. In this way, $H^m(\mathbb{R}^n)$ is interpreted as a set of continuous functions. The following theorem shows that $BL^m(\mathbb{R}^n) \subseteq C(\mathbb{R}^n)$ as well.

Theorem 6.1 ([48,116]). If $m > \dfrac{n}{2}$ then $BL^m(\mathbb{R}^n)$ is semi-Hilbert space of continuous functions on $\mathbb{R}^n$ and all the evaluation functionals with finite support in $\mathbb{R}^n$ that annihilate $\Pi_{m-1}(\mathbb{R}^n)$ are bounded.

Some of the ideas we have mentioned up to now (functionals, fundamental solutions, inner product spaces) can be linked using the ideas of Reproducing Kernel Hilbert Spaces (RKHS) [8,171,184,188].

6.3.5 Distributions and Mercer condition on kernels

In the theory of integral equations, the kernel $K(\mathbf{x},\mathbf{y})$ is positive definite when $K(\mathbf{x},\mathbf{y})$ satisfies

$$\int\int K(\mathbf{x},\mathbf{y}) f(\mathbf{x}) \overline{f(\mathbf{y})} \, d\mathbf{x} \, d\mathbf{y} = (Kf,f) \geq 0, \tag{6.9}$$

for any continuous function $f(\mathbf{x})$. In the beginning of XX-th century, Mercer [8] discovered that this condition is equivalent to the quadratic form

$$\sum_{i,j=1}^{M} \alpha_i \alpha_j K(a_i, a_j) \geq 0,$$

for any M points $a_1, a_2, \cdots, a_M \in \mathbb{R}^n$, and $\alpha_1, \alpha_2, \ldots, \alpha_M \in \mathbb{R} \setminus \{0\}$. If K is radial then $K(\mathbf{x},\mathbf{y}) = \Phi(\mathbf{x}-\mathbf{y})$ and (6.9) will be

$$\int\int \Phi(\mathbf{x}-\mathbf{y}) \varphi(\mathbf{x}) \overline{\varphi(\mathbf{y})} \, d\mathbf{x} \, d\mathbf{y} \geq 0 \text{ for all } \varphi \in C_0^\infty(\mathbb{R}^n).$$

To see this one only need to approximate this integral by a Riemann sum. This condition can be written as $\int\int f(\boldsymbol{\tau}) \varphi(\mathbf{x}) \overline{\varphi(\mathbf{x}-\boldsymbol{\tau})} \, d\boldsymbol{\tau} \, d\mathbf{x} = \int f(\boldsymbol{\tau})(\bar{\tilde{\varphi}} * \varphi)(\boldsymbol{\tau}) d\boldsymbol{\tau} \geq 0$, where $\tilde{\varphi}$ is the function $\tilde{\varphi}(\mathbf{x}) = \varphi(-\mathbf{x})$. This suggest to define a distribution $T \in \mathcal{D}'(\mathbb{R}^n)$ of **positive type** if

$$T(\bar{\tilde{\varphi}} * \varphi) \geq 0 \text{ for all } \varphi \in \mathcal{D}(\mathbb{R}^n). \tag{6.10}$$

If $\mathcal{H}$ is a Hilbert space of functions on an arbitrary set Ω whose inner product is written $(\cdot,\cdot)$, $\mathbb{R}^\Omega$ will be the space of mappings from Ω to $\mathbb{R}$ and $\mathbb{R}^{[\Omega]}$ is the vector space of finite

linear combinations of the Dirac, or evaluation functionals $L_{\mathbf{x}_0}(f) = \delta_{(\mathbf{x}_0)}(f) = f(\mathbf{x}_0)$ onto $\mathbb{R}$, $\mathbb{R}^{[\Omega]} = \{\sum\limits_{i=1}^{M} \alpha_i \, \delta_{a_i} : a_i \in \Omega, \alpha_i \in \mathbb{R}\}$. In this way, $\mathbb{R}^{[\Omega]}$ and $\mathbb{R}^{\Omega}$ are sets in duality by the bilinear form $\langle \cdot, \cdot \rangle : \mathbb{R}^{[\Omega]} \times \mathbb{R}^{\Omega} \to \mathbb{R}$ such that $\langle \sum\limits_{i=1}^{M} \alpha_i \, \delta_{a_i}, f \rangle = \sum\limits_{i=1}^{M} \alpha_i f(a_i)$. If the Dirac functional $L_{\mathbf{x}}(f)$ is bounded on $\mathcal{H}$, by Riesz representation theorem [35], there exists exactly one $K_{\mathbf{x}} \in \mathcal{H}$ such that

$$L_{\mathbf{x}}(f) = (f, K_{\mathbf{x}}) = f(\mathbf{x}), \text{ for all } f \in \mathcal{H}.$$

$K_{\mathbf{x}}$ is known as the *representer* of $L_{\mathbf{x}}$. Then $\mathcal{H}$ becomes a *Reproducing Kernel Hilbert Space* (RKHS) or *Hilbert space of functions* [35] and the representer is a unique positive definite function $K : \mathbb{R}^n \times \mathbb{R}^n \longrightarrow \mathbb{R}$, $(\mathbf{x}, \mathbf{y}) \to K(\mathbf{x}, \mathbf{y})$, called the reproducing kernel of $\mathcal{H}$; such that

$$f(\mathbf{x}) = (f(\mathbf{y}), K(\mathbf{x}, \mathbf{y}))_{\mathbf{y}} \ \forall f \in \mathcal{H}. \tag{6.11}$$

The kernels we deal with in this work are radial, thus they have the form $K(\mathbf{x}, \mathbf{y}) = \Phi(\| \mathbf{x} - \mathbf{y} \|)$, where $\Phi : [0, \infty[\to \mathbb{R}$ is a continuous function that depends of the distance between points. Φ is called a **radial basis function**. Table 6.1 gives a list of the most used radial basis functions.

Useful cases [154-157,188] of both positive definite and radial kernels are $K(\mathbf{x}, \mathbf{y}) = \Phi(\| \mathbf{x\text{-}y} \|)$ with Gaussians $\Phi(r) = e^{-r^2}$, inverse multiquadrics $\Phi(r) = \dfrac{1}{\sqrt{1 + r^2}}$ and Wendland compactly supported function $\Phi(r) = (1 - r)_+^4 (4r + 1)$. An especial case of conditionally positive definite kernel is obtained with the thin plate spline function $\Phi_{2,2}(r) = r^2 \ln r$, which is a particular case of (6.6).

The next theorem clearly illustrates the two trends that historically have been followed to study properties and applications of kernels. In the first trend, one is interested primarily in a class of functions $\mathcal{H}$, and the corresponding kernel $K(\mathbf{x}, \mathbf{y})$ is used essentially as a tool in the study of functions in this space. Those following the second trend consider a given kernel $K(\mathbf{x}, \mathbf{y})$ and study it in itself as a tool of research, the space $\mathcal{H}$ corresponding to $K(\mathbf{x}, \mathbf{y})$ is introduced *a posteriori*.

Theorem 6.2 (Moore-Aronszajn [188]). To every RKHS there corresponds a unique positive definite function (called the reproducing kernel) and conversely, given a positive-definite function $K(\mathbf{x}, \mathbf{y})$ on $\mathbb{R}^n \times \mathbb{R}^n$ it is possible to construct a unique RKHS of real valued functions on $\mathbb{R}^n$ with $K(\mathbf{x}, \mathbf{y})$ as its reproducing kernel, this space is called the **native space**.

It can be shown [191] that the native space for thin plate spline kernel $K(\mathbf{x},\mathbf{y}) = \Phi_{m,n}(\|\mathbf{x}-\mathbf{y}\|)$ is the Beppo-Levi space $\boldsymbol{BL}^m(\mathbb{R}^n)$ and the native space for $K(\mathbf{x},\mathbf{y}) = \Phi(\|\mathbf{x}-\mathbf{y}\|)$ with Wendland function $\Phi(r) = (1-r)_+^4(4r+1)$ is the classical Sobolev space $H^3(\mathbb{R}^n)$.

Name	$\Phi(r)$	Parameters	order
Linear	$\Phi(r) = r$		$m=1$
Cubic	$\Phi(r) = r^3$		$m=2$
Gaussian	$\Phi(r) = e^{-\beta r^2}$	$\beta > 0$	$m = 0$
Poli-harmonic	$\Phi(r) = r^\beta$	$\beta \in \mathbb{R}_{>0} \setminus 2\mathbb{Z}$	$m \geq \lceil \beta/2 \rceil$
Thin plate spline	$\Phi(r) = r^\beta \log(r)$	$\beta \in 2\mathbb{N}$	$m \geq \beta/2$
Multiquadric	$\Phi(r) = (c^2 + r^2)^{\beta/2}$	$\beta \in \mathbb{R}_{>0} \setminus 2\mathbb{Z}\ c>0$	$m \geq \lceil \beta/2 \rceil$
Inverse multiquadric	$\Phi(r) = 1/\sqrt{c^2 + r^2}$		$m = 0$
Wendland function	$\Phi(r) = (1-r)_+^4(4r+1)$		$m = 0$

Table 6.1: Some well known Radial Basis Functions.

Chapter 7

Interpolation of surfaces from point clouds

7.1 Introduction

Now we are going to apply the theory developed in the former chapter to solve the interpolation problem from a point cloud in any dimension $D = \{(a_i, z_i) \in \mathbb{R}^n \times \mathbb{R}\}_{i=1}^{M}$; this correspond to the problem (P1) proposed in (4.10a)

$$\min_{f \in \mathcal{X}} R[f], \qquad \text{with } \{f(a_i) = z_i\}_{i=1}^{M}. \qquad (7.1)$$

The approximation problem P2 in (4.10b) will be treated in the next chapter. Based on results from Hilbert space and distribution theory [35,48,56], we give a constructive proof to the problem of interpolation from scattered data. As a consequence of interpolation and smoothness conditions we obtain Thin Plate Spline (TPS), whose explicit expression is given in terms of the fundamental solution of the biharmonic differential operator. This spline is also written in terms of convolution with a fixed function.

TPS is a generalization to $\mathbb{R}^n$ of the well-known cubic spline in one variable [4,161,188]. Cubic spline was developed for solving interpolation problems in aircraft, shipbuilding and car industries at the 1950´s. Mathematicians soon realized that common interpolation methods as Lagrange Polynomials were not suitable for tackling these problems. It was necessary to build more subtle tools. After this achievement, there was a great interest to obtain the $\mathbb{R}^n$ equivalent to cubic spline. Several ways were tried but only the variational approach was successful. In the following lines we describe this approach.

7.2 D^m - Splines or Thin Plate Spline

D^m splines results as the application and generalization to n variables of the plate model discussed in chapter 5. This model was formalized by Duchon [48] and Meinguet [122,123]. To reconstruct a function (or surface), it is assumed that data $D = \{(a_i, z_i) \in \mathbb{R}^n \times \mathbb{R}\}_{i=1}^{M}$ comes from the sampling of a function f such that $f(a_i) = z_i$ and it is required to find an expression for f, in order to approximate $f(\mathbf{x})$ when $\mathbf{x}$ does

not belong to the set of nodes or centres $\mathcal{A} = \{a_1, a_2, \cdots, a_M\}$. This means that f should be a continuous function.

The idea is to find an element $S(\mathbf{x})$ in a proper subset or subspace and then use $S(\mathbf{x})$ to calculate $f(\mathbf{x})$. We suppose $\mathcal{A}$ contains a $\Pi_{m-1}(\mathbb{R}^n)$-unisolvent subset $\mathcal{B} = \{a_j\}_{j=1}^N$, $N = \dim \Pi_{m-1}(\mathbb{R}^n)$ and we want to find $S(\mathbf{x})$ such that $S(a_i) = f(a_i) = z_i$ for $i = 1, \ldots, M$ and minimizes the seminorm

$$R[u] = \int_{\mathbb{R}^n} \sum_{|\alpha|=m} c_\alpha \mid \partial^\alpha u(\mathbf{x}) \mid^2 d\mathbf{x}, \tag{7.2}$$

with null space $\Pi_{m-1}(\mathbb{R}^n)$; the $c_\alpha = \dfrac{m!}{\alpha!}$ are chosen for obtaining a rotational invariant seminorm. As a consequence, we begin assuming $S \in BL^m(\mathbb{R}^n)$, then by Sobolev embedding theorem, $BL^m(\mathbb{R}^n)$ is a linear subspace of $C(\mathbb{R}^n)$ for $m > \dfrac{n}{2}$.

The key idea is to apply theorems A.2 and A.3 on spaces of distributions and modify the semi inner product $[u, v] = \int_{\mathbb{R}^n} \sum_{|\alpha|=m} \dfrac{m!}{\alpha!} \partial^\alpha u(\mathbf{x}) \partial^\alpha v(\mathbf{x}) d\mathbf{x}$ on $BL^m(\mathbb{R}^n)$. We then obtain an inner product for building a complete space $\mathcal{H}$. Once this is done, we are enabled to use all the machinery of Hilbert spaces (see Appendix). The inner product is defined as

$$(u, v) = [u, v] + \sum_{a_i \in \mathcal{B}} u(a_i) v(a_i). \tag{7.3}$$

The solution $S(\mathbf{x})$ to the minimal norm interpolant is found using the projection operator technique on Hilbert Spaces. A linear transformation P of a linear space V into itself is said to be a projection if $P^2 = P$. The range $\mathcal{R}$ and the null space $\mathcal{K}$ of P are linear subspaces of V such that $V = \mathcal{R} + \mathcal{K}$. If $\mathcal{R} \perp \mathcal{K}$ then $I - P$ is also a projection and it is written $V = \mathcal{R} \oplus \mathcal{K}$

The ideas of the deduction are borrowed from Light [108] and Meinguet [122]. We give here the details necessary for showing the importance of fundamental solutions of differential operators.

Let $p_1, p_2, \ldots, p_N$ be the Lagrange basis for $\Pi_{m-1}(\mathbb{R}^n)$ with respect to the points $\mathcal{B} = \{a_1, a_2, \ldots, a_N\}$; we define $\mathcal{P} : \mathcal{H} \to \mathcal{H}$ with $\mathcal{P}f = \sum_{i=1}^N f(a_i) p_i$. Then $\Pi_{m-1}(\mathbb{R}^n)$ is the range of $\mathcal{P}$ and $\mathcal{H}_0 = \{u \in \mathcal{H} : u(a_j) = 0, \forall a_j \in \mathcal{B}\}$, its null space. By (7.3) it is seen that $\mathcal{H}_0 \perp \Pi_{m-1}(\mathbb{R}^n)$, then we have the representation formula $\mathcal{H} = \mathcal{H}_0 \oplus \Pi_{m-1}(\mathbb{R}^n)$, now it is predictable that S will be a term in $\mathcal{H}_0$ plus a polynomial. The idea is to find the

58

representers R_{a_i} on $\mathcal{H}$ and then use theorem A.2(see Appendix). If R_{a_i} is the representer for a_i on $BL^m(\mathbb{R}^n)$ then $R_{a_i} = h_{a_i} + p_{a_i}$ where h_{a_i} and p_{a_i} are the representers on $\mathcal{H}_0$ and Π_{m-1}, respectively . Now we find R_{a_i} using the distributional approach. The image of $\mathcal{H}$ under the projection operator $(I - \mathcal{P})$ is $\mathcal{H}_0$, then $\forall \varphi \in \mathcal{D}(\mathbb{R}^n)$

$$\varphi - (\mathcal{P}\,\varphi)(\mathbf{x}) = (\varphi - (\mathcal{P}\,\varphi), h_{\mathbf{x}}) = [\varphi - \mathcal{P}\,\varphi, h_{\mathbf{x}}] = [\varphi, h_{\mathbf{x}}]$$
$$= \sum_{|\alpha|=m} c_\alpha \int_{\mathbb{R}^n} (\partial^\alpha \varphi)(\partial^\alpha h_{\mathbf{x}}),$$

using derivative in the distributional sense in the last expression and by (6.2), we have

$$\varphi - (\mathcal{P}\,\varphi)(\mathbf{x}) = \sum_{|\alpha|=m} c_\alpha \langle \partial^\alpha \varphi, \partial^\alpha h_{\mathbf{x}} \rangle = \left\langle (-1)^m \sum_{|\alpha|=m} c_\alpha \partial^{2\alpha} h_{\mathbf{x}}, \varphi \right\rangle$$
$$= \left\langle (-1)^m \Delta^m h_{\mathbf{x}}, \varphi \right\rangle . \tag{7.4}$$

It is also seen that

$$\varphi - (\mathcal{P}\,\varphi)(\mathbf{x}) = \varphi - \sum_{i=1}^{N} f(a_i) p_i(\mathbf{x}) = \left\langle \delta_{(\mathbf{x})} - \sum_{i=1}^{q} p_i(\mathbf{x})\delta_{(a_i)}, \varphi \right\rangle , \tag{7.5}$$

so by equations (7.4) and (7.5) we have shown that $h_{\mathbf{x}}$ is a solution of the distributional differential equation

$$(-1)^m \Delta^m h_{\mathbf{x}} = \delta_{(\mathbf{x})} - \sum_{i=1}^{q} p_i(\mathbf{x})\delta_{(a_i)}. \tag{7.6}$$

Using the fundamental solutions (6.7) of the iterated Laplacian $(-1)^m \Delta^m K_{\mathbf{x}} = \delta_{(\mathbf{x})}$; then $K_{\mathbf{x}} - \sum_{i=1}^{l} p_i(\mathbf{x})K_{a_i}$ is a particular solution of the differential equation (7.6) . We project this solution on $\mathcal{H}_0$ to obtain

$$h_{\mathbf{x}} = (I - \mathcal{P})\left\{ K_{\mathbf{x}} - \sum_{i=1}^{l} p_i(\mathbf{x})K_{a_i} \right\}$$
$$= K_{\mathbf{x}} - \sum_{i=1}^{l} p_i(\mathbf{x})K_a - \sum_{i=1}^{l} K_{\mathbf{x}}(a)p_i + \sum_{i,i=1}^{l} K_{a_j}(a_i)p_j(x)p_i .$$

It can be shown that $p_x = \sum_{i=1}^{l} p_i(\mathbf{x})p_i$ then $R_{a_i} = h_{a_i} + \sum_{i=1}^{N} p_i(\mathbf{x})p_i$. Making some calculation we find the interpolant $S_{f,A}$ as a linear combination of translates of a fixed function plus a polynomial $p(\mathbf{x}) = \sum_{j=1}^{N} \beta_j p_j(\mathbf{x})$ where $\{p_j\}_{j=1}^{N}$ is a base for $\Pi_{m-1}(\mathbb{R}^n)$. Finally, it is obtained the following expression that solve the interpolation problem (7.1)

$$S_{f,A}(\mathbf{x}) = \sum_{i=1}^{M} \alpha_i \Phi_{m,n}(\| \mathbf{x} - a_i \|) + p(\mathbf{x}), \quad \Phi_{m,n}(r) = \begin{cases} c\, r^{2m-n} \ln r, & n \ even \\ d\, r^{2m-n}, & n \ odd \end{cases}, \quad (7.7)$$

where the constants c, d are known but are not necessary because they are absorbed by the linear combinations in $S_{f,A}$. This interpolant is known as D^m spline, polyharmonic spline, **Thin Plate Spline (TPS)** or surface spline. It is worth to say that $S_{f,A}$ is an orthogonal projection, therefore, is the best approximation with respect to the seminorm in the space $BL^m(\mathbb{R}^n)$, i.e.

$$| f - S_{f,A} |_m \leq | f - S |_m \quad \forall S \in BL^m(\mathbb{R}^n).$$

Given the data $D = \{(a_i, z_i) \in \mathbb{R}^n \times \mathbb{R}\}_{i=1}^{M}$, the interpolant $S_{f,A}$ is completely determined finding α_i's and β_i's. The interpolation conditions $S(a_i) = z_i$ $i = 1, \dots M$ produce M equations and the remaining N degrees of freedom are absorbed by the condition

$$\sum_{i=1}^{N} c_i p_j(a_i) = 0 \ \ \forall \ p_j \in \Pi_{m-1}, \quad (7.8)$$

yielding the system

$$\begin{bmatrix} A & P \\ P^t & 0 \end{bmatrix} \begin{bmatrix} \alpha \\ \beta \end{bmatrix} = \begin{bmatrix} z \\ 0 \end{bmatrix}, \quad (7.9)$$

where α_i, β_i are found by solving this linear system, where, A is an interpolation matrix (see Appendix), with

$$A_{i,j} = \Phi_{m,n}(\| a_i - a_j \|), \ i, j = 1, \cdots, M, \ P_{ij} = p_j(a_i) \ i = 1, \dots, M, \quad j = 1, \dots, N$$
$$\alpha = (\alpha_1, \dots, \alpha_M)^t, \ z = (z_1, \dots, z_M)^t.$$

It is interesting to note that $S_{f,A}$ may be written in terms of a convolution of a distribution with a function in the following way.

Let μ_α be the distribution $\mu_\alpha = \sum_{i=1}^{M} \alpha_i \delta_{(a_i)}$ such that $\mu_\alpha \in \Pi_{m-1}^{\perp} = \{ \mu \colon \mu(p) = 0 \}$, then by condition (7.8), we have that $\mu_\alpha(p) = 0$ if $p \in \Pi_{m-1}$. On the other hand, defining $\Psi(\mathbf{x}) = \Phi(\| \mathbf{x} \|)$, and using properties (6.3) of the delta function, the result is

$$\delta_{(a)} * \Psi(\mathbf{x}) = \Psi(\mathbf{x} - a),$$

thus, we can write

60

$$\sum_{i=1}^{M} \alpha_i \, \Phi(\mathbf{x} - a_i) = \mu_\alpha * \Psi(\mathbf{x}).$$

Therefore, taking $p \in \Pi_{m-1}$, $\mu_\alpha \in \Pi_{m-1}^{\perp}$ and $\operatorname{supp} \mu_\alpha \subseteq \mathcal{A} = \{a_1, a_2, \ldots, a_M\}$, the interpolant can be written as

$$S_{f,A} = \left(\sum_{i=1}^{M} \alpha_i \, \delta_{(a_i)} \right) * \Psi \; + \; p = \mu_\alpha * \Psi \; + \; p. \tag{7.10}$$

This suggests that $S_{f,A}$ can be seen as a very general form of a *low-pass filter*. These properties are completed with the following result.

Theorem 7.1 ([122]). If $m > \dfrac{n}{2}$, the D^m spline interpolation problem is well-posed: its solution exits, is unique, and depends continuously on the data $D = \{(a_i, z_i) \in \mathbb{R}^n \times \mathbb{R}\}_{i=1}^{M}$

Example 7.1 (Interpolation with D^m-splines). In the space $BL^2(\mathbb{R}^2)$ the corresponding semi-norm is

$$R[u] = \int_{\mathbb{R}^2} \left(\frac{\partial^2 u}{\partial x^2} \right)^2 + 2 \left(\frac{\partial^2 u}{\partial x \partial y} \right)^2 + \left(\frac{\partial^2 u}{\partial y^2} \right)^2 dx \, dy,$$

that represents the bending energy of an infinitely extended plate. With $\Phi(r) = r^2 \log r$, the interpolant (7.7) is

$$S(\mathbf{x}) = \sum_{i=1}^{M} \alpha_i \Phi(\| \mathbf{x} - a_i \|) + \beta_1 + \beta_2 x + \beta_3 y.$$

This spline interpolation, whether in one or two dimensions, physically corresponds to forcing a thin elastic beam or plate to pass through the data constraints. Away from the data points or centres the curve (or surface) will take on the shape that minimizes the strain energy given by $R[u]$. Figure 7.1 shows the results of interpolating Franke's test function $f(x, y)$ (7.11) [64], given by

$$f(x, y) = 0.75 e^{-\frac{1}{4}((9x-2)^2 + (9y-2)^2)} + 0.75 e^{-\left(\frac{(9x+1)^2}{49} + \frac{(9y+1)}{10} \right)}$$

$$+ 0.5 e^{-(9x-7)^2 - \frac{(9y-3)^2}{4}} + 0.2 e^{-((9x-4)^2 + (9y-7)^2)}, \tag{7.11}$$

using scattered data $D = \{(a_i, z_i) \in \mathbb{R}^2 \times \mathbb{R}\}_{i=1}^{M}$. The linear system to solve is

$$\begin{bmatrix} A_{11} & A_{12} & \cdots & A_{1M} & 1 & x_1 & y_1 \\ A_{21} & A_{22} & \cdots & A_{2M} & 1 & x_2 & y_2 \\ \vdots & \vdots & \ddots & \vdots & \vdots & \vdots & \vdots \\ A_{M1} & A_{M2} & \cdots & A_{MM} & 1 & x_M & y_M \\ 1 & 1 & \cdots & 1 & 0 & 0 & 0 \\ x_1 & x_2 & \cdots & x_M & 0 & 0 & 0 \\ y_1 & y_2 & \cdots & y_M & 0 & 0 & 0 \end{bmatrix} \begin{bmatrix} \alpha_1 \\ \alpha_2 \\ \vdots \\ \alpha_M \\ \beta_1 \\ \beta_2 \\ \beta_3 \end{bmatrix} = \begin{bmatrix} z_1 \\ z_2 \\ \vdots \\ z_M \\ 0 \\ 0 \\ 0 \end{bmatrix}, \tag{7.12}$$

where the coordinates of observation points are $a_i = (x_i, y_i)$, $A_{i,j} = \Phi(\| a_i - a_j \|)$. We solve this system to get the coefficients or weights α_i, β_j, $i = 1, \ldots, M$, $j = 1, 2, 3$.

(a) (b) (c)
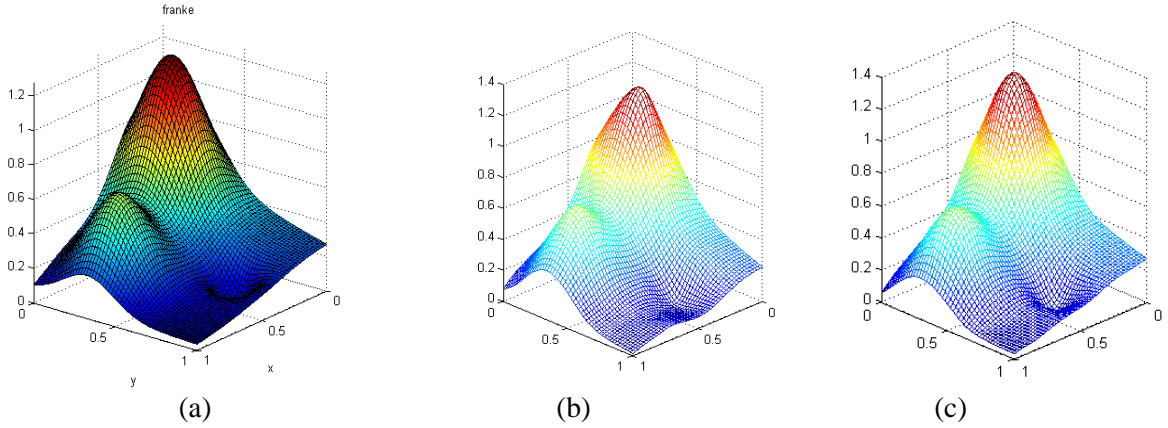
Fig. 7.1: Results interpolating Franke's test function (7.11) without noise in the interval $\Omega = [0,1] \times [0,1]$ (a) Original function. Interpolation with: (b) $M = 40$ points. (c) $M = 100$ points. The interpolation rapidly improves with an increasing number of random points.

Example 7.2 (Reconstruction of surfaces with discontinuities). The following is the mathematical expression for Franke's "landslide" in the interval $\Omega = [0,1] \times [0,1]$.

$$f(x, y) = \begin{cases} \dfrac{1}{2} & y \leq \dfrac{2}{5} \\[2mm] \dfrac{1}{2}\left(1 - \dfrac{25}{9}(y - \dfrac{2}{5})^2\right) & y > \dfrac{2}{5} \wedge x \leq \dfrac{1}{5} \\[2mm] \dfrac{125}{72}(1 - y)^2(1 - x) & y > \dfrac{2}{5} \wedge x > \dfrac{1}{5} \end{cases} \tag{7.13}$$

62
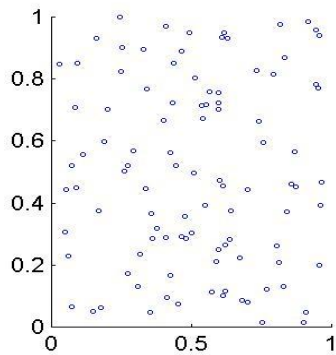
(a)
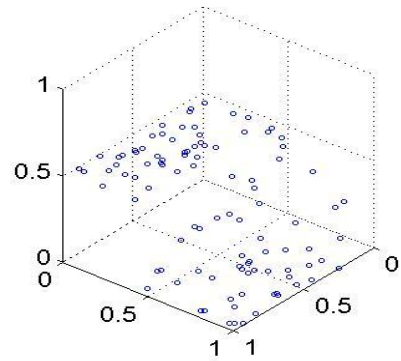
(b)
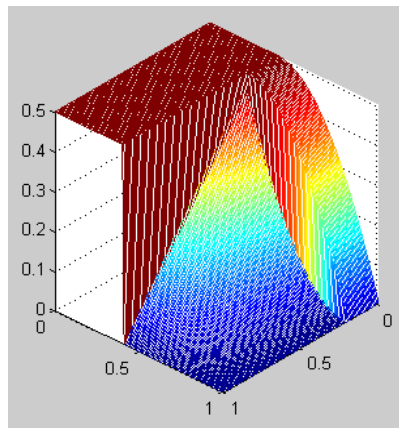
(c)
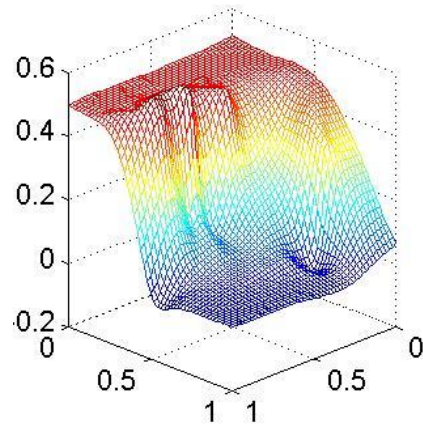
(d)

Fig. 7.2: (a) (x, y) coordinates of 100 scattered data on Franke's landslide surface (7.13) (b) 3D scatter plot of the points (c) The original surface (d) Interpolation of the scattered data. This is an extreme case very useful for testing approximation models in the reproduction of discontinuities. It has smooth zones as well as vertices, edges and faces.

$\mathbb{R}^n$	D^m	$\|u\|_{D_m}^2 = \int_{\mathbb{R}^n} \sum_{|\alpha|=m} \dfrac{m!}{\alpha!}|\partial^\alpha u|^2\, dx$ $\qquad\qquad u:\mathbb{R}^n \to \mathbb{R}$
$\mathbb{R}^1$	D^2	$\int (u''(x))^2\, dx$
$\mathbb{R}^1$	D^3	$\int (u'''(x))^2\, dx$
$\mathbb{R}^2$	D^2	$\iint_{\mathbb{R}^2}[(\dfrac{\partial^2 u}{\partial x^2})^2 + 2(\dfrac{\partial^2 u}{\partial x \partial y})^2 + (\dfrac{\partial^2 u}{\partial y^2})^2]\, dx\, dy$
$\mathbb{R}^2$	D^3	$\iint_{\mathbb{R}^2}[(\dfrac{\partial^3 u}{\partial x^3})^2 + 3(\dfrac{\partial^3 u}{\partial x^2 \partial y})^2 + 3(\dfrac{\partial^3 u}{\partial x \partial y^2})^2 + (\dfrac{\partial^3 u}{\partial y^3})^2]\, dx\, dy$
$\mathbb{R}^3$	D^2	$\iint_{\mathbb{R}^2}[(\dfrac{\partial^2 u}{\partial x^2})^2 + (\dfrac{\partial^2 u}{\partial y^2})^2 + (\dfrac{\partial^2 u}{\partial z^2})^2 + 2(\dfrac{\partial^2 u}{\partial x \partial y})^2 + 2(\dfrac{\partial^2 u}{\partial x \partial z^2})^2 + 2(\dfrac{\partial^2 u}{\partial y \partial z})^2]\, dx\, dy\, dz$

Table 7.1: Duchon seminorm (7.2) for some values of m, n ($m = 2,3$; $n = 1,2,3$) m represents the degree of derivatives and n the dimension of data.

$\mathbb{R}^n$	m	$p(\mathbf{x})$
$\mathbb{R}^1$	2	$c_0 + c_1 x$
$\mathbb{R}^1$	3	$c_0 + c_1 x + c_2 x^2$
$\mathbb{R}^2$	2	$c_0 + c_1 x + c_2 y$
$\mathbb{R}^2$	3	$c_0 + c_1 x + c_2 y + c_3 x^2 + c_4 y^2 + c_5 xy$
$\mathbb{R}^3$	2	$c_0 + c_1 x + c_2 y + c_3 z$

Table 7.2: Polynomial terms for D^m splines.

Now we will use the same variational approach to study other splines which are generalizarions of $D^m-splines$. The elements necessary to define these splines are a proper function space and semi-inner product. Once this is done is possible to find the explicit expressions for them on scattered data, solving systems of linear equations with the structure (7.9) and (7.12).

7.3 Generalizations of D^m splines and seminorms

There are some important splines that can be seen as particular cases of our proposed framework (4.11), with $\min_{f \in \mathcal{X}} \tau_{\lambda_1, \lambda_2, z_\delta}[f]$, by extending the framework used for D^m-splines. For this, it is convenient to use Fourier analysis on the semi-inner product

$$(u,v) = \sum_{|\alpha|=m}^{n} \frac{m!}{\alpha!} \int_{\mathbb{R}^n} (\partial^\alpha u)(\partial^\alpha v) d\mathbf{x} \,. \tag{7.14}$$

By Parseval's formula

$$\int_{\mathbb{R}^n} (\partial^\alpha u(\mathbf{x}))(\partial^\alpha v(\mathbf{x})) \, d\mathbf{x} = \int_{\mathbb{R}^n} (\partial^\alpha u(\mathbf{x}))(\partial^\alpha v(\mathbf{x})) \, d\mathbf{x} \,,$$

so, it is natural to modify the D^m semi-inner product (7.14)and try other inner products like

$$\sum_{|\alpha|=m}^{n} c_\alpha \int_{\mathbb{R}^n} (\partial^\alpha u(\mathbf{x}))(\partial^\alpha v(\mathbf{x})) \, w(\mathbf{x}) d\mathbf{x} \,,$$

In this way it is possible to show that the seminorm

$$R[f] = \sum_{|\alpha|=m}^{n} c_\alpha \int_{\mathbb{R}^n} |(\partial^\alpha f(\xi))|^2 \, \|\xi\|^{2s} d\xi \,, \tag{7.15}$$

defines a space of continuous functions $X^{m,s}$ under the assumption $-m + n/2 < s < n/2$ (see [48,122,123]). The (m,s)- **spline** σ is the unique function in $X^{m,s}$, which minimizes the seminorm $R[f]$ in (7.15) and interpolates f on $\mathcal{A} = \{a_1, a_2, \cdots, a_M\}$, i.e. $\sigma(a_i) = f(a_i) = z_i$, $i = 1, \ldots, M$. The (m,s) spline is given in the form

$$\sigma(\mathbf{x}) = \sum_{i=1}^{M} \alpha_i \Phi_{m,s}(\mathbf{x} - a_i) + p(\mathbf{x}), \tag{7.16}$$

where p is a polynomial in $\Pi_{m-1}(\mathbb{R}^n)$, the α_i's satisfy $\sum_{i=1}^{M} \alpha_i q(\mathbf{x}) = 0$, for any q in $\Pi_{m-1}(\mathbb{R}^n)$ and $\Phi_{m,s}$ is the radial basis function, given for $\mathbf{x} \in \mathbb{R}^n$, by

$$\Phi_{m,s}(\mathbf{x}) = \begin{cases} \|\mathbf{x}\|^{2m+2s-n} \log(\|\mathbf{x}\|), & 2m+2s-n \in 2\mathbb{N} \\ \|\mathbf{x}\|^{2m+2s-n}, & 2m+2s-n \notin 2\mathbb{N} \end{cases} \,. \tag{7.17}$$

This is a generalization of D^m spline, adding a new parameter s.

7.4 Splines in tension (τ-splines)

The thin plate spline with tension (TPST) [63] may be deduced from the model of a thin plate subjected to lateral loads and mid-plane forces. This equation may be found in Timoshenko's book [180, 181]

$$\Delta^2 f = \frac{1}{D}\left[q + N_x \frac{\partial^2 f}{\partial x^2} + N_y \frac{\partial^2 f}{\partial y^2} - N_{xy} \frac{\partial^2 f}{\partial x \partial y} \right],$$

where f is the lateral deflection, q is the lateral load, N_x N_y N_{xy}, are the mid-plane forces, and D depends on the properties of the plate material. Setting $N_x = N_y$ and $N_{xy} = 0$. From the former expression is obtained an equation of the form $\Delta^2 f - \tau \Delta f = p$. Where τ is a tension parameter. In this case the seminorm is

$$R[f] = \int_{\mathbb{R}^2} (\frac{\partial^2 f}{\partial x^2})^2 + 2(\frac{\partial^2 f}{\partial x \partial y})^2 + (\frac{\partial^2 f}{\partial y^2})^2 \, dx \, dy + \tau \int_{\mathbb{R}^2} (\frac{\partial f}{\partial x})^2 + (\frac{\partial f}{\partial y})^2 \, dx dy. \quad (7.18)$$

It can be proved that there exist a Hilbert space subspace of $C(\mathbb{R}^n)$ where there is an element σ_τ called spline in tension, that minimize the seminorm (7.18). σ_τ is given in the form

$$\boldsymbol{\sigma_\tau}(\mathbf{x}) = \sum_{i=1}^{M} \alpha_i \Phi_\tau(\|\mathbf{x} - a_i\|) + p(\mathbf{x}), \quad (7.19)$$

where p is a polynomial in $\Pi_{m-1}(\mathbb{R}^n)$, the α_i's satisfy $\sum_{i=1}^{M} \alpha_i q(\mathbf{x}) = 0$, for any q in $\Pi_{m-1}(\mathbb{R}^n)$ and $\Phi_\tau(\mathbf{x})$ is the radial basis function, given for $\mathbf{x} \in \mathbb{R}^n$, by

$$\Phi_\tau(\mathbf{x}) = \mathcal{K}_0(\tau \|\mathbf{x}\|) + \log(\|\mathbf{x}\|), \quad (7.20)$$

when the data have the form $D = \{(a_i, z_i) \in \mathbb{R}^n \times \mathbb{R}\}_{i=1}^{M}$ with $n = 2$. It is possible to show [26] that the function

$$\Phi_\tau(\mathbf{x}) = C(e^{-\tau\|\mathbf{x}\|} + \tau \|\mathbf{x}\|), \quad (7.21)$$

also gives a solution to the interpolation problem.

7.5 Conclusions

We have deduced an interpolating spline using a variational approach on Hilbert spaces. The most relevant features of these splines are their generalization and reproducing

properties applicable on scattered data, it is to say, there are not very restrictive conditions on the spatial distribution of centers. Following this method we show that (m,s) splines and tension splines are particular cases of our approach. These splines also minimize some seminorm with physical or geometrical interpretation.

Chapter **8**

Surface approximation from noisy data

8.1 Introduction

In the former chapter we have solved the minimal norm interpolation problem using the methods of reproducing kernels and projection on Hilbert spaces. Now, we consider the problem of smoothing of noisy data in the framework of Schwartz distributions. In other words, we want to solve the approximation problem (P2) proposed in (4.10b)

$$\min_{f \in \mathcal{X}} \boldsymbol{\tau}_{\lambda, z_\delta} = \frac{1}{M} \sum_{i=1}^{M} (f(a_i) - z_i)^2 \; + \; \lambda\, R\,[f], \text{ with } \{f(a_i) \approx z_i\}_{i=1}^{M}. \quad (8.1)$$

That is, to solve the inverse problem of reconstruction by Tikhonov regularization, in particular, the reconstruction of surfaces from scattered data. We also study the most general results about regularization of inverse problems. In this case data are considered with or without noise. The interesting thing is that these results provide a general answer for several forms of data and can be found by solving a linear system. The splines we obtain here include all the case studied in chapter TPS and splines in tension.

It was Hadamard [81], the first to speak about well-posed problems as having the properties of existence, uniqueness and stability of the solution. However, many important inverse problems in science and engineering lead to ill-posed inverse problems, though the corresponding direct problems are well posed. Frequently, existence and uniqueness can be forced by enlarging or reducing the solution space as we have done with distribution spaces.

8.2 Solution of smoothing in 3D

When the solution of a problem does not depend continuously on the data, the computed solution may be very different from the true solution. Again, we have that there is no way to overcome this difficulty unless additional information about the solution is available. Therefore, a reconstruction strategy requires additional *a priori* information about the solution.

As we have said before, this can be done by Tikhonov regularization. The main idea supporting Tikhonov regularization theory is that the solution of an ill-posed problem can

be obtained using a variational principle, which contains both the data and prior smoothness information.

Now we show the solution of (8.1) by finding the TPS for noisy point clouds, $D = \{(a_i, z_i) \in \mathbb{R}^2 \times \mathbb{R}\}_{i=1}^{M}$ and the smoothing functional $R[f]$ from (7.2), with $m = 2$

$$R[f] = \int_{\mathbb{R}^2} \left(\frac{\partial^2 f}{\partial x^2}\right)^2 + 2\left(\frac{\partial^2 f}{\partial x \partial y}\right)^2 + \left(\frac{\partial^2 f}{\partial y^2}\right)^2 dx\,dy.$$

We then have to minimize

$$\tau_\lambda [f] = \sum_{i=1}^{M} (f(a_i) - z_i)^2 + \lambda R[f]$$

$$= \sum_{i} (f(a_i) - z_i)^2 + \lambda \int_{\mathbb{R}^2} \left(\frac{\partial^2 f}{\partial x^2}\right)^2 + 2\left(\frac{\partial^2 f}{\partial x \partial y}\right)^2 + \left(\frac{\partial^2 f}{\partial y^2}\right)^2 dx\,dy$$

$$= \int_{\mathbb{R}^2} \sum_{i} (f(\mathbf{x}) - z_i)^2 \delta(x - a_i) + \lambda \int_{\mathbb{R}^2} \left(\frac{\partial^2 f}{\partial x^2}\right)^2 + 2\left(\frac{\partial^2 f}{\partial x \partial y}\right)^2 + \left(\frac{\partial^2 f}{\partial y^2}\right)^2 dx\,dy.$$

Using the Euler Lagrange equation

$$[F]_{\mathbf{u}} = F_u - \frac{\partial}{\partial x} F_{u_x} - \frac{\partial}{\partial y} F_{u_y} + \frac{\partial^2}{\partial x^2} F_{u_{xx}} + \frac{\partial^2}{\partial x \partial y} F_{u_{xy}} + \frac{\partial^2}{\partial y^2} F_{u_{yy}} + \cdots + (-1)^n \frac{\partial}{\partial y^n} F_{u_{yy\cdots y}} = 0,$$

,

for this functional we obtain

$$2\sum_{i} (f(\mathbf{x}) - z_i)^2 \delta(x - a_i) + 2\lambda \left(\frac{\partial^4 f}{\partial x^4} + \frac{\partial^4 f}{\partial x^2 \partial y^2} + \frac{\partial^4 f}{\partial y^4}\right) = 0,$$

and simplifying

$$\sum_{i} (f(\mathbf{x}) - z_i) \delta(x - a_i) + \lambda \Delta^2 f = 0,$$

where $\Delta^2 f = \frac{\partial^4 f}{\partial x^4} + \frac{\partial^4 f}{\partial x^2 \partial y^2} + \frac{\partial^4 f}{\partial y^4}$ is the biharmonic operator. In this way the differential

equation $\Delta^2 f = \sum_{i=1}^{M} \frac{(f(\mathbf{x}) - z_i)}{\lambda} \delta(x - a_i)$ is obtained and its solution is

$$f(\mathbf{x}) = K * \sum_{i=1}^{M} \frac{(f(\mathbf{x}) - z_i))}{\lambda} \delta(x - a_i),$$

where $K(\mathbf{x},\mathbf{y}) = \phi_{2,2}(\| \mathbf{x} - \mathbf{y} \|_2)$ is again the fundamental solution of the operator Δ^2. Doing $\alpha_i = \frac{(f(a_i) - z_i)}{\lambda}$, we have

$$f(\mathbf{x}) = K * \sum_{i} \alpha_i \delta(\mathbf{x} - a_i) = \sum_{i} \alpha_i K * \delta(\mathbf{x} - a_i) = \sum_{i} \alpha_i K(\mathbf{x} - a_i).$$

As the null space of (8.2) is $\Pi_1(\mathbb{R}^2)$ we have to add a term $p(\mathbf{x}) \in \Pi_1(\mathbb{R}^2)$ to the final expression for the solution of the optimization problem

$$S_\lambda(\mathbf{x}) = \sum_i \alpha_i K(\mathbf{x} - a_i) + p(\mathbf{x}) = \sum_{i=1}^{M} \alpha_i \Phi_{m,n}(\| \mathbf{x} - a_i \|) + p(\mathbf{x}).$$

This is the same expression obtained in (7.6) but with a change in the **interpolation matrix**, which has the form

$$\begin{bmatrix} A + \lambda I & P \\ P^t & 0 \end{bmatrix} \begin{bmatrix} \alpha \\ \beta \end{bmatrix} = \begin{bmatrix} z \\ 0 \end{bmatrix}, \qquad (8.2)$$

and I is the identity matrix of dimension M. These results are valid for data points on $\mathbb{R}^n$ with $D = \{(a_i, f_i) \in \mathbb{R}^n \times \mathbb{R}\}_{i=1}^{M}$. It is also possible to show that the solutions $S_\lambda(\mathbf{x})$, with $\lambda > 0$ are approximations $(S_\lambda(a_i) \approx f(a_i))$ that converge to the interpolation. This means that $\lim_{\lambda \to \infty} S(\mathbf{x})$ is the minimum square regression over $\Pi_{m-1}(\mathbb{R}^n)$ and $\lim_{\lambda \to 0} S(\mathbf{x})$ is the interpolant of the data D. In other words, the regularization approach gives a compact solution applied to both interpolation and approximation. This is shown in the following result for many kinds of data.

8.3 Extending Tikhonov regularization

Originally Tikhonov proposed the minimization of the functional.

$$\min_{f \in \mathcal{X}} \tau_{\lambda, z_\delta}[f] = \frac{1}{M} \sum_{i=1}^{M} (f(a_i) - z_i)^2 + \lambda R[f],$$

with $R[f] = \| f \|^2$. Later, other regularizers were introduced in the form $R[f] = | P f |_{\mathcal{X}}^2$, where $|*|_{\mathcal{X}}$ is a seminorm and P a differential operator. Now, we consider our proposed model in the form

$$\min_{f \in \mathcal{X}} \tau_{\lambda_1, \lambda_2, z_\delta}[f] = \frac{1}{M} \sum_{i=1}^{M} (f(a_i) - z_i)^2 + \lambda_1 R_1[f] + \lambda_2 R_2[f]. \qquad (8.3)$$

Observe that if we add two functionals of the form $\lambda_1 R_1[f] + \lambda_2 R_2[f]$, we could write $\lambda_1(R_1[f] + \frac{\lambda_2}{\lambda_1} R_2[f])$. So we will adopt this form. In particular our functionals are some instances of Duchon seminorm

$$R[f] = J_m[f] = \int_{\mathbb{R}^n} \sum_{|\alpha|=m} \frac{m!}{\alpha!} | \partial^\alpha f(\mathbf{x}) |^2 d\mathbf{x},$$

for different values of m. The key idea is to combine functionals with different degree of smoothness. We first consider J_2 with J_1 ($m = 1, 2$), obtaining the functional

$$\min_{f \in \mathcal{X}} \tau_{\lambda_1, \lambda_2, z_\delta}[f] = \frac{1}{M} \sum_{i=1}^{M} (f(a_i) - z_i)^2 + \lambda_1 (J_2[f] + \lambda_2^2 J_1[f])$$

$$= \frac{1}{M} \sum_{i=1}^{M} (f(a_i) - z_i)^2 \quad \lambda_1 \left(\int_{\mathbb{R}^2} (f_{xx}^2 + 2f_{xy}^2 + f_{yy}^2) + \lambda_2^2 \int_{\mathbb{R}^2} (f_x^2 + f_y^2) \right). \qquad (8.4)$$

Thus, applying the methods of variational calculus on $\tau_{\lambda_1, \lambda_2, z_\delta}[f]$ gives the PDE

$$(-\lambda_2^2 \Delta + \Delta^2) K = \delta, \qquad (8.5)$$

where K is a fundamental solution. The solution to this and other equations of the regularization functionals are given in table 8.1. They have been chosen following the criteria designed in chapter five, about the global or local character of the functionals. We try to mix both characteristics in the same expression.

The greater the value of m, the smoother the functional. Here it is important to remember that the variational derivative of $J_m[f]$ is $\Delta^m u$. Due to the physical interpretation of parameters we have used $\varphi = \lambda_1$ and $\tau = \lambda_2$.

Functional	PDE	Kernel
$J_2[f]$	$\Delta^2 K = \delta$	$\Phi_0(r) = r^2 \log r$
$J_2[f] + \tau^2 J_1[f]$	$(-\tau^2 \Delta + \Delta^2) K = \delta$	$\Phi_1(r) = -\dfrac{1}{2\pi \varphi^2}(\log r + K_0(\varphi r))$ $\Phi_\tau(\mathbf{x}) = C(e^{-\tau \|\mathbf{x}\|} + \tau \| \mathbf{x} \|)$
$J_2[f] + \tau^2 J_3[f]$	$(\Delta^2 - \tau^2 \Delta^3) K = \delta$	$\Phi_2(r) = \dfrac{1}{2\pi}(\tau^2 \log r + \dfrac{r^2}{4} \log r + \tau^2 K_0(\dfrac{r}{\tau}))$
$\varphi J_1[f] + J_2 + \tau^2 J_3[f]$	$(-\varphi\Delta + \Delta^2 - \tau^2 \Delta^3) K = \delta$	$\Phi_3(r) = -\dfrac{1}{2\pi\varphi^2}(-\log r + C_1 K_0(\sqrt{v}\, r) - C_2 K_0(\sqrt{w}\, r))$

Tab. 8.1: Splines deduced from variational approach, to be applied on scattered data. Each spline can be obtained by solving the Partial Difeerential Equation (PDE) that appears in the second column. Due to their physical origin we have used $\varphi = \lambda_1, \tau = \lambda_2$ in (8.3).

$$v = \frac{1 + \sqrt{1 - 4\tau^2 \varphi^2}}{2\tau^2}, \quad w = \frac{1 - \sqrt{1 - 4\tau^2 \varphi^2}}{2\tau^2}, \quad C_1 = \frac{w}{v - w}, \quad C_2 = \frac{v}{v - w},$$

$\mathcal{K}_0$ is the modified Bessel function of the second kind with $\mathcal{K}_v(z) = \dfrac{\pi}{2}\dfrac{I_{-v}(z)-I_v(z)}{\sin(v\pi)}$, and

$$I_v(z) = \left(\frac{z}{2}\right)^2 \sum_{k=0}^{\infty} \frac{\left(\dfrac{z^2}{4}\right)^k}{k\,!\,\Gamma(v+k+1)} \ . \text{ For our case } v = 0 \ .$$

8.5   The Relation with Radial basis functions

The generalization of splines to higher dimensions are called *surface splines* or radial *basis functions*, they are obtained by minimization of norms or functionals and have the rotational and translation invariance properties. Radial basis approximators have the form

$$S(\mathbf{x}) = \sum_{j=1}^{M} \alpha_j \Phi(\|\,\mathbf{x} - a_j\,\|) + p(\mathbf{x}), \tag{8.6}$$

where $p(\mathbf{x})$ is a low degree polynomial. For example, the cubic spline may be expressed in this way with $\Phi(r) = r^3$. If we use the spline S to interpolate the scattered data $\mathcal{A} = \{a_1, a_2, \cdots, a_M\}$ then S is completely determined by the scalars or weights α_i's. This is done solving the linear system

$$\sum_{j=1}^{M} \alpha_j K(a_k, a_j) + \sum_{i=1}^{N} \beta_i p_i(a_k) = z_k \quad 1 \le k \le M$$

$$\sum_{j=1}^{M} \alpha_i p_i(a_j) \quad + \quad 0 \quad = 0 \quad 1 \le i \le N \ , \tag{8.7}$$

such that $\boldsymbol{\alpha} = (\alpha_1, \ldots, \alpha_M) \in \mathbb{R}^M$ $\boldsymbol{\beta} = (\beta_1, \ldots, \beta_M) \in \mathbb{R}^N$ and the polynomials $\{p_j\}_{j=1}^{N}$ form a basis for $\Pi_{m-1}(\mathbb{R}^n)$. In this way the system can be written as

$$\begin{bmatrix} A & P \\ P^t & 0 \end{bmatrix} \begin{bmatrix} \alpha \\ \beta \end{bmatrix} = \begin{bmatrix} z \\ 0 \end{bmatrix} \ ,$$

with $A_{i,j} = K(a_i, a_j) = \Phi(\|\, a_i - a_j\,\|)$ $i, j = 1, \cdots, M$, $P_{ij} = p_j(a_i)$ $i = 1, \ldots, M, \quad j = 1, \ldots, N$ $\boldsymbol{\alpha} = (\alpha_1, \ldots, \alpha_M), z = (z_1, \ldots, z_M)$. Sometimes the spline does not have polynomial term $p(\mathbf{x})$, then we have $A\boldsymbol{\alpha} = z$.

We have seen (chapter 6) that under certain conditions $K(\mathbf{x}, \mathbf{y})$ produce positive definite matrices $A_{i,j} = K(a_i, a_j)$ and then the matrix is non-singular.

Chapter **9**

Applications, implementations and numerical experiments

9.1 Introduction

The variational framework we have built can be applied to multiple classes of data. In particular, this chapter is devoted to test and show the performance of our methods in the reconstruction of data coming from surfaces, given as point clouds or Cartesian coordinates. We analyze the splines of table 8.1, which can be derived using the theory of the last three chapters. For evaluating the performance of these splines we have chosen some 3D objects with different degree of complexity in their shape and topology. Our models are also analyzed in terms of the key ideas of approximation theory, density, convergence and error bounds of the approximators on scattered data. We also include some details about the algorithms developed, their implementation and condition number of the interpolation matrix. We obtain some results that may be surprising in current literature, because some of these splines may have an equal or better performance than thin plate splines.

9.2 Representation of surfaces

In real world problems we need a representation of surfaces in an operative form in order to be used into a computer. This representation is given as discrete points. Nevertheless it is important to represent a surface as a continuous set of points.

Explicit representation $z = f(x, y)$

This is the usual mathematical representation and corresponds to the definition of a function
$f : \mathbb{R}^2 \to \mathbb{R}$. It has the property that all the theories of functional analysis we develop in this work assume this representation. One disadvantage (fig.9.1) is that in many real point clouds there are points (x, y) with more than one value for z.

Fig. 9.1: This objects cannot be represented with an explicit form $z = f(x, y)$

The idea of a function $f : \mathbb{R}^n \to \mathbb{R}^m$ is the basic tool for any mathematical model and can be adapted for being applied to any kind of object or data.

Parametric representation $\mathbf{r}(u,v) = (x(u,v),\ y(u,v),\ z(u,v))$

This representation is more useful in the geometric methods described in chapter 2. It is the representation used in differential geometry, where any regular parametric surface can be described in the form, such that the vectors $\mathbf{r}_u, \mathbf{r}_v$ generate the tangent plane at each point of the surface with

$$\mathbf{r}_v = \frac{\partial \mathbf{r}}{\partial u} = (\frac{\partial x}{\partial u}, \frac{\partial y}{\partial u}, \frac{\partial z}{\partial u}), \qquad \mathbf{r}_v = \frac{\partial \mathbf{r}}{\partial v} = (\frac{\partial x}{\partial v}, \frac{\partial y}{\partial v}, \frac{\partial z}{\partial v}).$$

9.3 Models and objects analyzed

Our purpose is to evaluate our regulation framework as well as its extensions. In order to make comparisons with the big amount of classical and new literature, this evaluation has been done using some well known objects given as **point clouds**, in the **explicit** form $z = f(x, y)$ or in **parametric** form. The first publications with some of these objects appeared in the early 80's. Nowadays there exist a big repository and sources for point clouds that vary from very simple figures with thousands of points to very complex objects in the order of millions points. The models we have chosen by their relevance to our work are shown below.

1. *Franke's data ("landslide")*

$$f(x, y) = \begin{cases} \dfrac{1}{2} & y \le \dfrac{2}{5} \\ \dfrac{1}{2}\left(1 - \dfrac{25}{9}(y - \dfrac{2}{5})^2\right) & y > \dfrac{2}{5} \wedge x \le \dfrac{1}{5}, \\ \dfrac{125}{72}(1 - y)^2(1 - x) & y > \dfrac{2}{5} \wedge x > \dfrac{1}{5} \end{cases}$$

$$(9.1)$$

2. *Franke's function*

$$f(x,y) = 0.75\,e^{-\frac{1}{4}((9x-2)^2+(9y-2)^2)} + 0.75\,e^{-\frac{(9x+1)^2}{49}+\frac{(9y+1)}{10}}$$

$$+0.5e^{-(9x-7)^2-\frac{(9y-3)^2}{4}} + 0.2e^{-((9x-4)^2+(9y-7)^2)}. \qquad (9.2)$$

3. *Peaks surface*

$$f(x,y) = 3(1-x)^2 \exp(-x^2-(y+1)^2) - 10(\frac{x}{5}-x^3-y^5)\exp(-x^2-y^2)$$

$$-\frac{1}{3}\exp(-(x+1)^2-y^2). \qquad (9.3)$$

4. *The Tube.*

$$z(u,v) = 1 - e^{\frac{u}{3\pi}} - \sin v + e^{\frac{u}{6\pi}}\sin v$$

$$y(u,v) = 2(-1+e^{\frac{u}{6\pi}})\sin u \cos^2(\frac{v}{2})$$

$$x(u,v) = 2(1-e^{\frac{u}{6\pi}})\cos u \cos^2(\frac{v}{2}). \qquad (9.4)$$
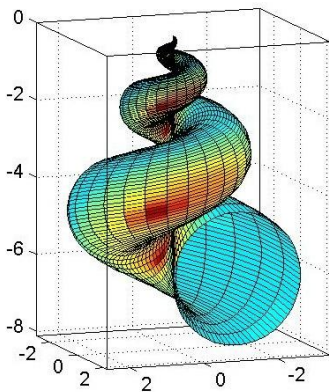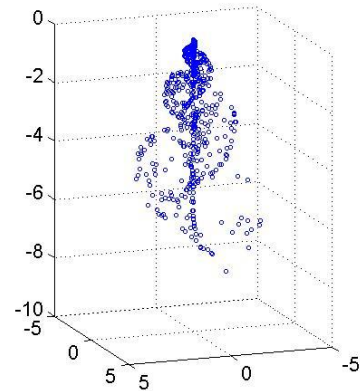
(a)   (b)

Fig. 9.2: The surface in (a) represents the parametric equation (9.4). In (b) we show a set of 200 sample points on this surface.
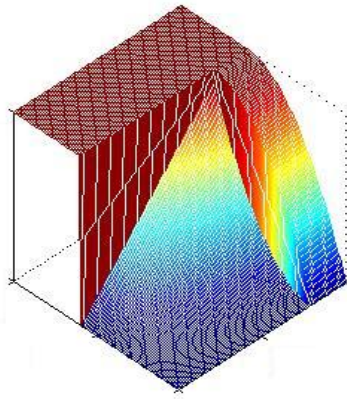
(a)
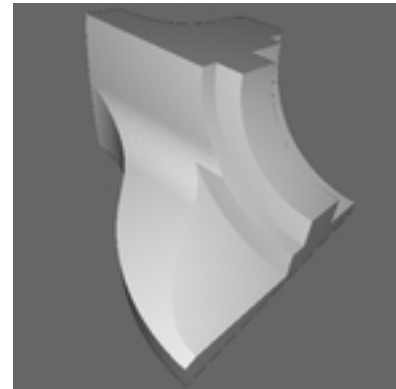
(b)
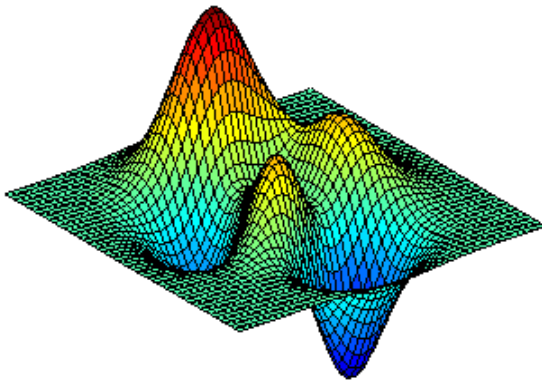
(c)
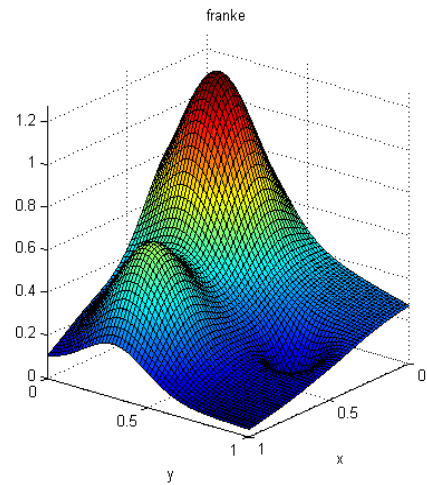
(d)

Fig. 9.3: The surface in (a) corresponds to equation (9.1), it is known as Franke´s data. This surface shares many features with the "fandisk" in (b). By their edges and vertices, they are both used to test reconstruction of discontinuities. The surface in (c) is generated by the function (9.3) and it is well known to MATLAB users with the name "peaks". The surface (d) is known as Franke's function and is the graph of (9.2). It has been widely used in many publications and has become a standard test for surface reconstruction methods.

(a)	(b)
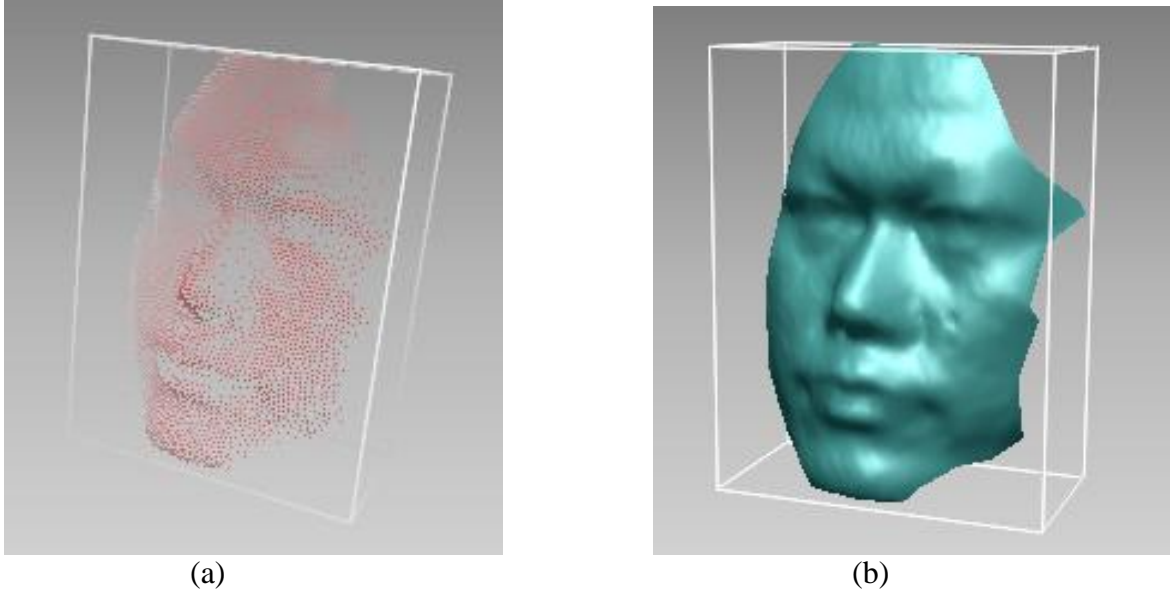
Fig. 9.4: The range scanning point cloud in (a) has 10.000 points and we have used it to test our method. In (b) is shown a reconstruction of these noisy data taking 2000 points from (a) and applying TPS.

9.4 Interpolation and Smoothing with surface splines

The theory developed in this thesis produce surface splines represented as radial basis functions. This property makes them very suitable for applications on scattered data. These splines have the form

$$S_{f,A}(\mathbf{x}) = \sum_{i=1}^{M} \alpha_i \Phi(\| \mathbf{x} - a_i \|) + p(\mathbf{x}), \qquad (9.5)$$

where $p(\mathbf{x})$ is a low degree polynomial. Although we can use any base for these polynomial terms, it is common to use the base $\mathbf{x}^{\alpha} = x_1^{\alpha_1} x_2^{\alpha_2} \cdots x_n^{\alpha_n}$, thus, $\{1, x, y\}$, $\{1, x, y, x^2, y^2, xy\}$, $\{1, x, y, z, x^2, y^2, z^2, xy, xz, yz\}$ are taken as basis for $\Pi_1(\mathbb{R}^2), \Pi_2(\mathbb{R}^2)$ and $\Pi_2(\mathbb{R}^3)$, respectively. In general, $\{\mathbf{x}^{\alpha}\}, \alpha \in Z^n, |\alpha| \leq k$ is taken as a basis for $\Pi_k(\mathbb{R}^n)$.

We have shown (chapter 6, 7, 8) that these interpolants are linear combinations in terms of the fundamental solutions of some partial differential equations. In particular, we studied splines related with the PDE's of table 8.1, where $\mathcal{K}_0$ is the modified Bessel function of the second kind (*besselk* in Matlab) and where $\Phi(r)$ is one of the functions in (9.2).

$$
\begin{cases}
\Phi_0(r) = r^2 \log r \qquad (TPS) \\[2mm]
\Phi_1(r) = -\dfrac{1}{2\pi\,\varphi^2}\,(\log r + \mathcal{K}_0(\varphi\, r)) \\[3mm]
\Phi_2(r) = \dfrac{1}{2\pi}\,(\tau^2 \log r + \dfrac{r^2}{4}\log r + \tau^2 \mathcal{K}_0(\dfrac{r}{\tau})) \\[3mm]
\Phi_3(r) = -\dfrac{1}{2\pi\varphi^2}\,(-\log r + C_1 \mathcal{K}_0(\sqrt{v}\, r) - C_2 \mathcal{K}_0(\sqrt{w}\, r)) \\[3mm]
\Phi_\tau(\mathbf{x}) = C(e^{-\tau\|\mathbf{x}\|} + \tau\,\|\,\mathbf{x}\,\|) \quad \textit{tension spline}
\end{cases}
\qquad . \qquad (9.6)
$$

From this list, we have already studied thin plate spline $\Phi_0(r) = r^2 \log r$ in our paper [129]; showing that it has a very good performance for interpolation and smoothing of scattered data. Our results are similar to those quoted in the literature. However there exist few reports or no one about the application and performance of the other functions in (9.6), so in this chapter we are going to develop algorithms and numerical tests to measure the performance of these functions and compare it with thin plate spline, which is considered up to now one of the most efficient interpolators. It is possible to show that the functions of this family are conditionally positive definite [27].

For finding the explicit expression of the spline $S_{f,A}(\mathbf{x}) = \sum_{i=1}^{M} \alpha_i \Phi(\|\,\mathbf{x} - a_i\,\|) + p(\mathbf{x})$ it is necessary to determine the coefficients α_i's in the first term and c_i's for the polynomial $p(\mathbf{x}) \in \Pi_{m-1}(\mathbb{R}^n)$. This is done solving the $(M + N)$ system (8.5) of linear equations, where $N = \dim \Pi_{m-1}(\mathbb{R}^n)$. In real cases N is always very small compared to M so the complexity of solving the system is $O(M^3)$.

Other source for increasing the computer time is represented by the evaluation of $S_{f,A}(\mathbf{x})$ on a grid. When the grid is very large there exist different strategies and fast algorithms [15]. We have implemented numerical algorithms for solving the system and evaluating the spline using Matlab with $M \approx 2000$. It is worth to observe in fig.9.5 that a relatively small number of points produce a good visualization. This fact suggests splines as a good method for mesh and image compression.

9.5 How to choose an interpolant

There are three very useful criteria to judge effectiveness of an interpolant or approximator: *density, interpolation* and *order of convergence.*

Density

A subset U in a normed space $\mathcal{X}$ is said to be fundamental if the set of all linear combinations from U is **dense** in $\mathcal{X}$. Otherwise, $\forall f \in \mathcal{X}$ and $\forall \varepsilon > 0$ there is a vector $\sum_{j=1}^{M} \alpha_j u_j$ with $u_j \in U$, such that

$$\left\| f - \sum_{j=1}^{M} \alpha_j u_j \right\| \leq \varepsilon .$$

This is crucial because our interpolators are constructed on linear combinations of translates of a fixed function. It is known that if Ω is a compact subset of $\mathbb{R}^n$ and $\mathcal{G}$ is the subspace of $C(\mathcal{G})$ defined by $\mathcal{G} = span\{ x \mapsto \Phi(\| \mathbf{x} - a_i \|) : \mathbf{x} \in \Omega \}$ then $\mathcal{G}$ is dense in $C(\mathcal{G})$ for functions $\Phi(r)$ of (9.6), among others. For example, it can be proved [7,109] that the space $\mathcal{S} + \Pi_{m-1}(\mathbb{R}^n)$ is dense in the space $X^{m,s}$ of (m,s)-splines.

Interpolation and error bounds

The splines S we have studied are interpolating, that is $S(a_i) = f(a_i)$ $i = 1, \dots, M$ or simply $S|_{\mathcal{A}} = f$. One important observation is that we can always interpolate uniquely with conditionally positive definite functions if we add polynomials to the interpolant and if the only polynomial that vanishes on our set of data centers is zero, that is, $\mathcal{A}$ is $\Pi_{m-1}(\mathbb{R}^n)$-unisolvent.

Theorem 9.1 ([191]) Let Φ be a conditionally positive definite function of order m on $\Omega \subseteq \mathbb{R}^n$, and let the data set $\mathcal{A} = \{a_1, a_2, \dots, a_M\} \subseteq \Omega$ be $\Pi_{m-1}(\mathbb{R}^n)$-unisolvent. Then the system (8.10) is uniquely solvable.

The accuracy of the interpolant can be estimated applying the setting of theorem A.2 (see appendix) with $V = \{u \in \mathcal{H} : L_i(u) = 0, i = 1, \dots, M\}$. We have

Theorem 9.2. Let $L_i(f) = f(a_i)$, $i = 1, \dots, M$, be continuous linear functionals on $\mathcal{H}$ such that $u_\mathbf{x}$ is the representer for the point $\mathbf{x}$. Let $f \in \mathcal{H}$ have minimal norm interpolant S with $S = \sum_{i=1}^{M} \alpha_i u_i$. Let P be the orthogonal projection from $\mathcal{H}$ onto V, then

$$\left| f(\mathbf{x}) - S(\mathbf{x}) \right| \leq \left\| P u_\mathbf{x} \right\| \sqrt{[f,f]} .$$

Convergence

The convergence of interpolants on scattered data can be studied in terms of the spatial density of the set of nodes $\mathcal{A} = \{a_1, a_2, \dots, a_M\}$. For this purpose the Hausdorff or fill distance

$$h_{A,\Omega} := \sup_{y \in \Omega} \min_{a_j \in A} \| y - a_j \|, \tag{9.7}$$

of the set $\mathcal{A}$ within an enclosing domain Ω is used. $h_{A,\Omega}$ gives the radius of the largest ball without data sites or "data-site free ball" in Ω.

(a) MAX   (b) RMS   (c) $h_{A,\Omega}$
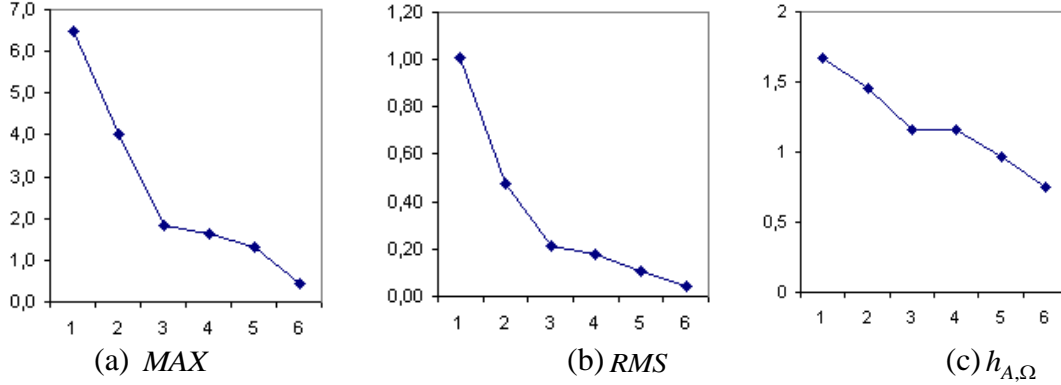
Fig. 9.5: Illustration of the convergence of $S_{f,A}$. (a) The Maximum Error MAX and (b) Root Mean Square Error RMS decrease when the Hausdorff measure (c) $h_{A,\Omega} \rightarrow 0$ as a consequence of increasing M.

A central idea in the interpolation problem is that as the set $\mathcal{A}$ "fills" Ω, the error between the function and its interpolant should go to zero.; this is seen in the values of $h_{A,\Omega}$. If $f \in C(\Omega)$ say, and S_f is the interpolant, then one might hope to obtain $\| f - S_f \| = \mathcal{O}(h^k)$ as $h \rightarrow 0$, where k is some measure of the smoothness of f. If we take a sequence of observational data such that $h_{A,\Omega}$ tends to zero, the reproduction error always behaves like a power $h_{A,\Omega}^k$, where $k > 0$ increases with the smoothness of $\Phi(r)$. If $\Phi(r)$ is an analytic function as the Gaussian and Multiquadrics, the error decreases exponentially like $ce^{-c/h}$ with $c > 0$ as shown by Madych and Nelson [112].

But sometimes things are not so easy because this excellent convergence may have the problem of an ill-conditioned system, when $h \rightarrow 0$. In some cases it is necessary to apply additional techniques as preconditioning. Duchon [48] showed that under certain conditions

$$\lim_{h_{A,\Omega} \rightarrow 0} \| S_{f,A} - f^{\Omega} \|_{m,s} = 0,$$

where f^{Ω} denotes the unique element of minimal seminorm $R[u] = J_m[u]$ in the set
$$\{ u \in X_{m,s} : u \mid_{\Omega} = f \}.$$

There exist similar results for interpolating and smoothing splines that include (9.6) [7].

Example 9.1 Testing interpolation and convergence by splines. In this example we test the convergence behavior of TPS for interpolating the peaks surface on different number of scattered data in the region $\Omega = [-4, 4] \times [-4, 4]$. We have obtained the model (9.1) for TPS using a set $\mathcal{A} = \{a_i, a_2, \ldots, a_M\}$ of M scattered data, then this spline is used to approximate the peaks surface with explicit representation

$$f(x, y) = 3(1 - x)^2 \exp(-x^2 - (y+1)^2) - 10(\frac{x}{5} - x^3 - y^5)\exp(-x^2 - y^2) - \frac{1}{3}\exp(-(x+1)^2 - y^2),$$

on a second fixed set of points $\mathcal{B}$. In the fig. 9.3 the improvement of accuracy with decreasing values for max error (MAX) (see equation 9.9) and Root Mean Square Error (RMS) (9.10) as the Hausdorff measure $h_{A,\Omega} \to 0$ is observed. This behavior is also illustrated in table 9.1.

Test	M	$h_{A,\Omega}$	RMS	MAX
1	50	1,6653	1,0076	6,4676
2	100	1,4504	1,4760	4,0028
3	200	1,1573	0,2146	1,8246
4	300	1,1573	0,1769	1,6232
5	400	0,9695	0,1044	1,3003
6	500	0,7486	0,0420	0,4374

Tab. 9.1: Results of numerical experiment for interpolation of peaks surface. Increase in the number of points M, implies decreasing values in $h_{A,\Omega}$, RMS and MAX.

Most of the existing results about interpolation, convergence and error bounds for radial basis functions depend on the variational properties and positive definiteness of $\Phi(r)$, so they are applicable to the interpolants studied here, for more details see [191].

9.6 Reconstruction of data without noise

Although real point clouds are commonly noisy, the interpolation of exact data it is an important criteria for surface reconstruction methods and it is the first numerical test performed on the splines studied here. In this case our splines have a very similar behavior in their reproducing quality of the tested functions but they may have great differences in the execution time.

The table 9.2 shows the execution time in seconds of the splines in (9.6). For obtaining the data in this table we have interpolated peaks surface, taking $M = 300$ scattered points (x, y) in the region $\Omega = [-3,3] \times [-3,3]$.

The time includes all the steps from the generation of the points up to the visualization of the spline. Obviously the interpolation improves with an increasing number of points M.

M	$\Phi_0 (TPS)$	Φ_1	Φ_2	Φ_3	Φ_τ
50	6.5310	37.5780	37.5630	70.5000	6.5150
100	6.5310	76.0160	76.0000	144.4220	6.9840
300	40.8910	240.7660	240.8590	451.6400	41.0930
600	90.8280	525.5470	518.2500	975.7660	90.2180
1000	168.6720	958.2190	951.3910	1783.3750	171.4220

Tab. 9.2: Execution time (in seconds) of interpolation with splines.
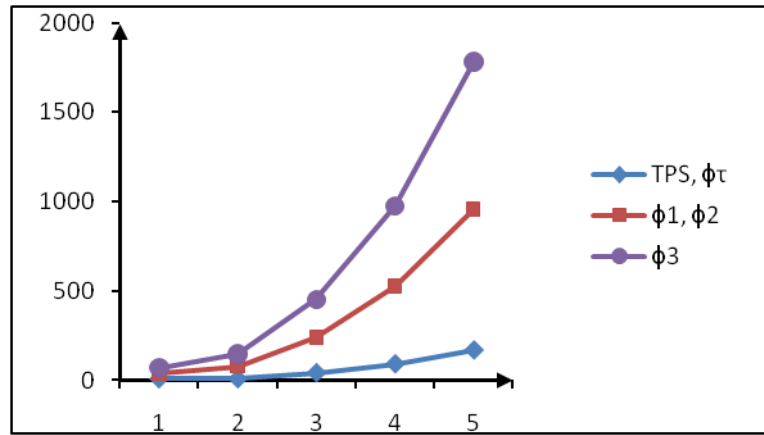
Fig. 9.6: Visual comparison of execution times for splines. As we can see the execution times for the interpolation are longer for Φ_1, Φ_2, Φ_3 due to the evaluation of Bessel function in these splines. As we can see in table 9.2, the values of Φ_1 and Φ_2 are very similar, so their graphs are superimposed . A similar situation occurs for TPS and tension spline.

(a) $M = 200$

(b) $M = 200$, Φ_0 (TPS)

(c) $M = 200$, Φ_1, $\tau = 0.1$
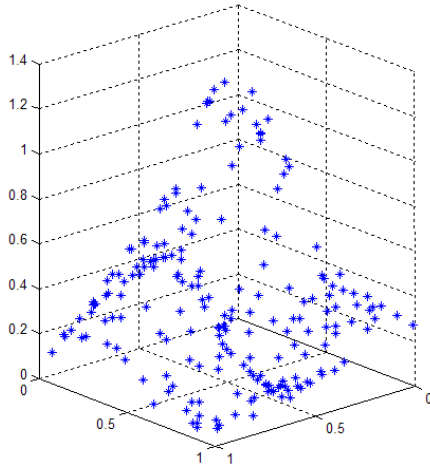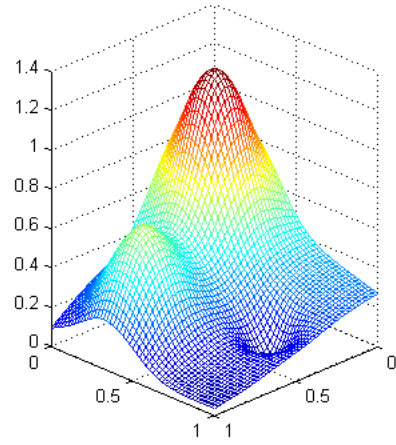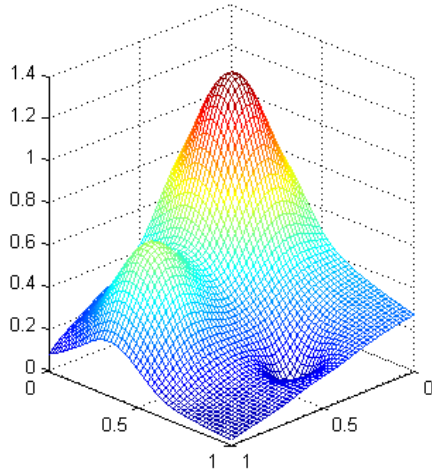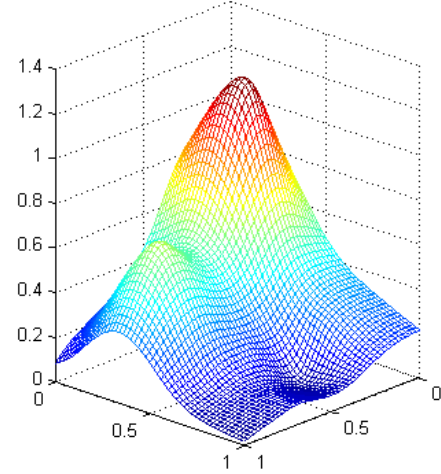
(d) $M = 40$, Φ_1, $\tau = 0.1$

Fig. 9.7: (a) Three dimensional scatter plot of $M = 200$ points on Franke's surface. These points are used to reconstruct the surface. Figures (b), (c) ,(d) show a similar accuracy for TPS and spline Φ_1; nevertheless, the performance of Φ_1 can be improved by tuning the parameter τ.
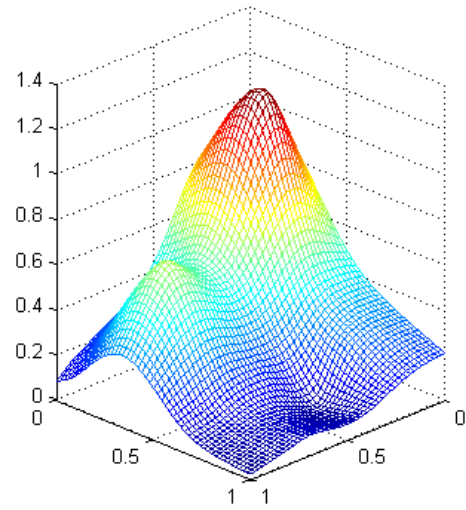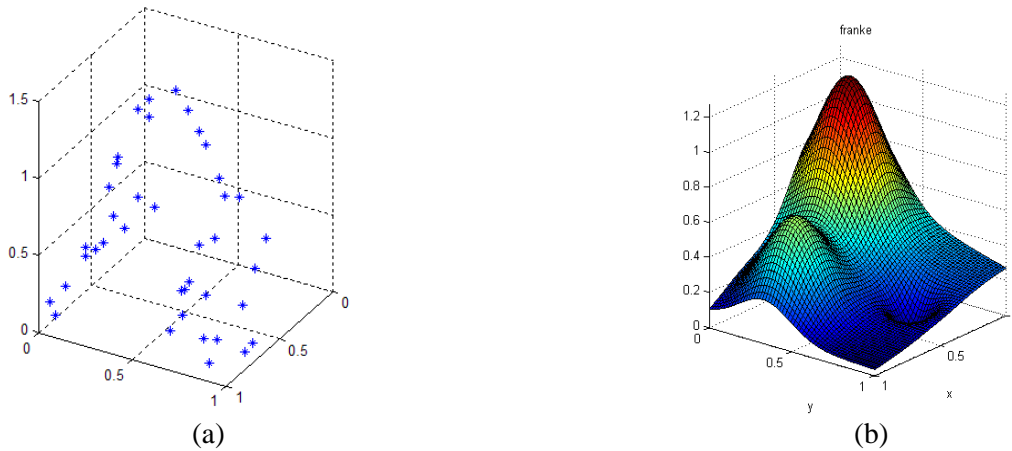
(a) $M = 40$, Φ_τ, $\tau = 0.1$

(b) $M = 40$ Φ_0 (TPS)

(c) $M = 40$, Φ_2, $\tau = 0.1$
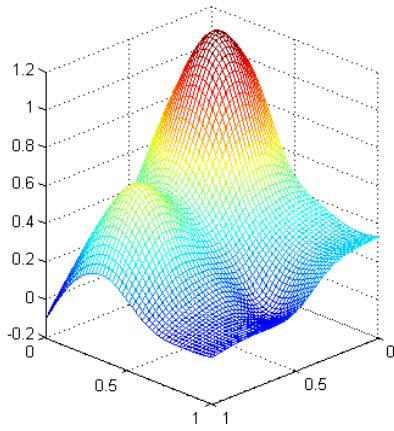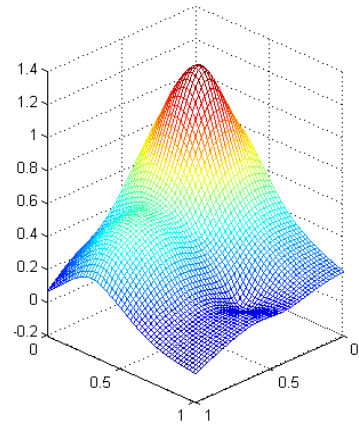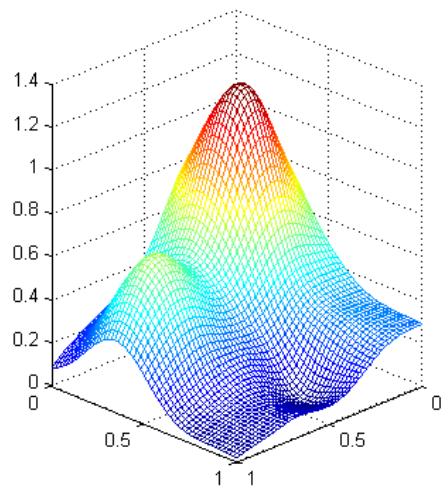
$M = 40$, Φ_3, $\varphi = 1$, $\tau = 0.001$

Fig. 9.8 In these figures, we see that it is only required a small number of points for obtaining a good reproduction with all the splines listed in (9.6). In general, the numerical experiments show a very similar behavior. As we show later, the great differences appears when dealing with noisy data.

(a)   (b)

Fig. 9.9: Many numerical experiments have been run for surface interpolation. Figure (a) shows a typical scatter plot for points on Franke's surface and (b) the exact surface.

An important test for visualization is to reconstruct a surface by interpolation from a small number of scattered data. We have run many numerical experiments for surface interpolation. In figures 9.7 and 9.8 we show some remarkable cases. For this task, we have used Franke´s function with different values for M in the region $\Omega = [0,1] \times [0,1]$.

9.7 Condition numbers and error bounds

Associated with the solution of a linear system $A\mathbf{x} = \mathbf{b}$ there is a number $\kappa(A)$ called the condition number of the matrix A and is defined as a product of the magnitudes of A and its inverse; that is

$$\kappa(A) = \| A \| \cdot \| A^{-1} \|, \qquad (9.8)$$

where $\| \cdot \|$ is a matrix norm. If the solution of $A\mathbf{x} = \mathbf{b}$ is insensitive to small changes in the right-hand side $\mathbf{b}$ then small perturbations in $\mathbf{b}$ result in only small perturbations in the computed solution $\mathbf{x}$. In this case, A is said to be well conditioned and corresponds to small values of $\kappa(A)$. If the condition number is large then A is ill conditioned and the numerical solutions of $A\mathbf{x} = \mathbf{b}$ cannot be trusted.

To understand the numerical behavior of the spline approximations it is essential to have bounds on the approximation error and on the condition numbers of the interpolation matrix in the system

$$\begin{bmatrix} A & P \\ P^t & 0 \end{bmatrix} \begin{bmatrix} \alpha \\ \beta \end{bmatrix} = \begin{bmatrix} z \\ 0 \end{bmatrix}.$$

These bounds are usually expressed employing two different geometric measures. For the approximation error is crucial to know how well the data sites $\mathcal{A} = \{a_1, a_2, \ldots, a_M\} \subset \Omega$ fill the region Ω. This can be also measured by the Hausdorff distance (9.7), which gives the radius of the largest "data-site free" ball in Ω.

M	$\Phi_0 (TPS)$ 10^8	Φ_1 10^{12}	Φ_2 10^9	Φ_3 10^{10}	Φ_τ 10^{16}
50	0,002479	0,002831	0,000207	0,271619	0,001333
100	0,027472	0,005665	0,000239	0,554171	0,002685
300	0,742896	0,279228	0,010356	1,684353	0,008065
600	0,656841	0,217310	0,285977	3,379575	0,016223
1000	8,446342	1,707619	1,335015	5,640198	2,390499

Tab. 9.3: Condition numbers for the interpolation matrix of splines. It is remarkable that although these values may be very high, the regularization parameters control the ill-posedness of the interpolation matrix.

The condition number, however, will obviously only depend on the data sites $\mathcal{A}$ and not on the region Ω. Moreover, if two data sites tend to coalesce then the corresponding interpolation matrix has two rows which are almost identical. Hence, it is reasonable to measure the condition number in terms of the separation distance

$$q_A := \frac{1}{2} \min_{j \neq k} \| a_j - a_k \|.$$

In the table 9.3 we report the behavior of the condition number $\kappa(A)$ of the interpolation matrix for every spline from the list (9.6). We observe an increasing value of $\kappa(A)$ with respect to an increasing number of scattered data and in comparison with TPS. In spite of these large values, the solution of the system and the reconstruction of the surface are possible under very general conditions.

9.8 Evaluation Criteria for the approximation methods

9.8.1 Accuracy

For these criteria we use known surfaces defined in the form $z = f(x, y)$, taking samples with or without noise and approximating the whole surface, using the spline obtained from the scattered data. We then compare exact and approximated values of the function. Certainly in the usual and real applications of reconstruction methods we do not have a

representation of the object in the form $z = f(x, y)$, nevertheless, if the method makes a faithful approximation of a variety of surfaces; we expect it to give reasonable results in other instances. In order to test the accuracy of interpolation of exact data with splines in (9.6) We have taken a fixed test set $B = \{b_1, b_2, \ldots, b_N\}$ and interpolated the function peaks using M scattered data points $A = \{a_1, a_2, \ldots, a_M\}$ in such a way that A and B are disjoint sets, its to say they have no common point, then $A \cap B = \varnothing$. We use the indicators

Maximum Error (MAX)

$$(MAX)(S, f) = \max \left\{ \| S(b_i) - f(b_i) \| \right\}_{i=1}^{M}, \tag{9.9}$$

and Root Mean Square Error (RMS)

$$(RMS)(S, f) = \sqrt{\frac{1}{N} \sum_{i=1}^{N} | S(b_i) - f(b_i) |^2}. \tag{9.10}$$

M	$\Phi_0(TPS)$	Φ_1	Φ_2	Φ_3	Φ_τ
50	0.8963	0.9087	0.9829	0.6876	0.7530
100	0.5725	0.6096	0.4666	0.4988	0.4739
300	0.1108	0.0928	0.1677	0.2837	0.0647
600	0.0684	0.0180	0.0148	0.0611	0.0092
1000	0.0144	0.0226	0.0060	0.0161	0.0090

Tab. 9.4: Results for RMS interpolating Matlab peaks function. A remarkable fact it is the high degree of accuracy of Φ_2 and Φ_τ, better than TPS.

M	$\Phi_0(TPS)$	Φ_1	Φ_2	Φ_3	Φ_τ
50	4,6211	5,2151	3,4896	4,8581	3,6658
100	3,2655	2,4901	1,1351	2,5254	1,0782
300	0,5999	0,4793	1,0159	2,6755	0,5417
600	0,4003	0,1051	0,1226	0,2318	0,0486
1000	0,0721	0,1728	0,0447	0,1151	0,1114

Tab. 9.5: Results for MAX interpolating Matlab peaks function.
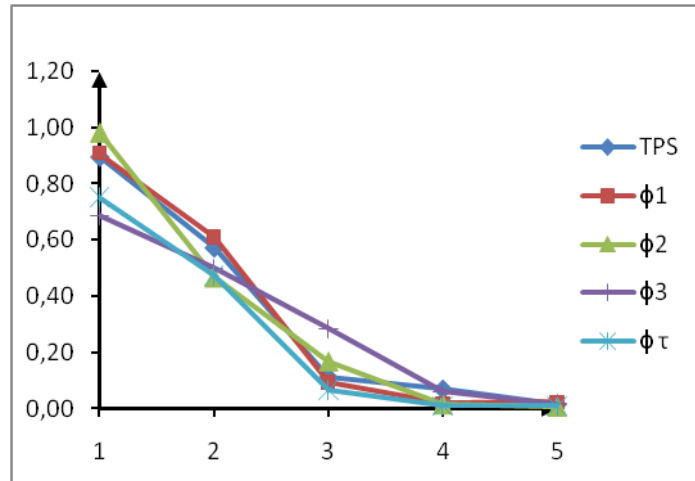
Fig. 9.10: This figure shows the accuracy of surface reconstruction with our splines. The vertical axis shows the values of *RMS* for each spline using data without noise. The results tend to be different as increases the number of points *M*. As we shall see later, the differences are more evident when dealing with noisy data.

On tables 9.4 and 9.5 we can see some of the typical results obtained in testing the accuracy of splines compared with TPS. Here is evident that our splines are sometimes equal or better than TPS for the reproducing quality. The performance of Tension splines is again very remarkable.

9.8.2 Visual Aspects

As we said in the beginning of this work, human visual perception is a very powerful skill in our comprehension of reality. Point clouds come from laser scanning of real objects, so visualization is a critical task in the performance of the models.

In general we observe that the visual aspects are similar for all the splines when we use exact data. As an example, we can see (fig 9.11) the excellent interpolation of Franke's function by TPS. Nevertheless the differences between TPS and the rest of splines may be remarkable when dealing with noisy data. In figure 9.11(b) we can observe that the performance of TPS for interpolating the noisy "peaks" surface is very poor; but is very good using the spline corresponding to Φ_3. In general this is the typical behavior of our family of splines (9.6).
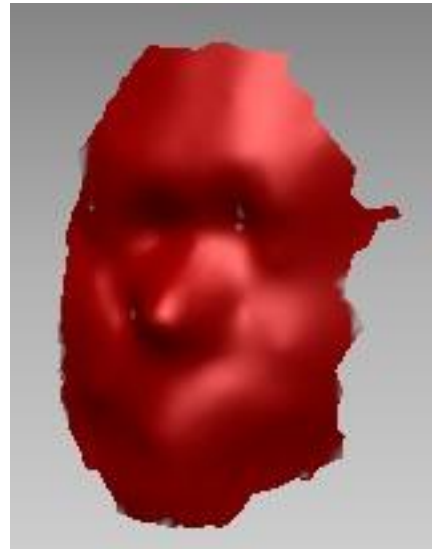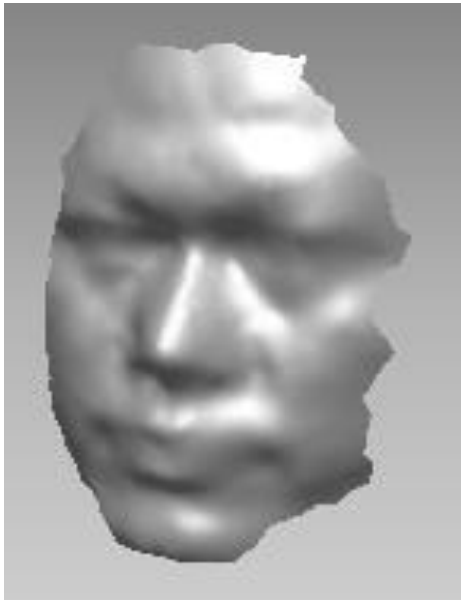
(a)

(b)

(c)

(d)
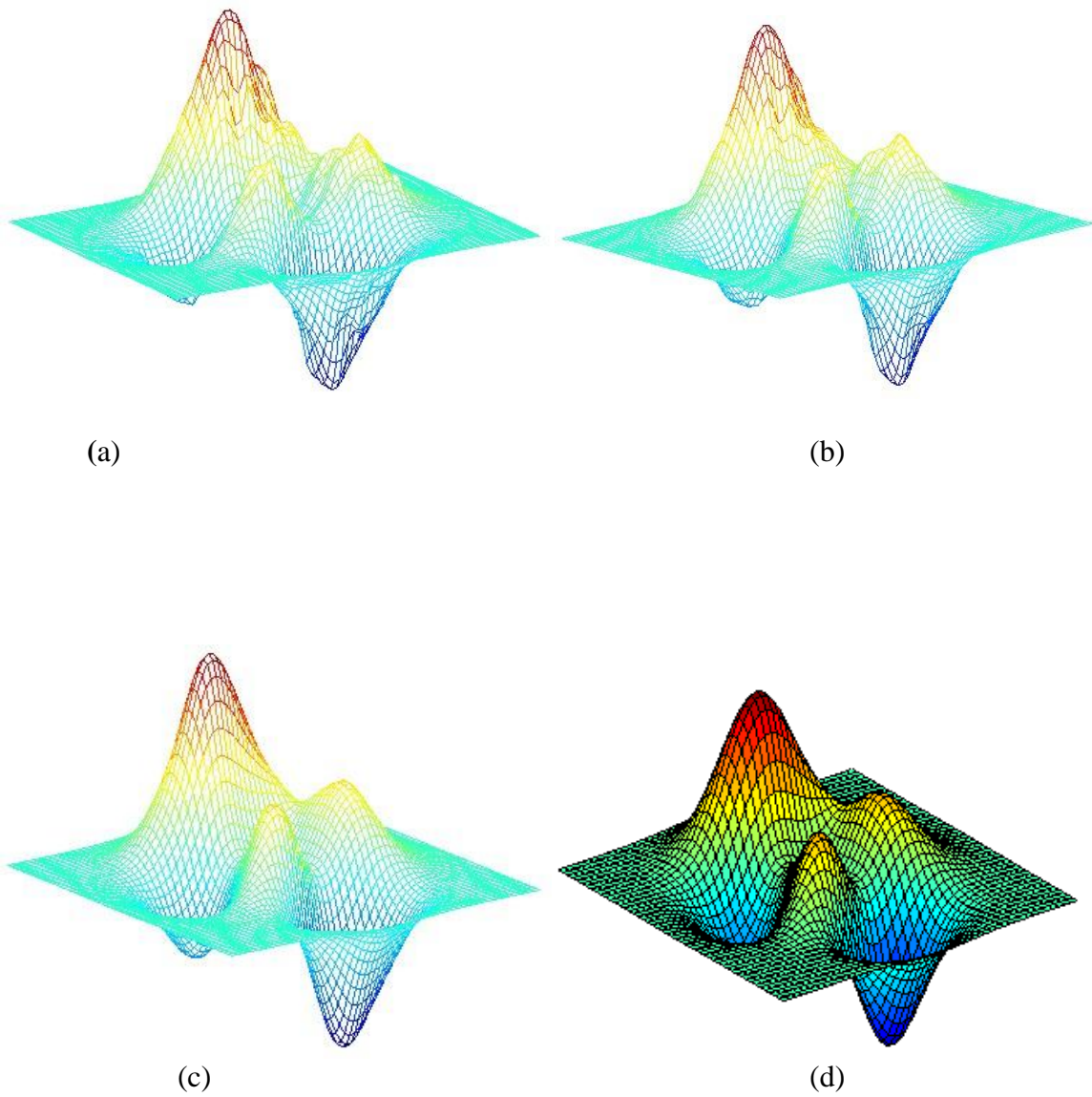
Fig. 9.11: In this numerical experiment we have taken a very noisy peaks surface (a) and applying TPS we obtain the surface in (b). But tuning the parameters of Φ_3, we finally obtain the improved surface (c) that can be compared with the exact surface (d).
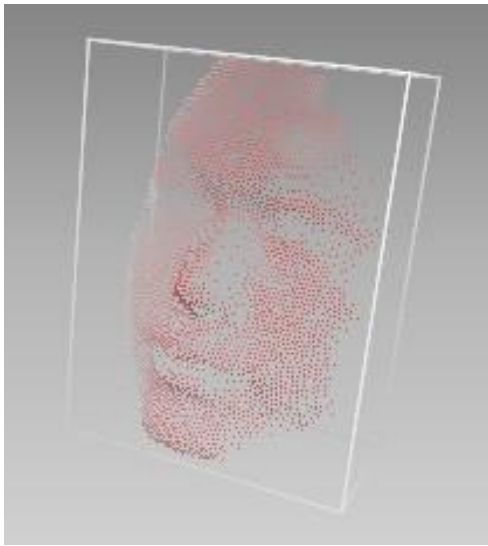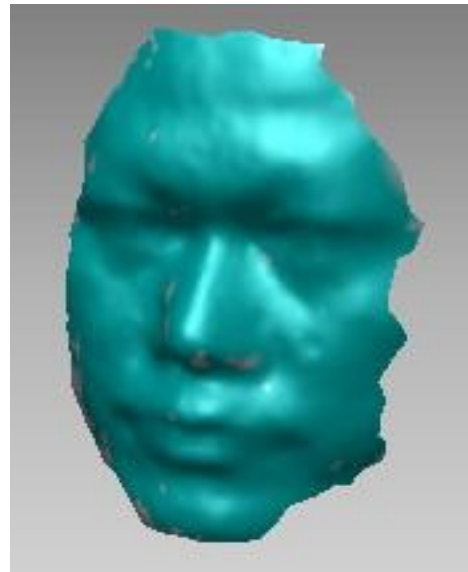
(a)   (b)

(c)   (d)

Fig. 9.12: We use the point cloud in (a) to test our splines in the reconstruction of free form objects. In this example, applying TPS, with $\lambda = 0.00002$ and an increasing number of points: (b) 100 points (c) 800 points (d) 2000 points.

90

9.8.3 Sensitivity to parameters

Tuning of parameters permits to enhance or decrease some features of the object. The models based on regularization have this remarkable property. Tuning of parameters is very useful for fitting different requirements on different applications and it is essential for noisy data. TPS doesn't have parameters into its mathematical expression, the rest of splines have one or two parameters we denoted φ, τ. The main trend of the curves shows that the optimal φ, τ value seems to fall in an interval where the accuracy behavior of the interpolant may be unstable. If the same experiment is performed with a slightly different data point resolution or different φ, τ resolution, the main trend of the resulting curves remains similar, but the oscillatory segments change. This sawtooth instability has not yet been well understood although it has been recognized in the literature studying other radial basis functions [57]. Nevertheless, our numerical experiments show that it is always possible to tune the values of parameters for obtaining good approximators.

In our experiment we have evaluated splines by calculating RMS and MAX on noisy data. The values of RMS show a similar performance as in the graphs of figure 9.7. They show an oscillatory behavior and then grows rapidly. These experiments have shown us that the best values for φ, τ are in the interval [0, 1] and sometimes in a larger interval but not larger than [0,10].

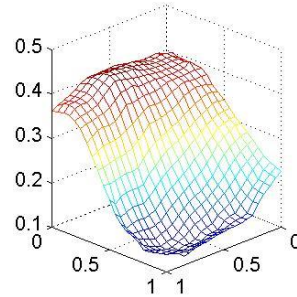(a)   (b)
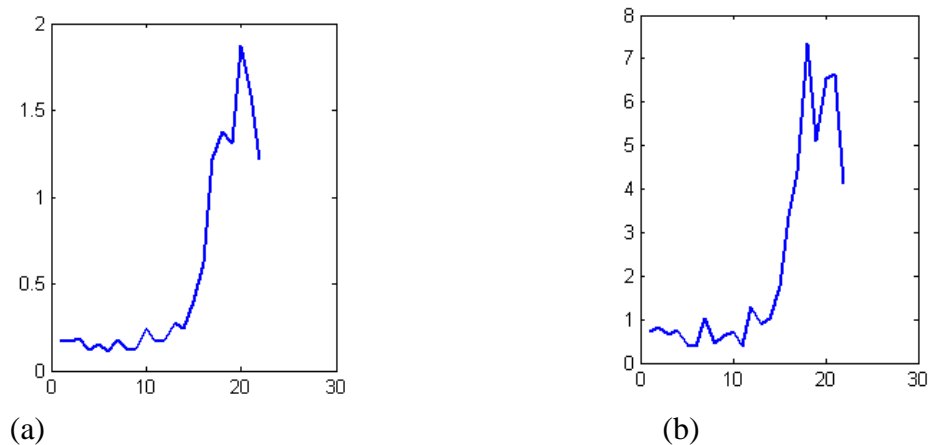
Fig.. 9.13: We made a lot of experiments varying randomly the values for φ and τ in the intervals [0,1] and $[1,10^5]$. They all have tend to stabilize in the interval [0,1]. (a) RMS . (b) MAX .
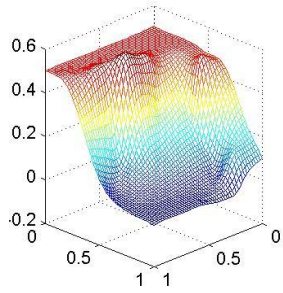
In Fig. 9.14 we show more results with reconstruction (interpolation) for the Franke's data with 100 scattered points for different values of φ and τ .
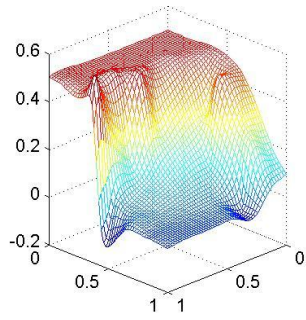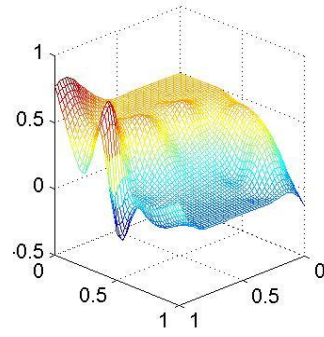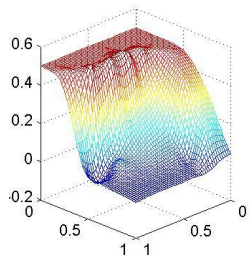
(a) $\Phi_3 \; \varphi = 1 \; \tau = 0.00001$

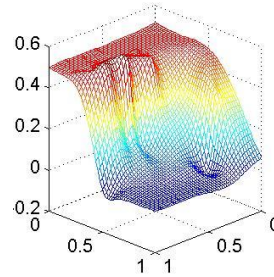(b) $\Phi_3 \; \varphi = 1 \; \tau = 10^{-10}$

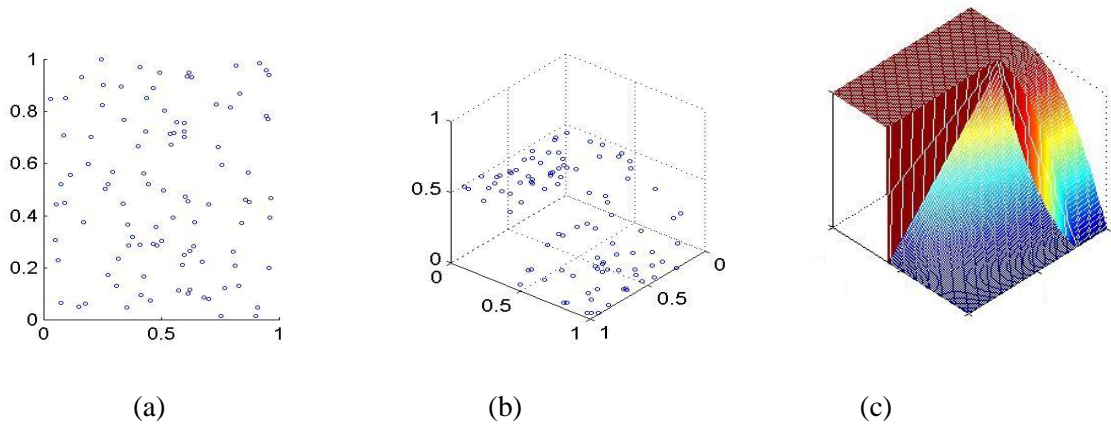(c) $\Phi_2 \;\; \tau = eps$ (machine)

(d) $\Phi_2 , \; \tau = 1$

(e) $\Phi_1 , \tau = 1$

(f) Φ_0 TPS $\;\; \lambda = 0$

Fig. 9.14: This figure shows some results from different tests on regularization parameters. We have used Franke´s data for testing an extreme case of discontinuities reconstruction. The results show how to preserve discontinuities by tuning the values of parameters.

Fig. 9.15 Figures (a), (b) shows 100 points, taken randomly on Franke's data (c).

9.8.4 Timing

The execution time of an algorithm is measured by its computational complexity which, as we said in chapter 3, it is an intrinsic problem in reconstruction. Nevertheless a method that is slow now, may be not so much in a better hardware, or if the method worth the effort, we can develop faster algorithms. This is the case of all our splines; although they may require a huge number of floating points operations in a computer, the results on reconstruction capabilities are very encouraging. In table 9.2 we show some typical performance times (in seconds) of our splines family (9.6). It is easily observed, as we may hope, that the splines containing Bessel function $\mathcal{K}_0$ are very time consuming, specially Φ_3. They have the form

$$S_{f,A}(\mathbf{x}) = \sum_{i=1}^{M} \alpha_i \Phi(\| \mathbf{x} - a_i \|) + p(\mathbf{x}),$$

where M is the number of centres, so this evaluation is proportional to M and may take very long time.

9.8.5 Ease of implementation.

Our purpose has been to obtain explicit analytic expressions for approximators in order to develop better applications. From this point of view our splines are very well-suited for implementation in any computer language. They are linear combinations of a fixed function Φ, given in terms of polynomials, exponentials and logarithms. Nevertheless TPS and tension spline require simpler expressions than Φ_1, Φ_2, Φ_3 which contain the Bessel function $\mathcal{K}_0$.

9.9 Reconstruction from noisy data. Cross validation

Other important task is the determination of the smoothing parameter λ. Visual appearance is a good criterion for visualization problems, so in these case the values for λ may be determined by trial and error. λ is a very sensitive parameter, so small changes in its values may cause large changes in the visualization of the surface as observed in former figures. λ is penalizing large values of the functional $R[f]$. The functional contains a great amount of derivatives such that should assume large values for non smooth functions and small for smooth functions. It is possible to find optimal values $\hat{\lambda}$ for the smoothing parameter in the sense of some criteria. One of them is cross validation.

The basic idea of cross validation for evaluating the performance of an approximator of the data $D = \{(a_i, z_i) \in \mathbb{R}^n \times \mathbb{R}\}_{i=1}^M$ is to build the approximator over the set $\{a_i : i \neq k\}$, that is, without considering the knot a_k and then repeat this procedure for $k = 1, \ldots, M$. Let $f_\lambda^{[k]}$ be the minimizer of

$$H[f] = \frac{1}{M} \sum_{\substack{i=1 \\ i \neq k}}^M (f(a_i) - z_i)^2 \; + \; \lambda R[f],$$

then it is reasonable to look for the model which minimizes the ordinary cross validation function $V_0(\lambda)$, defined as

$$V_0(\lambda) = \frac{1}{M} \sum_{k=1}^M (z_k - f_\lambda^{[k]}(a_k))^2,$$

The minimizer of $V_0(\lambda)$ is known as the "leaving-out-one" estimator of λ. However, in computational terms, finding this value is very expensive. An alternative is to use the influence matrix B, which may be found [188] with

$$\begin{bmatrix} f_\lambda(a_1) \\ f_\lambda(a_2) \\ \vdots \\ f_\lambda(a_M) \end{bmatrix} = B(\lambda) z.$$

It can be shown that $(z_k - f_\lambda^{[k]}(a_k)) \equiv \dfrac{(z_k - f_\lambda(a_k))}{(1 - b_{kk}(\lambda))}$, then

$$V_0(\lambda) = \frac{1}{M} \sum_{k=1}^M \frac{(z_k - f_\lambda(a_k))^2}{(1 - b_{kk}(\lambda))}.$$

Minimization of the function $V_0(\lambda)$ is a powerful criterion for the choice of an optimal λ. But there exist an even easier method called Generalized Cross Validation (GCV), where

$$V(\lambda) = \frac{(1/M) \, \| \mathbf{I} - \mathbf{B}(\lambda) \mathbf{z} \|^2}{[(1/M) \, tr \, (\mathbf{I} - \mathbf{B}(\lambda))]^2},$$

and $\boldsymbol{B}(\lambda)$ is the $M \times M$ "hat" matrix of the ridge regression [13,188] $\boldsymbol{B}(\lambda) = \mathbf{X}(\mathbf{X}^T\mathbf{X} + M\lambda\mathbf{I})^{-1}\mathbf{X}^T$. At first glance, optimization of $V(\lambda)$ seems a formidable computational problem since each value of λ has its corresponding $\boldsymbol{B}(\lambda)$. However, [13] gave a method of expressing $V(\lambda)$ as an easily-calculated rational function based in the singular value decomposition (SVD) $\mathbf{X} = \mathbf{UDV}^T$, where $\mathbf{U}$ is $M \times p$ with orthonormal columns, $\mathbf{V}$ is $p \times p$ and orthogonal, and $\mathbf{D}$ is $p \times p$ and diagonal with diagonal elements $d_1 \geq d_2 \geq \cdots \geq d_p \geq 0$, which are the nonnegative square roots of the eigenvalues of $\mathbf{X}^T\mathbf{X}$. Finally we obtain the expression

$$V(\lambda) = \frac{M \sum_{j=1}^{M-t} \left(\dfrac{n\lambda}{d_j^2 + n\lambda} \right)^2 z_j^2}{\left(\sum_{j=1}^{M-t} \dfrac{n\lambda}{d_j^2 + n\lambda} \right)^2}. \tag{9.11}$$

Example 9.2: Interpolation and Cross validation. The results for this example are shown in Figure 9.16. For this experiment we have taken 400 noisy points $\mathcal{A} = \{a_1, a_2, \ldots, a_M\}$ on Franke's function in $\Omega = [0,1] \times [0,1]$ to be approximated with the Thin Plate Spline. We can allow the surface to pass close to, but not necessarily through, the known data points, by setting $\lambda > 0$. When $\lambda = 0$, the function interpolates the data points. As λ approaches zero, the surface becomes rougher because it is constrained to pass closer to the data points. At $\lambda = 0$, the surface interpolates the data, and overshoots are much more evident . The optimum value λ_0 for λ is determined minimizing the GCV function $V(\lambda)$ to obtain a smooth surface with fidelity to data.

At larger values of λ ($\lambda > \lambda_0$), the reconstructed model is smoother and approaches an amorphous bubble (e). It has been calculated an error (Error =0.01082745537985) for this experiment with

$$Error = \frac{1}{M} \sum_{j=1}^{M} |z_j - f(a_i)|,$$

where $f(a_j)$ are the exact values on the data points and z_j obtained using GCV. In example 9.4 we study a case in which we apply the other splines to data with higher degree of noise.

Example 9.3 Testing regularization parameters. The approximator TPS, has also been tested using k-fold cross validation. In this method the data set (Fig.9.11 (a)) is divided into k subsets whose points are chosen randomly. Each time, one of the k subsets is used as the test set and the other $(k-1)$ subsets are put together to form a training set.
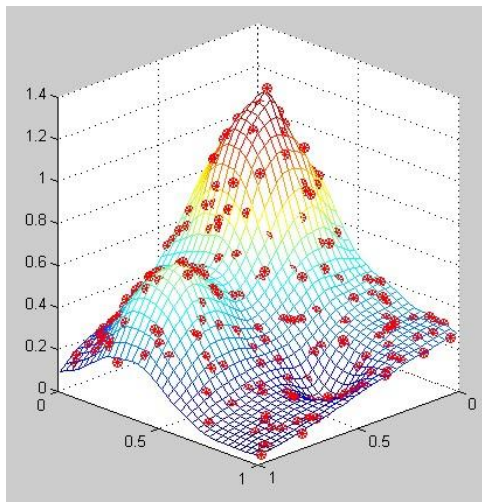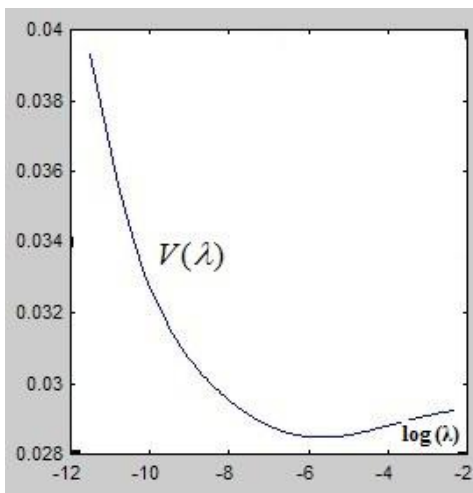
(a)
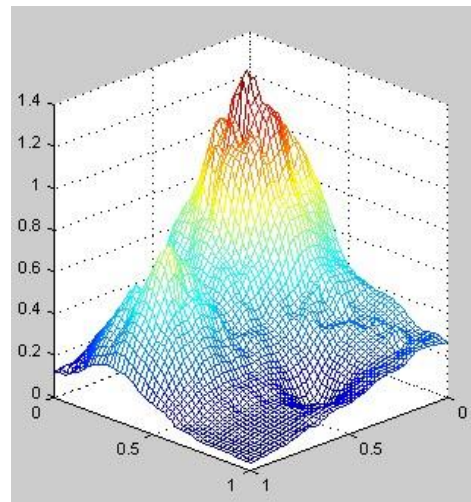
(b)

(c)
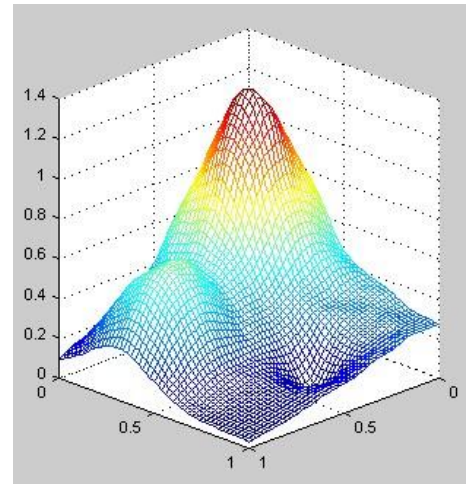
(d)

Fig. 9.16: This example shows the potential of splines to smooth a noisy surface by tuning regularization parameters by Generalized Cross- validation (GCV). Figure (a) depicts the noisy data near the surface. In (b) we see the interpolation of the original data with $\lambda = 0$, without smoothing. (c) The optimum value λ_0 for the regularization parameter λ is found by minimizing the function $V(\lambda)$ and the resulting surface is shown in figure (d).

(a)   (b)
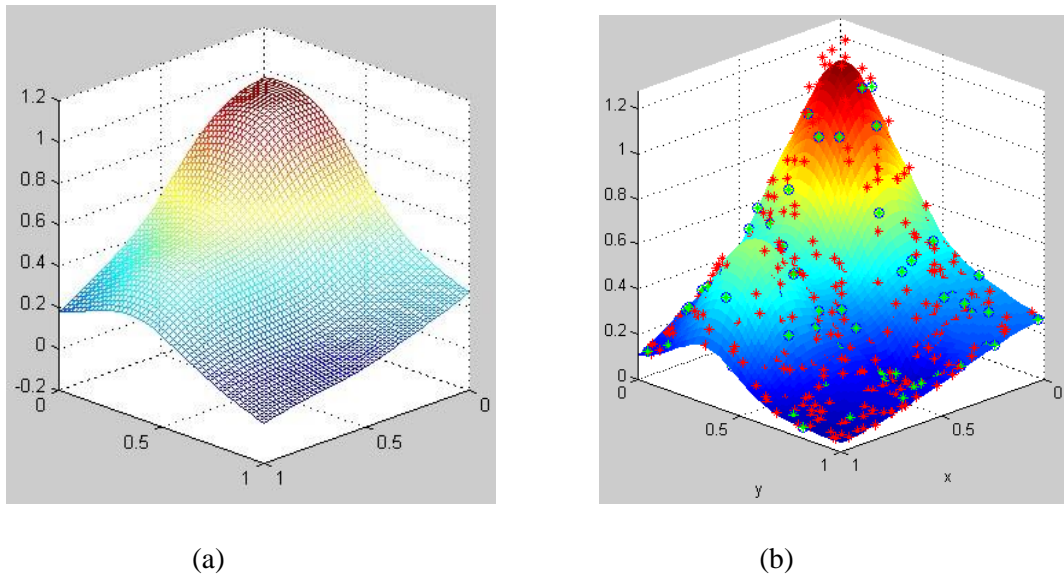
Fig. 9.17: When the surface is reconstructed by using values larger than λ_0 the surface is too smoothed and loses fidelity to data as it is the case shown in figure (a), with $\lambda = 1$. The data used for k-fold cross validation are shown in (b).

The function approximator fits a function using the training set only. Then the function approximator is asked to predict the output values for the data in the testing set. In this case we have taken $k = 5$. In figure 9.11 (f) is shown one case for training set (red) and test set (green) The errors for each test set were very similar, showing the robustness of the method to different degrees of complexity of the surface or data. The errors were accumulated to give a mean absolute test set error (0.010559412144).

Test set	Error
1	1.0671e-002
2	1.0374e-002
3	1.0110e-002
4	1.0562e-002
5	1.1080e-002

Tab. 9.6: Results for k-fold Cross Validation.

(a)

(b)
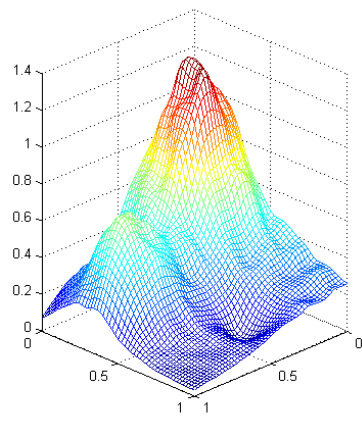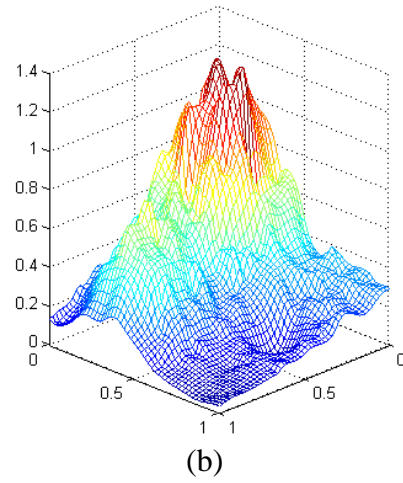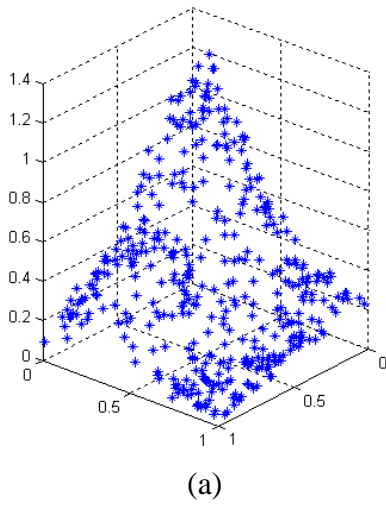
(c) Φ_0 (TPS), $\lambda = GCV$
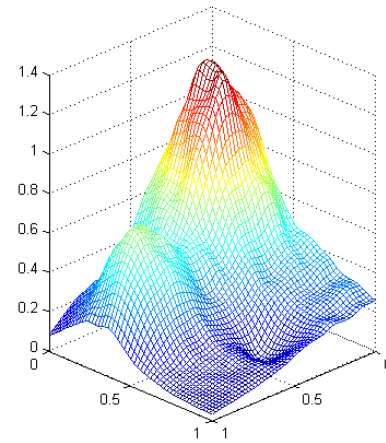
(d) Φ_3, $\varphi = 1$, $\tau = 10^{-4}$, $\lambda = 10^{-4}$

Fig. 9.18. Figure (a) shows a noisy point cloud from Franke's surface. (b) interpolation of the former data. In (c) we reconstruct the surface with TPS and choosing $\lambda = \lambda_0$ by GCV, but the result still has noise. In (d) we try the same problem with Φ_3 but the result is similar to TPS. Nevertheless, as we show next (see Fig. 9.19), it is possible to choose adequate values for regularization parameters to obtain high accuracy in surface reconstruction even in highly noisy data.

(e) Φ_3, $\varphi = 1$ $\tau = 0.0001$, $\lambda = 0.01$

(f) Φ_τ, $\tau = 0.1$, $\lambda = 0.0002$
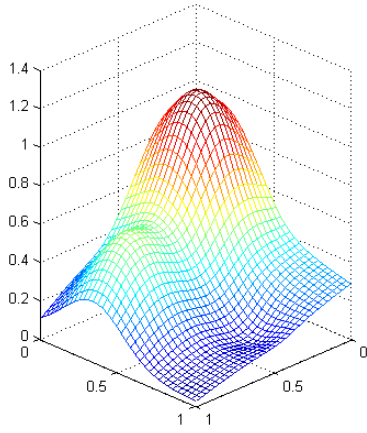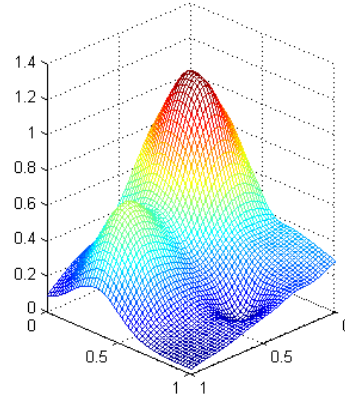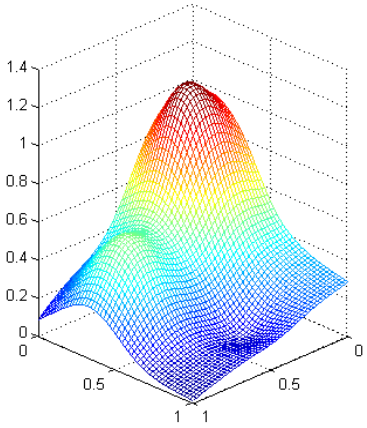
(g) Φ_1, $\tau = 0.1$, $\lambda = 0.009$
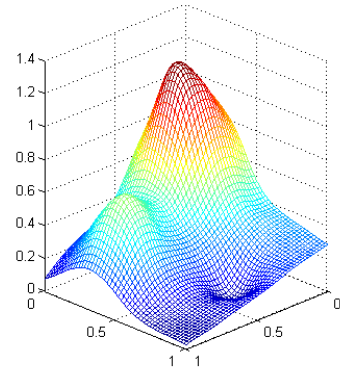
(h) Φ_1, $\tau = 0.05$, $\lambda = 0.001$

Fig. 9.18 (cont.): Now, we show a successful surface reconstruction that remarkably improves the performance of TPS. Figure (e) shows that although Φ_3 fails to smooth the noise in (d), the parameters can be tuned to obtain good results. In (f), we show that Φ_τ not only eliminates the noise on data, it also gets a high accuracy in the reconstruction of the original surface. The other splines have a similar performance, as seen in (g) and (h).

Example 9.4: Regularization of an extremely noisy data set. Now we take a more noisy point cloud for Franke's function in fig 9.12(a). In this case we take 400 highly noisy data on Franke's surface. In figure 9.12 (b) is depicted the interpolation of the noisy surface. The reconstruction of the surface is done using the regularization parameter λ by GCV. We observe in (c) and (d) that TPS and Φ_3 have a similar quality and it is really remarkable the smoothing done by the spline in tension Φ_τ. The picture (f) shows that Φ_τ performs much better than TPS when treating very noisy data.. Furthermore, (f), (g), (h) show how these splines eliminate the noise from data by tuning the values of regularization parameters.

Example 9.5: Reconstruction with larger number of points. Now we show the performance of regularization of data coming from free form objects and taken by range scanners, so in general, we assume the data are noisy. We show some results obtained by splines in tension with parameter τ around 0.1 and $\lambda = 0.0001$. Further experiments with the other splines have shown similar behavior. A sample is shown in Fig. 9.19
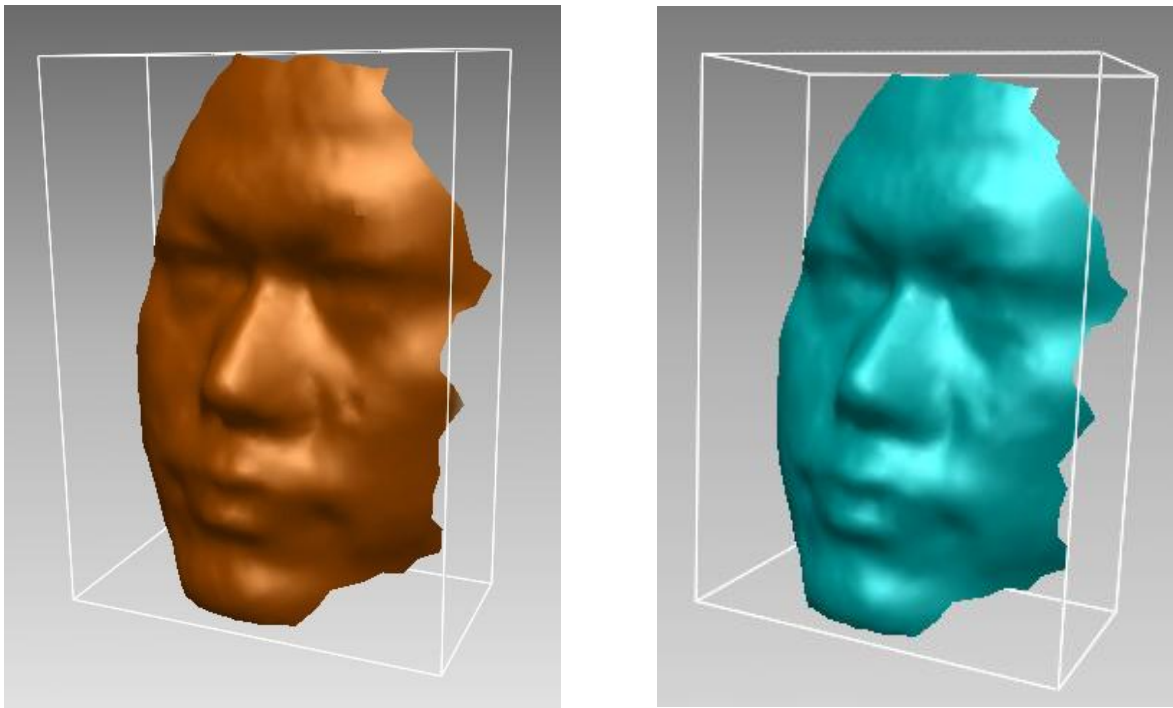
Fig. 9.19: Example of reconstruction of the "face" from a large point cloud with tension spline.

9.10   Comparisons with other methods

From the splines tested here only thin plate splines have been extensively studied and although other authors have studied splines in tension, this has been commonly done for data without noise and mainly for curves [38,153]. After the success of thin plate splines at the 1970's there has been a great interest in improving its performance in regularization problems. Basically, from the physical interpretations in chapter 5, we can understand the limitations of TPS because the material aspects of an elastic plate are rather limiting with respect to its physical reality. That is, one may abstract from its third dimension; it is elastic, hence it doesn't deform, only bend, and it is a plate, not a membrane, which means it is stiff. Its behaviour is rather that of steel than that of gum. The splines studied in this work deal with this problem integrating local and global features in regularization model.

One of the first to propose surface in tension was Franke [63,64], who made extensive study of different splines. Nevertheless, the research of Franke was done only for interpolation. Perhaps due to the limited computational resources of the 1980's, there is not much research comparing the properties of the splines we study here. The studies of Franke were done around 1982, so we can say that the availability of better computational resources we have today allowed us a better analysis and visualization.

9.11 Conclusions

In this chapter we have performed numerical tests that show how an adequate choice of regularization functionals conduct to stable solutions of severely ill posed inverse problems, with a high degree of accuracy. We have shown that our spline family (9.6) is a set of adequate approximators of surfaces given as scattered data; including free form objects coming from range scanners. It is possible to find intervals for adjusting regularization parameters and we can find their values by GCV or by trial and error. This last option does not mean chaotic choice, because we provide some intervals and key values that become very useful in practical problems. Comparing with other works as Franke's, our numerical tests have similar performance in some cases, and in other cases we find better results.

Chapter 10

Conclusions and open problems

10.1   General conclusions of the thesis

In the first part of the thesis, we mainly focused on building a general framework for solving reconstruction problems with different kinds of data, in that way we obtained a formulation that joins the classical inverse problems theory with ideas from Schwartz distribution theory. This general formulation can be applied to a wide class of inverse problems, in particular we dealt with Lagrange data.

Constructing this formulation we encountered and solved the following issues:

- In order to select the most appropriate framework, we have applied inverse theory to determine and classify the most relevant problems that arise in reconstruction problems. In this way we saw that the most critical point is how to include local and global features in the approach to be applied. We found that the regularization framework has enough generality for fulfilling these requirements. We found that it is possible to include multiple functionals in order to capture local and global properties on the data.

- We found that the inclusion of regularization functionals can be conducted by physical and geometrical criteria. We have chosen as regularizers the family of Duchon seminorms which have an interpretation in elasticity theory. A very important idea is the resolution of the functional, given by its null space. This space should not be too large in order to capture the complexity of data.

- In deciding what kind of functional spaces are adequate for solving reconstruction problems we found Schwartz distribution theory as a powerful mathematical tool for designing splines. By converting the addition of functionals into an optimization problem, we obtain solutions that satisfy local and global properties which can be tuned using regularization parameters. This method is not only for particular cases, it can be generalized to n-dimensional data and different kind of problems. We obtained explicit expressions in the form of robustly implementable radial basis functions.

In the second part of the thesis we explore applications of the regularization framework to problems of surface reconstruction and visualization. In this field, ill-posedness appears in the form of having to decide a trade-off between a good fit of the data and some model requirements that comes expressed in the degree of localness (or globalness) of regularization functionals.

We drew the following conclusions:

- The splines family studied here unifies several spline formulations and yields radial basis functions which produce practical implementations. These splines perform, in some cases, equal results to thin plate splines and better results in other cases. The results are similar for all the splines when dealing with data without noise and they are really better in reconstruction of noisy data.

- The splines studied have two terms. The first one contains a linear combination of translates of a fixed function (parametric part in statistical language) and a linear polynomial term, that are implementable in stable form.

- The optimum regularization parameters are determined by generalized cross validation and others are found to belong to short-length intervals. The tuning of these parameters permit us to obtain a trade-off between local an global features.

- The concepts of regularization theory give a comprehensive framework to formulation of the problems in vision: at all three levels of problem, algorithm, and implementation. Furthermore, the mathematical theory of regularization provides a useful theory for incorporating prior knowledge, constraints, and quality of solution. The exciting prospect is that the analogies with elasticity theory and physics will continue to provide fruitful ideas for development of regularization theory and for understanding human perception.

10.1 Future research and open problems

We have given a wide theoretical framework for dealing with many kinds of reconstruction problems whose data are given as a set $D = \{L_1(f), L_2(f)..., L_M(f)\}$ of bounded linear functionals. Applying this theory on surface reconstruction, very good results are obtained, that promise similar performance applied to other kind of data and non linear functionals $L_i(f)$. So, we have a great amount of possibilities for future work in the following subjects.

Non linear inverse problems

In reconstruction problems the relationship between object and image has the most general representation in the form of a non linear integral equation $g(s) = \int h(s,t,f(t))dt$, where h is a continuous function. This equation gives the solution of the direct problem and the

inverse problem is obtained by exchanging the roles of the data and the solution: in these cases we must find the object f for a given image g. The solution of this equation is very difficult from both the theoretical and practical points of view. No general theory exists for such a non linear integral equation and each problem requires specific analysis, moreover the problem may be ill posed and no general regularization theory exists for wide classes of non linear problems.

Biomedical imaging

In general the new techniques of medical imaging are based on the interrogation of the human body by means of radiation transmitted, reflected or emitted by the body: the effect of the body on the radiation is observed and a mathematical model for the body-radiation interaction is developed. The invention of computed tomography (CT) by G. H. Hounsfield at the beginning of the seventies was a breakthrough in medical imaging. The conception of CT is based on ideas which opened new and wide perspectives. CT requires a mathematical model of X-ray absorption.

A specific feature of medical imaging is that the problems to be solved are ill-posed in the sense of Hadamard; this means that although the available data contains a big amount of information, the fact that the problem is ill posed, combined with the presence of noise, implies that the extraction of this information is not trivial. This is a very important challenge for the future.

Fast algorithms

During this work we have faced problems regarding the algorithmic complexity of splines, especially for those expressions that contains the Bessel function of the second kind $\mathcal{K}_0$. The applications of radial basis functions imply two basic problems:

1. The solution of very large linear systems, and
2. The evaluation of very long linear combinations on a very large amount of points.

These two facts could be sometimes disappointing; nevertheless the methods are very promising, so they deserve the analysis and design of algorithms able to lower its complexity. Fortunately, this has been done for some radial basis functions, but there remains more research about these algorithms, which become necessary when dealing with thousands or millions of data.

Appendix

The reconstruction problem on Hilbert spaces

Regularization problems in finite or infinite-dimensional spaces can be modeled under the following framework [35].

Let $\mathcal{X}$ be a normed linear space and $D = \{L_1(f), L_2(f)..., L_M(f)\}$ are linear "information functionals" on $\mathcal{X}$. The idea is that for a given $f \in \mathcal{X}$, the following information

$$L_i(f) = z_i \quad i = 1, \cdots, M,$$

is available. From this information we want to compute a value $L(f)$ where L is another linear functional. In particular, for reconstruction of point clouds the L_i's are point evaluation functionals of the form $L_i(f) = f(a_i)$.

From the information given by the L_i's, the goal is to "learn" f (i.e. to find a good approximation of f) from random samples. But without any restrictions on the class of functions f, there is no hope of controlling $L(f)$, simply by knowing the values $L_1(f), L_2(f)..., L_M(f)$. So, we will look for an approximation to f on a Hilbert space $\mathcal{H}$. At first instance the only information is that the desired element is in the linear manifold

$$U = \{u \in \mathcal{H} : L_i(u) = L_i(f), i = 1, ...M\}.$$

Then the problem may be treated as a minimal norm interpolation on the manifold U, where U is a translate of the subspace $V = \{u \in \mathcal{H} : L_i(u) = 0, i = 1, ..., M\}$. If S is the element of minimal norm, then $S \perp V$ and $L_i(S) = L_i(f)$, $i = 1, ..., M$.

Theorem A.1 (Riesz representation theorem). If L is a bounded linear functional on a Hilbert space $\mathcal{H}$ there exists exactly one $\mathbf{x}_0 \in \mathcal{H}$ such that $L(\mathbf{x}) = (\mathbf{x}_0, \mathbf{x}) \ \forall \mathbf{x} \in \mathcal{H}$. The element $\mathbf{x}_0$ is called the **representer** of L in $\mathcal{H}$.

In other words, this theorem reveals that bounded linear functionals on a Hilbert space have a very simple form and the representers of the functionals $L_i(f)$ can be used to find the minimal norm interpolant S.

Theorem A.2. Let $L_1(f), L_1(f), ..., L_M(f)$ be continuous linear functionals on $\mathcal{H}$, with representers $u_1, u_2, ..., u_M$, respectively. Let $f \in \mathcal{H}$ have minimal norm interpolant S on $L_1(f), L_2(f)..., L_M(f)$. Then

$$S = \sum_{i=1}^{M} \alpha_i \, \boldsymbol{u}_i,$$

where the coefficients α_i are chosen to solve the system of linear equations

$$\sum_{j=1}^{M} \alpha_i \, (\boldsymbol{u}_i, \boldsymbol{u}_j) = (f, \boldsymbol{u}_i), \qquad i = 1, \ldots, M.$$

Proof. Using representers, $\boldsymbol{L}_1(f) = (f, \boldsymbol{u}_i)$, then

$$\boldsymbol{V} = \{u \in \mathcal{H} : \boldsymbol{L}_i(u) = 0\}_{i=1}^{M}$$
$$= \{u \in \mathcal{H} : (f, \boldsymbol{u}_i) = 0\}_{i=1}^{M} = \bigcap_{i=1}^{M} K_i^{\perp} = span \{\boldsymbol{u}_1, \boldsymbol{u}_2, \ldots, \boldsymbol{u}_M\}.$$

On the other hand $S \perp \boldsymbol{V}$ then $S \in (\bigcap_{i=1}^{M} \boldsymbol{u}_i^{\perp})^{\perp} = span \{\boldsymbol{u}_1, \boldsymbol{u}_2, \ldots, \boldsymbol{u}_M\}$, hence it is possible to write $S = \sum_{i=1}^{M} \alpha_i \, \boldsymbol{u}_i$.

The second part of the theorem comes from $\boldsymbol{L}_i(f) = \boldsymbol{L}_i(S)$, $i = 1, \ldots, M$, then

$$(f, \boldsymbol{u}_i) = \boldsymbol{L}_i(f) = \boldsymbol{L}_i(S) = \boldsymbol{L}_i(\sum_{j=1}^{M} \alpha_j \, \boldsymbol{u}_j) = \sum_{j=1}^{M} \alpha_j \, \boldsymbol{L}_i(\boldsymbol{u}_j) = \sum_{j=1}^{M} \alpha_j \, (\boldsymbol{u}_i, \boldsymbol{u}_j),$$

and finally

$$\sum_{j=1}^{M} \alpha_i \, (\boldsymbol{u}_i, \boldsymbol{u}_j) = (f, \boldsymbol{u}_i).$$

Let us now suppose that $\mathcal{H}$ has a semi-inner product $[\cdot, \cdot]$ with null space N such that $\dim(N) = N$. Now let us choose this same number of elements $\{\boldsymbol{L}_1(f), \boldsymbol{L}_2(f) \ldots, \boldsymbol{L}_N(f)\}$ from the original data $\boldsymbol{L}_1(f), \boldsymbol{L}_2(f) \ldots, \boldsymbol{L}_M(f)$ and suppose the inner product $(\cdot, \cdot)$ of $\mathcal{H}$ can be expressed as

$$(u, v) = [u, v] + \sum_{i=1}^{N} \boldsymbol{L}_i(u) \boldsymbol{L}_i(v).$$

Theorem A.3. The set of representers $\{\boldsymbol{u}_1, \boldsymbol{u}_2, \ldots, \boldsymbol{u}_N\}$ of $\{\boldsymbol{L}_1(f), \boldsymbol{L}_2(f) \ldots, \boldsymbol{L}_N(f)\}$ is an orthonormal base for N, and $N \perp \boldsymbol{V}$.

This can be seen by

$$(u, v) = [u, v] + \sum_{i=1}^{N} \boldsymbol{L}_i(u) \boldsymbol{L}_i(v) = \sum_{i=1}^{N} \boldsymbol{L}_i(u) \boldsymbol{L}_i(v) = \sum_{i=1}^{N} (u, \boldsymbol{u}_i)(v, \boldsymbol{u}_i) = \left(\sum_{i=1}^{N} (u, \boldsymbol{u}_i) \boldsymbol{u}_i, v \right),$$

then $u = \sum_{i=1}^{N} (u, u_i) u_i$ hence $\{u_1, u_2, \ldots, u_N\}$ generates N, and is a basis since $\dim(N) = N$.

On the other hand $u_j = \sum_{i=1}^{N} (u_j, u_i) u_i$, then $(u_i, u_j) = \delta_{ij}$ and $\{u_1, u_2, \ldots, u_N\}$ is orthonormal. $u_j \perp V$ because $(v, u_j) = L_j(v) = 0 \ \forall \ v \in V$, thus $N \perp V$.

Definition A.1. A Hilbert space $\mathcal{H}$ is called a **Hilbert function space** if the elements of $\mathcal{H}$ are complex valued functions on a set Ω and for each $\mathbf{x} \in \Omega$, there exists a positive constant $C_{\mathbf{x}}$ such that $|f(\mathbf{x})| \leq C_{\mathbf{x}} \|f\|$ for all f in $\mathcal{H}$.

It is to say; in a Hilbert function space the point evaluation functionals $L_{\mathbf{x}}(f) = f(\mathbf{x})$ are bounded. Then it is possible to apply the Riesz representation theorem. For each $\mathbf{x}$ in Ω there exists a unique representer $K_{\mathbf{x}} \in \mathcal{H}$ such that

$$L_{\mathbf{x}}(f) = (f, K_{\mathbf{x}}) = f(\mathbf{x}).$$

Definition A.2. The mapping $K : \Omega \times \Omega \to \mathbb{C}$ such that $K(\mathbf{x}, \mathbf{y}) = K_{\mathbf{x}}(\mathbf{y})$ is called the **reproducing kernel** (or simply kernel) of $\mathcal{H}$. The reproducing kernel is so called because it has the potential of reproducing each function in $\mathcal{H}$: $(f, K_{\mathbf{x}}) = f(\mathbf{x})$ for all f in $\mathcal{H}$ and all $\mathbf{x}$ in Ω. Some properties of a kernel are

- $K(\mathbf{x}, \mathbf{y}) = (K_{\mathbf{x}}, K_{\mathbf{y}})$ $\forall \ \mathbf{x}, \mathbf{y}$ in Ω.
- $K(\mathbf{x}, \mathbf{y}) = \overline{K(\mathbf{y}, \mathbf{x})}$ $\forall \ \mathbf{x}, \mathbf{y}$ in Ω.
- $K(\mathbf{x}, \mathbf{x}) \geq 0$ $\forall \ \mathbf{x}$ in Ω.

Positive definite functions

Usually, we have to deal with approximation on an arbitrary set $\mathcal{A} = \{a_1, a_2, \cdots, a_M\}$ $\subset \Omega \subset \mathbb{R}^n$ of M distinct centres or knots and a symmetric kernel $K(\mathbf{x}, \mathbf{y})$ on Ω. We can form linear combinations

$$S(\mathbf{x}) = \sum_{j=1}^{M} \alpha_j K(a_j, \mathbf{x}), \qquad \mathbf{x} \in \Omega.$$

With such a set we can form the symmetric $M \times M$ matrix $A = (K(a_j, a_k))_{1 \leq j, k \leq M}$ and pose the interpolation problem

$$S(a_k) = z_k \quad 1 \leq k \leq M$$
$$= \sum_{j=1}^{M} \alpha_j K(a_j, a_k).$$

From these interpolation conditions we obtain the matrix linear system $A\alpha = z$, with $\alpha = (\alpha_1,\ldots,\alpha_M)$, $\mathbf{y} = (y_1,\ldots,y_M)$ and the **interpolation matrix**

$$A = \begin{bmatrix} K(a_1,a_1) & \cdots & K(a_1,a_M) \\ \vdots & \ddots & \vdots \\ K(a_M,a_1) & \cdots & K(a_M,a_M) \end{bmatrix}. \tag{A.1}$$

Definition 4.2. We say the function $K(\mathbf{x},\mathbf{y})$ is *positive definite* if for any M points $a_1,a_2,\cdots,a_M \in \mathbb{R}^n$, and $\alpha = (\alpha_1,\alpha_2,\cdots,\alpha_M) \in \mathbb{R}^M \setminus \{0\}$ the quadratic form

$$\alpha^t A \alpha = \sum_{i,j=1}^{M} \alpha_i \alpha_j K(a_i,a_j) \geq 0, \tag{A.2a}$$

and *strictly positive definite* if ">" holds. More generally we say that

Definition A.3. $K(\mathbf{x},\mathbf{y})$ is a conditionally positive definite kernel of order m (m-CPD) on Ω if for any choice of finite subsets $A = \{a_1,a_2,\ldots,a_M\} \subseteq \Omega \subset \mathbb{R}^n$ of M different points and all $\alpha = (\alpha_1,\alpha_2,\cdots,\alpha_M) \in \mathbb{R}^M \setminus \{0\}$ satisfying

$$\sum_{j=1}^{M} \alpha_j p(x_j) = 0, \ \forall p \in \Pi_{m-1}(\mathbb{R}^n), \tag{A.2b}$$

the quadratic form $\sum_{i,j=1}^{M} \alpha_i \alpha_j K(a_i,a_j)$ is positive. If $m = 0$, this definition is reduced to the case of positive definite functions and the condition (A.2b) is empty.

Definition A.4. The points $A = \{a_1,a_2,\ldots,a_M\} \subset \Omega \subset \mathbb{R}^n$ with $M \geq N = \dim \Pi_m(\mathbb{R}^n)$ are called $\Pi_m(\mathbb{R}^n)$- unisolvent if the zero polynomial is the only polynomial from $\Pi_m(\mathbb{R}^n)$ that vanishes in all of them.

Theorem A.4 ([26]). Let us consider the space $X^{m,l,s}$ and a family $\mathcal{L} = \{L_1,L_2,\ldots,L_M\}$ of compactly supported distributions representing our data, with $M > N = \dim \Pi_{m-1}(\mathbb{R}^n)$. We assume:

- The L_i's are of order $\leq r$, i.e. continuous linear functionals defined on C^r, where r satisfies the condition $-m + r + \dfrac{n}{2} < s < \dfrac{n}{2}$

- The family $\mathcal{L}$ is linearly independent in $\mathcal{D}'$ and contains a subfamily $\tilde{\mathcal{L}}$ which is Π_{m-1} -unisolvent.

And let $\mathbf{Z} = (z_1, z_2, \ldots, z_M)^t$ be a given vector in $\mathbb{R}^M$. Consider the following interpolation problem

(P1). Find $\boldsymbol{\sigma} \in X^{m,l,s}$ such that
$$|\sigma|_{m,l,s} = \min R[u] = |u|_{m,l,s}$$
$$u \in X^{m,l,s}$$
$$\langle L_i, u \rangle = z_i, i = 1, \ldots, M$$

and the smoothing problem

(P2). Find $\sigma \in X^{m,l,s}$ that minimize

$$H_\lambda[u] = \sum_{i=1}^{M}(L_i(u) - z_i)^2 + \lambda R[u], \qquad R[u] = |u|_{m.l.s}^2$$

The solutions to problems (P1) and (P2) are given explicitly by an spline of the form

$$\boldsymbol{\sigma} = \sum_{i=1}^{M}\alpha_i \overline{L}_i * K_{m,l,s} + \sum_{j=1}^{N}\beta_j p_j, \qquad (A.3)$$

where $\{p_j\}_{j=1}^{N}$ is a basis for Π_{m-1} and $K_{m,l,s}$ is a fundamental solution in C^{2r} of the operator $\Delta_{m,l,s}$, i.e. $\Delta_{m,l,s} K_{m,l,s} = \delta$.

In the interpolation problem **(P1)**, the coefficients α_i $i = 1, \ldots, M$, β_j $j = 1, \ldots, N$ satisfying the interpolating conditions and the orthogonal conditions, are solutions of the following system of linear equations

$$\begin{cases} \sum_{i=1}^{M}\alpha_i \langle L_k, \overline{L}_i * K_{m,l,s} \rangle + \sum_{j=1}^{N}\beta_j \langle L_k, p_j \rangle = z_k, & k = 1, \ldots, M \\ \sum_{j=1}^{N}\alpha_i \langle L_i, p_j \rangle = 0, & j = 1, \ldots, N \end{cases} \qquad (A.4)$$

The system can be written in the form

$$\begin{bmatrix} K & P \\ P^t & 0 \end{bmatrix} \begin{bmatrix} \alpha \\ \beta \end{bmatrix} = \begin{bmatrix} Z \\ 0 \end{bmatrix}, \tag{A.5}$$

where

- $K = [\langle L_i, \bar{L}_j * K_{m,l,s} \rangle]_{1 \le i,j \le M}$ is an $M \times M$ matrix
- $P = [\langle L_i, p_j \rangle]_{1 \le i \le M, 1 \le j \le N}$ is an $M \times N$ matrix
- $\alpha = (\alpha_1, \alpha_2, \ldots, \alpha_M)^t$
- $\beta = (\beta_1, \beta_2, \ldots, \beta_N)^t$
- $Z = (z_1, z_2, \ldots, z_M)^t$ is the data vector.

In case of smoothing problem (**P2**) we have to solve the system

$$\begin{bmatrix} K + \lambda I_M & P \\ P^t & 0 \end{bmatrix} \begin{bmatrix} \alpha \\ \beta \end{bmatrix} = \begin{bmatrix} Z \\ 0 \end{bmatrix}, \tag{A.6}$$

where I_M is the identity matrix.

References

[1] Abramowitz, M. and Stegun, I.A. (1970). *Handbook of mathematical functions with formulas, graphs and mathematical tables*. National Bureau of Standards, Applied Mathematics Series. Washington

[2] Adams, R. A. (1975). *Sobolev Spaces*. Academic Press, New York, USA.

[3] Adi, B. and Greville, T. (2003). *Generalized inverses. Theory and applications*. Springer.

[4] Ahlberg, J., Nilson, H.E. and Walsh, J. L. (1967). *The Theory of Splines and Their Applications*. Academic Press, New York.

[5] Alexa, M., Behr, J., Cohen-Or, D., Fleishman, S. and Silva, C.T. (2001). Point set surfaces. In *Proc. IEEE Visualization 2001*, p.21-28.

[6] Amenta, N., Bern, M. and Eppstein, D. (1998). The crust and the b-skeleton: combinatorial curve reconstruction, *Graph. Models Image Process*. 60 (2) pp. 125-135.

[7] Arcangéli, R., Lopez, M.C. and Torrens, J. (2004). *Multidimensional Minimizing Splines*. Kluwer Academic Publishers, Dordrecht.

[8] Aronszajn, N. (1950). Theory of reproducing kernels. *Trans. Amer. Math. Soc.*, 68, pp. 337- 404.

[9] Atkinson, G. and Hancock, E. R. (2006). Recovery of surface orientation from diffuse polarization, *IEEE Trans. Image. Process.*, **15** (6), pp. 1653-1664.

[10] Atteia, M. (1992). *Hilbertian Kernels and Spline Functions*. North-Holland, Elsevier Science, Amsterdam, Holland.

[11] Bajaj, C. Bernardini, F. and Xu, G. (1995). Automatic reconstruction of surfaces and scalar fields from 3d scans. *SIGGRAPH'95 Proceedings*, pp. 193-198.

[12] Barrow, H. G. and Tenenbaum, J. M. (1981). Computational vision, *Proc. IEEE*, **69** (5), pp. 572-595.

[13] Bates, D., Lindstrom, M., Wahba, G. and Yandell, B. (1986). GCVPACK-Routines for Generalized Cross Validation Department of Statistics, University of Wisconsin. Technical Report No.775.

[14]   Beatson R. K. and Powell, M. J. D. (1992). Univariate interpolation on a regular grid by a multiquadric plus a linear polynomial. *IMA J. of Numerical Anal.*, **12**, pp. 107-133.

[15]   Beatson, R. K., Carr, J.C., McCallum, B.C., Fright, W.R., Mclennan, T.J. and Mitchell, T.J. (2003). Smooth surface reconstruction from noisy range data. *In Proc. Graphite 2003,* pp. 119-126.

[16]   Bellman, R. (1961). *Adaptive Control Processes*: A Guided Tour. Princeton University Press, Princeton.

[17]   Bellman, R.E. (1957). *DynamicProgramming*. Princeton University Press, Princeton.

[18]   Bertero, M., Poggio,T. and Torre,V. (1986). Ill-Posed Problems in Early Vision. Artifitial intelligence Laboratory Memo, No.924.MIT.

[19]   Bezhaev, A.Y. and Vasilenko, V.A. (2001). *Variational Theory of Splines*. Kluwer.New York, USA.

[20]   Blais, F. (2004). Review of 20 years of range sensor development. *Journal of Electronic Imaging* **13** (1), pp. 231-240.

[21]   Bloomenthal, J., Bajaj, C., Blinn, J., Cani-Gascuel, M.P., Rockwood, A., Wyvill, B. and Wyvill, G. (1997). *Introduction to Implicit Surfaces*. Morgan Kaufman, San Francisco, USA.

[22]   Bobenko, A.I., Schröder, P., Sullivan, J.M., Ziegler, G.M. (2008*). Discrete differential geometry*. Birkhäuser.

[23]   Bochner, S. (1932). *Vorlesungen• uber Fouriersche Integrale*, Akademische Verlagsgesellschaft, Leipzig.

[24]   Bochner, S. (1933). Monotone Funktionen, Stieltjes Integrale und harmonische Analyse, *Math. Ann.,* **108** pp. 378-410.

[25]   Boissonnat, J.D. and Cazals, F. (2002). Smooth shape reconstruction via natural neighbor interpolation of distance functions. *Computational Geometry*, **22**, (1-3), pp. 185-203.

[26]   Bouhamidi, A. and Le Méhauté, A. (1999). Multivariate interpolating (m, l, s)-splines. *Adv. Comput. Math.* **11**, pp. 287-314.

[27]   Bouhamidi, A. (2005). Weighted thin plate splines. *Anal. Appl.* **3**(3), pp. 297-324.

[28]   Bouhamidi, A. (2007). Error estimates in Sobolev spaces for interpolating thin plate splines under tension. *J. Computational and Applied Mathematics,* **200,** pp. 208-216.

[29]   Boult, T. E. and Kender, J. R. (1986). Visual surface reconstruction using sparse depth data, in Proc. *IEEE Conf Comp. Vision and Pattern Recognition*, pp. 68-76.

[30]   Branch, J. W. (2007). Reconstrucción de objetos de forma libre a partir de imágenes de rango empleando una red de parches NURB. Tesis de doctorado. Facultad de Minas Universidad Nacional de Colombia. Sede Medellín. Colombia.

[31]   Breen, D.E., Mauch, S. and Whitaker, R.T. (1998). 3D scan conversion of CSG models into distance. *Volume Visualization Symposium*, pp. 7-14.

[32]   Buhmann, M.D. (2003).   *Radial basis functions*. Cambridge Monographs on Applied and Computational Mathematics, Cambridge University Press, Cambridge.

[33]   Carr, J. C., Beatson, R. K.., Cherrie, J. B., Mitchell, T. J., Fright, W. R., Mccallum, B. C. and Evans, T. R. (2001). Reconstruction and representation Of 3D objects with radial basis functions. In *proceedings of ACM SIGGRAPH 2001*, pp. 67-76.

[34]   Chen, C.Y. and Cheng, H. Y. (2005). A sharpness dependent filter for mesh smoothing. *Computer Aided Geometric Design*, **22** (5), pp. 376-391.

[35]   Cheney, E.W. and Light, W.A. (2000). *A Course in Approximation Theory*. Brooks Cole Publishing Company. Pacific Grove.

[36]   Choi J., Young-seok, H. and Moon, G. K. (2008). High Dynamic range image reconstruction using multiple images. *The 23rd International Conference on Circuits/Systems, Computers and Communications* (ITC-CSCC 2008).

[37]   Clarenz, U. Diewald, U. and Rumpf, M. (2000). Anisotropic geometric diffusion in surface processing. In Proc. Conf. Visualization. *IEEE Computer Society*, pp. 397-405.

[38]   Curless, B. and Levoy, M. (1996). A volumetric method for building complex models from range images. In H. Rushmeier, editor, *SIGGRAPH 96 Conference Proceedings*, Addison Wesley, pp. 303- 312.

[39]   Cyganek, B. and Siebert, J. P. (Eds.). (2009). *An Introduction to 3d Computer Vision Techniques and Algorithms*. Wiley.

[40]   Deny, J. and Lions, J.L. (1954). Les espaces du type de Beppo-Levi. *Ann. Inst. Fourier* 5, pp. 305-370.

[41]   Desbrun, M. and Cani-Gascuel, M.P. (1998). Active Implicit Surface for Animation, *Graphics Interface '98*, 143-150.

[42]   Desbrun, M., Meyer, M., Schroder, P. and Barr, A. H. (1999). Implicit fairing of irregular meshes using diffusion and curvature flow. In *Proc. 26th Conf. Computer Graphics and Interactive Techniques*, CM Press/Addison-Wesley Publishing Co, pp. 317-324.

[43]   Dey, T.K. and Sun, J. (2005). Adaptive MLS surfaces for reconstruction with guarantees. In *Eurographics Symposium on Geometry Processing 2005*, pp. 43-52.

[44]   Diebel, J. R., Thrun, S. and Brunig, M. (2006). A Bayesian method for probable surface reconstruction and decimation. *ACM Trans. Graphics*, **25** (1), pp. 39-59.

[45]   Dinh, H. Q., Turk G. and Slabaugh, G. (2002). Reconstructing Surfaces By Volumetric Regularization Using Radial Basis Functions. *IEEE Trans. Pattern Anal. Machine Intell*, pp. 1358-1371.

[46]   Dubrovin, B.A., Fomenko, A.T. and Novikov, S.P. (1984). *Modern Geometry: Methods and Applications*. Springer.

[47]   Duchon, J. (1976). Interpolation des fonctions de deux variables suivant le principe de la exion des plaques minces, Rev. *Francaise Automat. Informat. Rech. Oper., Anal. Numer.* 10, pp. 5-12.

[48]   Duchon, J. (1977). Splines minimizing rotation-invariant semi-norms in Sobolev spaces, in *Constructive Theory of Functions of Several Variables, Oberwolfach 1976*, W. Schempp and K. Zeller (Eds.), Springer Lecture Notes in Math. 571, Springer-Verlag, Berlin, pp. 85-100.

[49]   Duchon, J. (1978). Sur l'erreur d'interpolation des fonctions de plusieurs variables par les Dm-splines, *Rev. Francaise Automat. Informat. Rech. Oper. Anal. Numer.* **12**, pp. 325-334.

[50]   Duchon, J. (1980). Fonctions splines homogenes a plusiers variables. Universite de Grenoble.

[51]   Dunford, N. and Schwartz, J.T. (1958-1971). *Linear Operators.*, Part 1, *General Theory*, 1958; Part 2, *Spectral Theory*, 1963; Part 3 *Spectral Operators*. Interscience Publishers, Inc., New York.

[52]   Edelsbrunner, H. (1998). Shape reconstruction with delaunay complex, in *Proceedings of LATIN'98*. Theoretical Informatics, Lecture Notes in Computer Science, vol. 1380, Springer- Verlag, pp. 119-132.

[53]   Edelsbrunner, H., Kirkpatrick, D. and Seidel, R. (1983). On the shape of a set of points in the plane, *IEEE Trans. Inf. Theory,* **29** (4), pp. 551-559.

[54]   Edelsbrunner, H. and Mücke, E.P. (1994). Three-dimensional alpha shapes, *ACM Trans. Graph*. **13**, pp. 43-72.

[55]   Engl, H.W., Hanke, M. and Neubauer, A. (1996). *Regularization of inverse problems*. Springer.

[56]   Epstein, C. (2003). *Introduction to the Mathematics of Medical Imaging*. Pearson.

[57]   Fasshauer, G. (2007). *Meshfree Approximation Methods with Matlab*. Interdisciplinary Mathematical Sciences. World Scientific Publishers.

[58]   Faugeras, O. D. and Keriven, R. (1998). Variational principles, surface evolution, pdes, level set methods, and the stereo problem, *IEEE Trans. Image Process*., **7** (3), pp. 336-344.

[59]   Faul, A.C., Goodsell, G. and Powell, M. J. D. (2005). A Krylov subspace algorithm for multiquadric interpolation in many dimensions. *IMA Journal of Numerical Analysis,* **25**, pp.1-24.

[60]   Fenn, M. and Steidl, G. (2005). Robust local approximation of scattered data. In Geometric *Properties from Incomplete Data*. R. Klette, R. Kozera, L. Noakes, J. Weickert (Eds.), Springer, pp. 317-334.

[61]   Flint, A. and van den Hengel, D. A. (2008). Local 3D structure recognition in range images *IET Comput. Vis*., **2**(4), pp. 208-217.

[62]   Folland, G.B. (1992). *Fourier analysis and its Applications*. Amer. Mathematical Society.

[63]   Franke, R. (1985). Thin plate splines with tension. *Comput. Aided Geom. Des*. 2, 87-95.

[64]   Franke, R. (1982). Scattered data interpolation: tests of some methods, *Math. Comp*., 48, pp. 181-200.

[65]   Friedlander, F.G. and Joshi, M. (2008). *Introduction to the Theory of Distributions*. Cambridge University Press.

[66]   Gel'fand, I.M. and Shilov, G.E. (1964, 1968, 1967). *Generalized Functions*. Vol. 1-3. Academic Press, New York.

[67] Ghane, M., Sattaria, M., Samadzadegan, F. and Azizib, A. (2008). A review of recent range image reconstruction algorithms. The International Archives of the Photogrammetry, *Remote Sensing and Spatial Information Sciences*.

[68] Gibson, J.J. (1979). *The ecological approach to visual perception*. Houghton Mifflin.

[69] Girosi, F. and Anzellotti, G. (1995). Convergence Rates of Approximation by Translates.A.I. Memo No. 1288-Massachusetts Institute of Technology Artificial Intelligence Laboratory.

[70] Girosi, F., Jones, M. and Poggio, T. (1995). Regularization Theory and Neural Networks Architectures, *Neural Computation*, **7** (2), pp. 219-269.

[71] Girosi, F. and Poggio, T. (1990). Networks and the best approximation property. *Biol. Cybernet*. **63**, 169-176.

[72] Girosi, F. (1993). Regularization theory, radial basis functions and networks. In *From Statistics to Neural Networks. Theory and Pattern Recognition Applications*, V. herkassky, J. H. Friedman, and H. Wechsler (Eds.). Springer-Verlag, Berlin.

[73] Girosi, F., Jones, M. and Poggio, T. (1993). Priors, Stabilizers and Basis Functions: From Regularization to Radial, Tensor and Additive Splines, A.I. Memo No. 1430, C.B.C.L. Paper No.75, Massachusetts Institute of Technology Arti cial Intelligence Lab.

[74] Glennerster, A. (2002) Computational theories of vision. *Current Biology*, **12** (20), pp. 682-685.

[75] Glennerster, A. (2007). Marr's vision: Twenty-five years on. *Current Biology*, **17** (11) pp. 397-399.

[76] Gokmen, M. and Li, C. C. (1993). Edge Detection and Surface Reconstruction Using Refined Regularization. *IEEE Trans. Pattern Analysis and Machine Intelligence*, **15** (5), pp. 492-499.

[77] Golomb, M. and Weinberger, H.F. (1959). Optimal approximation and error bounds. In *Numerical Approximation*. Langer, R. E. Ed., University of Wisconsin Press, Madison, pp. 117-190.

[78] Grimson, W.E.L. (1983). An implementation of computational theory for visual surface interpolation, *Comput. Viiwn, Graphics, Image Processing*, **6** (22), pp. 39-69.

[79] Grimson, W.E.L. (1981). *From images to surfaces: A Computational study of the human early vision system*, MIT Press, Cambridge, MA.

[80] Gumerov, N. A. and Duraiswami, R. (2007). Fast radial basis function interpolation via preconditioned Krylov iteration, *SIAM Journal on Scientific Computing*, **29** (5), pp. 1876-1899.

[81] Hadamard, H. (1923). *Lectures on the Cauchy problem in linear partial differential equations*. Yale University Press. New Haven.

[82] Hansen, P. C. (1998). *Rank-deficient and discrete ill-posed problems: numerical aspects of linear inversion*. Society for Industrial Mathematics.

[83] Hansen, P. C. (2008). *Regularization Tools. A Matlab Package for Analysis and Solution of Discrete Ill-Posed Problems.* Version 4.1 for Matlab 7.3.

[84] Harder, J. R., Desmarais, R. N. (1972). Interpolation using surface splines; *Journal Aircraft*; **9**, pp. 189-197.

[85] Hardy, R. L., (1971), Multiquadric equations of topography and other irregular surfaces, *J. Geophys. Res*., **76**, pp. 1905-1915.

[86] Hartmann, F. and Katz, C. (2007). *Structural analysis with finite elements*. Springer

[87] Hilbert, D. and Courant, R. (1989). *Methods of Mathematical Physics*. Wiley.

[88] Hilton, A. Stoddart, A.J., Illingworth, J. and Windeatt, T. (1998). Implicit surface - based geometric fusion. *Comput. Vision and image Understanding*, **69**, pp. 273-291.

[89] Hinestroza, D., Murio, A. and Zhan, S. (1999). Regularization techniques for nonlinear problems. *Computers and Mathematics with Applications*, **37**, pp. 145-159.

[90] Hoppe, H. (1994). Surface reconstruction from unorganized points, Ph.D. Thesis in Computer Science and Engineering, University of Washington.

[91] Hormander, L. (1963). *Linear Partial Differential Operators*. Springer-Verlag, Berlin.

[92] Horn, B. K. P. and Brooks, M. J. (1986). The variational approach to shape from shading, *Comp. vision, Graphics, and Image Processing*, **33** (2), pp. 174-208.

[93] Hwang, W.L., Lu, C.S. and Chung, P.C. (1998). Shape from texture: Estimation of planar surface orientation through the ridge surfaces of continuous wavelet transform, *IEEE Trans. Image Process.*, **7** (5), pp. 773-780.

[94] Isakov, V. (2006). *Inverse Problems for partial Differential Equations*. Springer.

[95]   Ivrissimtzis, I., Lee, Y., Lee, S., Jeong, W.K. and Seidel, H.P. (2004). Neural mesh ensembles. In *2nd International Symposium on 3D Data Processing, Visualization, and Transmission*, Y. Aloimonos, G. Taubin (Eds.), pp. 308-315.

[96]   Jones, T. R., Durand, F. and Desbrun, M. (2003). Non-iterative, feature-preserving mesh smoothing. *ACM Trans. Graphics*, **22**(3), pp. 943-949.

[97]   June, H. and Chelberg, D.M. (1995). Discontinuity-Preserving and Viewpoint Invariant Reconstruction of Visible Surfaces Using a First Order Regularization *IEEE Trans. Pattern Anal. Machine Intell.,* **17** (6), pp. 624-629.

[98]   Kelly, A. R. and E. Hancock. (2004). A graph-spectral approach to shape-from-shading, *IEEE Trans. Image Process.*, **13** (7), pp. 912-926.

[99]   Keren, D. and Werman, M. (1999). A Full Bayesian Approach to Curve and Surface Reconstruction, *Journal of Mathematical Imaging and Vision,* **11**, pp. 27-43.

[100] Kirsch, A. (1996). *An Introduction to the Mathematical Theory of Inverse Problems*. Springer.

[101] Koivunen, V. (1995). A robust nonlinear filter for image restoration. *IEEE Trans. Image Process*. **4**, pp. 569-578.

[102] Kress, R. (1999). *Linear Integral Equations*. Springer.

[103] Lange, C. and Polthier, K. (2005). Anisotropic fairing of point sets. *Comput. Aided Geom. Des*. **22** (7), pp. 680-692.

[104] Laurent, P.J. (1972). *Approximation et optimisation*. Hermann, Paris.

[105] Lee, K.M., Meer, P. and Park, R.H. (1998). Robust adaptive segmentation of range images. *IEEE Trans. Pattern Anal. Machine Intell*. **20**, pp. 200-205.

[106] Levoy, M., Pulli, K., Curless, B., Rusinkiewicz, S., Koller, D., Pereira, L., Ginzton, M., Anderson, S., Davis, J. Ginsberg, J. Shade, J. and Fulk, D. (2000). The digital michelangelo project: 3D scanning of large statues. *Proceedings of SIGGRAPH 2000*, pp. 131-144.

[107] Light, W. A. and Wayne, H. (1998). On power functions and error estimates for radial basis function interpolation, *J. Approx. Theory* **92**, pp. 245-266.

[108] Light, W. (1998). Variational Methods for interpolation, Particularly by Radial Basis Functions. University of Leicester. Technical Report.

[109] Light, W. and Wayne, H. (1997). Spaces of Distributions and Interpolation by Translates of a Basis Function. University of Leicester. Technical Report.

[110] Linsen, L. (2001). Point cloud representation. Tech. Rep. 2001-3, Fakultät für Informatik, Universität Karlsruhe.

[111] Madych, W. R. and Nelson, S. A. (1983). Multivariate interpolation: a variational theory, manuscript.

[112] Madych, W. and Nelson, S. (1988). Multivariate interpolation and conditionally positive definite functions, *Approx. Theory Appl*. **4**, pp. 77-89.

[113] Marr, D. (1982). *Vision: A Computational Investigation into the Human Representation and Processing of Visual Information*. W. H. Freeman and Company New York.

[114] Marr, D. and Poggio, T. (1976). Cooperative computation of stereo disparity. *Science*, **194**, pp. 283-287.

[115] Marr, D. and Poggio, T. (1977). From understanding computation to understanding neural circuitry. *Neurosciences Res. Prog. Bull*., **15**, pp. 470-488.

[116] Marr, D. and Poggio, T. (1979). A computational theory of human stereo vision. *Proceedings of the Royal Society of London B*, **204**, pp. 301-328.

[117] Marr, D. and T. Poggio, (1979). A theory of human stereo vision, *Proc. Roy, Soc. London B,* **204**, pp. 301-328.

[118] Marr, D. and Poggio, T. (1976) Cooperative computation of stereo disparity. *Science*, **194**, pp. 283-287.

[119] Marroquin, J., Mitter, S. and Poggio, T. (1987). Probabilistic Solution of Ill-posed Problems in Computational Vision, *Journal of American Statistical Association*, **82** (397), pp. 76-89.

[120] Mederos, B., Velho, L. and de Figueiredo, L.H. (2004). Smooth surface reconstruction from noisy clouds. *J. Brazilian Comput. Soc*.

[121] Meer, P., Mintz, D., Rosenfeld, A. and Kim, D.Y. (1991). Robust regression methods for computer vision. *Areview. Internat. J. Comput. Vision* **6**, pp. 59-70.

[122] Meinguet, J. (1979). Multivariate interpolation at arbitrary points made simple, *Z. Angew. Math. Phys*., **30**, pp. 292-304.

[123] Meinguet, J. (1979). An intrinsic approach to multivariate spline interpolation at arbitrary points, in *Polynomial and Spline Approximations*, N. B. Sahney (ed.), Reidel, Dordrecht, pp. 163-190.

[124] Meinguet, J. (1979). Basic mathematical aspects of surface spline interpolation, in *Numerische Integration*, G. Hammerlin (ed.), Birkhauser, Basel, pp. 211-220.

[125] Meinguet, J. (1984). Surface spline interpolation: basic theory and computational aspects, in *Approximation Theory and Spline Functions*, S. P. Singh, J. H. W. Burry, and B. Watson (Eds.), Reidel, Dordrecht, pp. 127-142.

[126] Micchelli, C. A. (1986). Interpolation of scattered data: distance matrices and conditionally positive definite functions, *Constr. Approx.*, **2**, pp. 11-22.

[127] Micchelli, C. A. and Rivlin, T. J (1977). A survey of optimal recovery, in *Optimal estimation in approximation theory*, C. A. Micchelli and T. J. Rivlin (Eds.), Plenum Press, New York, pp. 1-54.

[128] Micchelli, C. A and Rivlin, T. J. (1980). Optimal recovery of best approximations, *Resultate Math*. **3** (1), pp. 25-32.

[129] Montegranario, H. and Espinosa, J. (2007). Regularization Approach for Surface Reconstruction from Point Clouds. *Applied Mathematics and Computation*, **188**, pp. 583-595.

[130] Montegranario, H. (2008). A unified framework for 3D reconstruction. *PAMM - Proc. Appl. Math. Mech.* 7, 2140017-2140018.

[131] Montegranario, H. and Espinosa, J. (2009). A general framework for regularization of n-dimensional inverse problems. VII Congreso Colombiano de Modelamiento Numerico. Bogota. Colombia.

[132] Morozov, V. A. (1993). *Regularization Methods for Ill-Posed Problems*. CRC Press;

[133] Muraki, S. (1991). Volumetric shape description of range data using "blobby model". In Computer Graphics. *Proc. SIGGRAPH '91*, **25**, pp. 227-235.

[134] Narayanan, K. A., O'Leary, D. P. and Rosenfeld, A. (1982). Image smoothing and segmentation by cost minimization, *IEEE Trans. Syst. Man, Cybernetics*, vol. SMC-12, pp. 91-96.

[135] Ning, P. and Bloomenthal, J. (1993). An evaluation of implicit surface tilers. *IEEE Computer Graphics and Applications*, **13**(6), pp. 33-41.

[136] O'Neill, B. (1966). *Elementary Differential Geometry*. Academic Press.

[137] Osher, S. and Sethian, J. (1988) Fronts propagating with curvature dependent speed, algorithms based on a Hamilton-Jacobi formulation. *J. Comp. Phys.*, **79**, pp. 12-49.

[138] Park, D.J., Nam, K.M. and Park, R.H. (1995). Multiresolution edge detection techniques. *Pattern Recognition* 28, 211-229.

[139] Pasko, A., Adzhiev, V. Sourin, A. and Savchenko, V. (1995). Function representation in geometric modeling: concepts, implementation and applications. *The Visual Computer*, **11** (8), pp. 429-446.

[140] Piegel, L. and Tiller, W. (1996). *The NURBS Book*, Springer-Verlag.

[141] Poggio, T. and Girosi, F. (1990) Regularization Algorithms for Learning that are Equivalent to Multilayer Networks, *Science*, 247, 978-982.

[142] Poggio, T. and Torre, V. (1984). Ill-posed problems and regularization analysis in early vision. MIT Artifitial Intelligence Lab.A.I. Memo 773.

[143] Poggio, T., Voorhees, H. and Yuille, A. (1988). A Regularized Solution to Edge Detection, *Journal of Complexity*, **4**, pp.106-123.

[144] Poggio, T., Torre, V. and Koch, C. (1985). Computational Vision and Regularization Theory, *Nature*, 317, pp. 314-319.

[145] Poggio T. and Torre, V. (1984). Ill-Posed Problems and Regularization Analysis in Early Vision. AI Memo 773/CBIP Paper 1, Massachusetts Institute of Technology, Cambridge, MA.

[146] Raja, V. and Fernandes, K. J. (Eds.). (2008). *Reverse Engineering. An Industrial Perspective*. Springer.

[147] Reddy, J.N. (1984). *Energy and variational methods in applied mechanics*. John Wiley and Sons.

[148] Rigling, B. D. and Moses, R. L. (2005). Three-dimensional surface reconstruction from multistatic SAR images, *IEEE Trans. Image Process*., **14** (8), pp. 1159-1171.

[149] Rogers, D.F. (2000). *An Introduction to NURBS*, Morgan Kaufman.

[150] Rongjiang, P., Meng, X. and Whangbo, T. (2009). Hermite variational implicit surface reconstruction. *Sci China Ser F-Inf Sci*., **52** (2), pp. 308-315.

[151] Rousseeuw, P.J. and Leroy, A.M. (1987). Robust Regression and Outlier Detection. Wiley, New York, USA.

[152] Rudin, W. (1973). *Functional Analysis*. McGraw-Hill, New York.

[153] Saxena, A. and Sahay, B. (2005). *Computer Aided Engineering Design*. Springer.

[154] Schaback, R. (1995). Creating Surfaces from Scattered Data using Radial Basis Functions, in *Mathematical Methods for Curve and Surfaces*, M. Dæhlen, T. Lyche, and L. Schumaker (Eds.), Vanderbilt University Press, Nashville, pp. 477-496.

[155] Schaback, R. (1999). Native Hilbert spaces for radial basis functions I, in *New Developments in Approximation Theory*, M. W. Muller, M. D. Buhmann, D. H. Mache and M. Felten (Eds.), Birkhauser, Basel, pp. 255-282.

[156] Schaback, R. (2000). A unified theory of radial basis functions. Native Hilbert spaces for radial basis functions II, *J. Comput. Appl. Math*. **121**, pp. 165-177.

[157] Schall, O., Belyaev, A. and Seidel, H.P. (2007). Feature-preserving non-local denoising of static and time-varying range data. In *Proc. ACM Symp. Solid and Physical Modeling*, ACM Press, pp. 217-222.

[158] Schoenberg, I. J. (1938). Metric spaces and completely monotone functions, *Ann. of Math.*, **39**, pp. 811-841.

[159] Schoenberg, I. J. (1964). Spline functions and the problem of graduation, *Proc. Nat. Acad. Sci.* **52**, pp. 947-950.

[160] Scholkopf, B., Giesen, J. and Spalinger, S. (2005). Kernel methods for implicit surface modeling. In *Advances in Neural Information Processing Systems* **17**, pp. 1193-1200.

[161] Schultz, M. H. (1973). *Spline Analysis*. Prentice Hall, Englewood Cliffs, N. J.

[162] Schumaker, L. L. (1976). Fitting surfaces to scattered data, in *Approximation Theory II*, G. G. Lorentz, C. K. Chui, and L. L. Schumaker, (Eds.). Academic Press, pp. 203-267.

[163] Schwartz, L. (1966). *Théorie des distributions*. Hermann, Paris.

[164] Schwartz, L. (1966). *Mathematics for the Physical Sciences*. Addison-Wesley.

[165] Shepard, D. (1968) A two dimensional interpolation function for irregularly spaced data, *Proc. 23rd Nat. Conf. ACM*, pp. 517-523.

[166] Shin, D. and Tjahjadi, T. (2008). Local hull-based surface construction of volumetric data from silhouettes, *IEEE Trans. Image. Process*., **17** (8), pp. 1251-1260.

[167] Sobolev, S.L. (1936). Méthode nouvelle à résoudre le problème de Cauchy pour les équations linéaires hyperboliques normales. *Matematicheskiĭ Sbornik*. **1** (43) (1), pp. 39-72.

[168] Speckman, P. and Sun, D. (2003). Fully Bayesian spline smoothing and intrinsic autoregressive priors, *Biometrika*, **90** (2), pp. 289-302.

[169] Steinke, F., Schölkopf, B. and Blanz, V. (2005). Support vector machines for 3D shape processing. *Comput. Graph. Forum* **24**(3), pp. 285-294.

[170] Sun, X., Rosin, P. L., Martin, R. R. and Langbein, F. C. (2007). Fast and effective feature-preserving mesh denoising. *IEEE Trans. Visualization and Computer Graphics*, **13**(5), pp. 925-938.

[171] Suykens, J. A. K., Gestel, T. V., Brabanter, J. D., Moor, B. D. and Vandewalle, J. (2003). *Least Squares Support Vector Machines*. World Scientific Publishing Company.

[172] Tarantola, A. (2005). *Inverse Problem Theory and Model Parameter Estimation*, SIAM.

[173] Taubin, G. (1995). A signal processing approach to fair surface design. In R. Cook, editor, *SIGGRAPH 95 Conference Proceedings*, Addison Wesley, pp. 351-358.

[174] Terzopoulos, D. (1988). The Computation of Visible- surface representation.IEEE Transactions on Pattern Analysis and Machine Intelligence. **10** (4), pp. 417 - 438.

[175] Terzopoulos, D. (1983). Multilevel computational processes for visible surface reconstruction. *Comput. Vision, Graphics and Image Processing*, **24**, pp. 52-96.

[176] Terzopoulos, D. (1984).Multiresolution computation of visible-surface representations. Ph.D. dissertation, Massachusetts Institute of Technology, Dept. of Electrical Engineering and Computer Science, Cambridge.

[177] Terzopoulos, D. Witkin, D. A. and Kass, M. (1988) Constraints on deformable models: Recovering 3D shape and nonrigid motion, *Artificial Intell.*, **36**, pp. 91 - 123.

[178] Terzopoulos, D. (1986). Regularization of Inverse Visual Problems Involving Discontinuities, *IEEE Trans. Pattern Analysis and Machine Intelligence*, **8**(4), pp. 413-424.

[179] Tikhonov, N. and Arsenin, V.Y. (1977). *Solutions of ill-posed problems*. W. H. Winston, Washington D.C.

[180] Timoshenko, S. and Woinowsky, S. (1981). *Theory of Plates and Shells*. McGraw-Hill.

[181] Timoshenko, S P. and Gere, J. M. (1952). *Theory of Elastic Stability*. Wiley and sons.

[182] Turk, G. and O'Brien, J.F. (2002). Modelling with Implicit Surfaces that Interpolate. *ACM Transactions on Graphics*, **21** (4), pp. 855-873.

[183] Turk, G. and O`Brien, J.F (1999). Shape transformation using variational implicit functions. *SIGGRAPH99*, pp. 335-342.

[184] Vapnik, V. N. (1998). *Statistical Learning Theory*. Wiley, New York.

[185] Vinesh, R. and Fernández, K. J. (Eds.). (2008). *Reverse Engineering. An Industrial Perspective*. Springer.

[186] Wahba, G. and Luo, Z. (1997). Smoothing spline ANOVA ts for very large, nearly regular data sets, with application to historical global climate data, in *The Heritage of P. L. Chebyshev: a Festschrift in honor of the 70th birthday of T. J. Rivlin*, Ann. Numer. Math. **4** (1-4), pp. 579-597.

[187] Wahba, G. (1979). Convergence rate of "thin plate" smoothing splines when the data are noisy, *Springer Lecture Notes in Math.*, 757, pp. 233-245.

[188] Wahba, G. (1990). *Spline Models for Observational Data*. CBMS-NSF, Regional Conference Series in Applied Mathematics, SIAM, Philadelphia.

[189] Wahba, G. and Wendelberger, J. (1980). Some new mathematical methods for variational objective analysis using splines and cross validation; *Mon.Wea.Rev.*, **108**, pp. 1122-1143.

[190] Waqar, S., Schall, O., Patan, G., Belyaev, A. and Seidel, H.P. (2007). On stochastic methods for surface reconstruction. *Visual Comput.,* **23**, pp. 381-395.

[191] Wendland, H. (2010). *Scattered Data Approximation*. Cambridge University Press.

[192] Wendland, H. (1994). Ein Beitrag zur Interpolation mit radialen Basisfunktionen, Diplomarbeit. Universitat, Gottingen.

[193] Westermann. R. (2000). Volume models. In *Principles of 3D Image Analysis and Synthesis*, B. Girod, G. Greiner, and H. Niemann, (Eds). Kluwer Academic Publishers, Boston-Dordrecht-London, pp. 245-251.

[194] Wyvill, B., Guy, A. and Galin, E. (1999). Extending the CSG tree, warping, blending and boolean operations in an implicit surface modeling system. *Computer Graphics Forum*, **18**(2), pp. 149-158.

[195] Wyvill, B. McPheeters, C. and Wyvill, G. (1986). Data structure for soft objects. The Visual Computer, **2** (4), pp. 227-234.

[196] Yoshizawa, S., Belyaev, A. and Seidel, H.P. (2006). Smoothing by example: Mesh denoising by averaging with similarity-based weights. In *Proce. Shape Modeling and Applications*, IEEE Computer Society, pp. 9.

[197] Yosida, K. (1995). *Functional Analysis*, Springer-Verlag, Berlin.

[198] Yu, Y., Zhou, K., Xu, D., Shi, X., Bao, H., Guo, B. and Shum, H. (2004). Mesh editing with Poisson-based gradient field manipulation. *ACM Trans. Graphics*, **23** (3), pp. 644-651.

[199] Zeidler, E. (1984). *Nonlinear Functional Analysis and Its Applications*: Part II and III. Springer.

[200] Zexiao, X., Jianguo, W. and Qiumei, Z. (2005). Complete 3D measurement in reverse engineering using a multi-probe system. *International Journal of Machine Tools & Manufacture,* **45**, pp. 1474-1486.

[201] Zhao, H.K., Osher, S. and Fedki, R. (2001). Fast Surface Reconstruction Using the Level Set Method. Proceedings. IEEE Workshop on Variational and Level Set Methods in Computer Vision, pp. 194-201.

[202] Zuily, C. (1988). *Problems in Distributions and Partial Differential Equations*. Elsevier Science.